frontiers | Research Topics

Advanced use of materials in orthodontics

Edited by
Domenico Ciavarella, Michele Tepedino
and Paolo M. Cattaneo

Published in
Frontiers in Materials
Frontiers in Bioengineering and Biotechnology
Frontiers in Dental Medicine

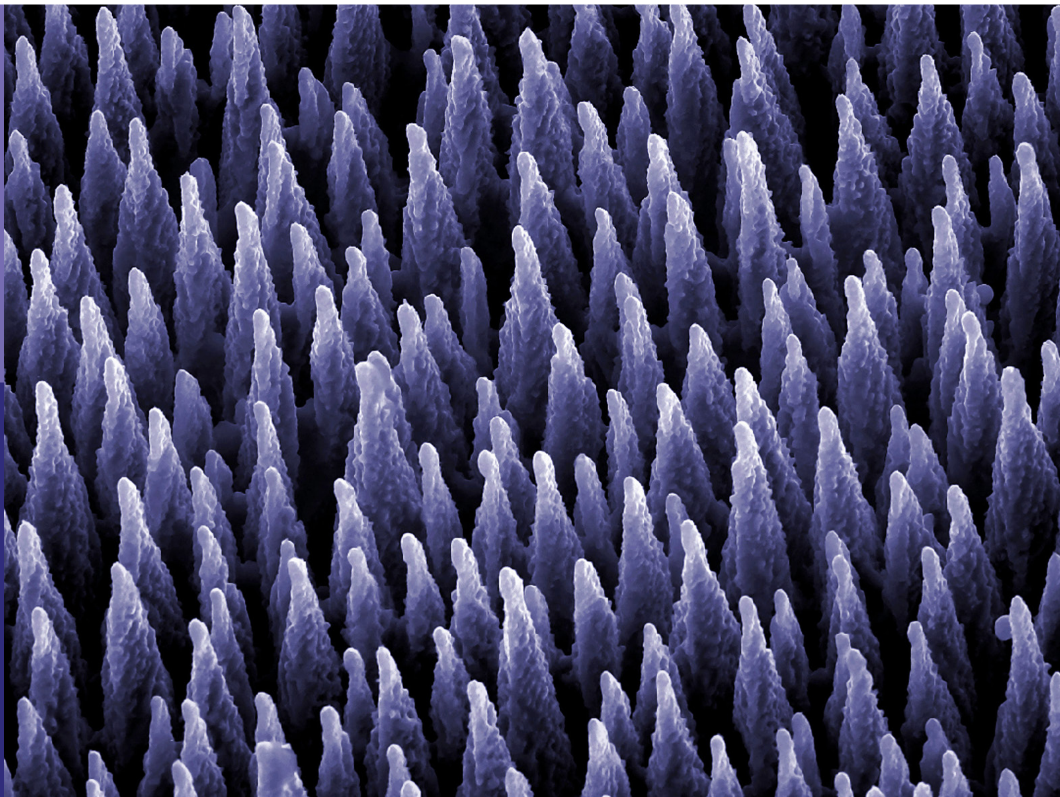

ISSN 1664-8714
ISBN 978-2-83251-197-8
DOI 10.3389/978-2-83251-197-8

About Frontiers

Frontiers is more than just an open access publisher of scholarly articles: it is a pioneering approach to the world of academia, radically improving the way scholarly research is managed. The grand vision of Frontiers is a world where all people have an equal opportunity to seek, share and generate knowledge. Frontiers provides immediate and permanent online open access to all its publications, but this alone is not enough to realize our grand goals.

Frontiers journal series

The Frontiers journal series is a multi-tier and interdisciplinary set of open-access, online journals, promising a paradigm shift from the current review, selection and dissemination processes in academic publishing. All Frontiers journals are driven by researchers for researchers; therefore, they constitute a service to the scholarly community. At the same time, the *Frontiers journal series* operates on a revolutionary invention, the tiered publishing system, initially addressing specific communities of scholars, and gradually climbing up to broader public understanding, thus serving the interests of the lay society, too.

Dedication to quality

Each Frontiers article is a landmark of the highest quality, thanks to genuinely collaborative interactions between authors and review editors, who include some of the world's best academicians. Research must be certified by peers before entering a stream of knowledge that may eventually reach the public - and shape society; therefore, Frontiers only applies the most rigorous and unbiased reviews. Frontiers revolutionizes research publishing by freely delivering the most outstanding research, evaluated with no bias from both the academic and social point of view. By applying the most advanced information technologies, Frontiers is catapulting scholarly publishing into a new generation.

What are Frontiers Research Topics?

Frontiers Research Topics are very popular trademarks of the *Frontiers journals series*: they are collections of at least ten articles, all centered on a particular subject. With their unique mix of varied contributions from Original Research to Review Articles, Frontiers Research Topics unify the most influential researchers, the latest key findings and historical advances in a hot research area.

Find out more on how to host your own Frontiers Research Topic or contribute to one as an author by contacting the Frontiers editorial office: frontiersin.org/about/contact

Advanced use of materials in orthodontics

Topic editors
Domenico Ciavarella — University of Foggia, Italy
Michele Tepedino — University of L'Aquila, Italy
Paolo M. Cattaneo — University of Melbourne, Australia

Citation
Ciavarella, D., Tepedino, M., Cattaneo, P. M., eds. (2023). *Advanced use of materials in orthodontics*. Lausanne: Frontiers Media SA. doi: 10.3389/978-2-83251-197-8

Table of contents

frontiers | Frontiers in Materials

TYPE Editorial
PUBLISHED 09 November 2022
DOI 10.3389/fmats.2022.1062940

Check for updates

OPEN ACCESS

EDITED AND REVIEWED BY
Hafiz M. N. Iqbal,
Monterrey Institute of Technology and Higher Education (ITESM), Mexico

*CORRESPONDENCE
Michele Tepedino,
m.tepedino@hotmail.it

†Those authors contributed equally and share first authorship.

SPECIALTY SECTION
This article was submitted to Biomaterials and Bio-Inspired Materials, a section of the journal Frontiers in Materials

RECEIVED 06 October 2022
ACCEPTED 31 October 2022
PUBLISHED 09 November 2022

CITATION
Cattaneo PM, Tepedino M and Ciavarella D (2022), Editorial: Advanced use of materials in orthodontics. *Front. Mater.* 9:1062940.
doi: 10.3389/fmats.2022.1062940

Editorial: Advanced use of materials in orthodontics

Paolo M. Cattaneo[1†], Michele Tepedino[2*†] and Domenico Ciavarella[3]

[1]Melbourne Dental School, Faculty of Medicine, Dentistry and Health Sciences, The University of Melbourne, Melbourne, VIC, Australia, [2]Department of Biotechnological and Applied Clinical Sciences, University of L'Aquila, L'Aquila, Italy, [3]Department of Clinical and Experimental Medicine, University of Foggia, Foggia, Italy

KEYWORDS

CAD-CAM appliances, 3D printing, patient-specific treatment, aligners, digital workflow, thermoplastic material, biocompatible materials

Editorial on the Research Topic
Advanced use of materials in orthodontics

New technologies and new materials have a profound impact on Dentistry in general and in Orthodontics in particular, like the introduction of CAD/CAM techniques for digital appliance design and manufacturing and new 3D-printed materials. This was main thought behind the decision to have the Research Topic "*Advanced Use of Materials in Orthodontics*".

Among the recent innovations that changed many aspects of our specialty, CAD/CAM technologies are the most important: surely they have changed the way Orthodontics is nowadays provided, and will definitely play a key role in the future development of Orthodontics. In the Research Topic, Ludwig et al., studied the application of 3D-printed resin insertion guides for orthodontic miniscrew placement in an *in-vitro* environment. They found out that not all kinds of resin are suitable for the realization of surgical insertion guides, because the sterilization process can have a large impact on some materials' dimensional properties. On the other hand, an adequate resin can take advantage from the sterilization process, resulting in an improved insertion accuracy.

When thinking about CAD/CAM technologies in Orthodontics, probably clear aligners are the biggest players. This is reflected by the number of articles submitted to this Research Topic dealing on various aspects of clear aligners technology. Macrì et al. provided an interesting narrative review on different clinical and technological aspects of clear aligners. We believe this article is a great starting lecture for everyone willing to know more about aligners clinical performance, but also a stimulus for young researchers looking for project ideas. The use of attachments represented also an alluring topic for different research groups, and this is not surprising since attachments are a crucial medium introduced to improve the transfer of forces and moments from the aligner to the teeth, thus substantially contributing to clear aligners' clinical effectiveness. Gazzani et al. evaluated the type of composite resin used for the application of attachments, concluding that conventional nanocomposites are the materials best suited for the clinical needs.

Moreover, Ferlias et al. analyzed different shapes of attachments in an *in-vitro* setting to evaluate which geometry provided the highest derotational moment on an upper second premolar. This study could have a great clinical impact, since it highlights the importance in choosing the appropriate attachment geometry for various types of dental movement. Moreover, this study highlights that each attachment has some side-effects: for example, a vertical rectangular attachment seems to provide the greatest rotational moment, but at the cost of higher intrusion and inclination movement.

Elshazly et al. presented a highly innovative *in-vitro* study by evaluating the forces produced by 3D-printed aligners made of shape memory polymers, so-called "four dimensional aligners". Indeed, the possibility to directly 3D printing the aligners – avoiding the steps of printing the models, thermoforming and then refining the aligners – the possibility to have materials with a high shape memory, and the possibility to have different thickness of the walls within the same aligner represent an incredible advantage over conventional produced aligners. Studies like the one presented in this Research Topic show the future direction in the clinical use of aligners, which will probably become the "new-normal" in the near future.

Furthermore, biomaterials' innovation means the possibility to have materials that carry a biological effect. Crawford et al., presented the possible application of nanoparticles releasing nitric oxide for tooth movement modulation. Many researchers studied methods to influence tooth movement acting at a biochemical level, with alternating fortune. However, the use of locally injected nanoparticles with the ability to release active ingredients could be a promising technology. Crawford et al. obtained a significant result in Sprague-Dawley rats, inhibiting tooth movement for 1 week to achieve an "orthodontic anchorage effect"; nevertheless, further studies are needed to better understand the biological mechanism and to optimize nitric oxide treatment efficacy and longevity.

Even old materials like elastomers, which are extensively used in daily practice, may reveal new features and clinically useful information: Castroflorio et al. evaluated the forces produced by different types of Class II intermaxillary elastics, concluding that 3/16" 4.5 oz elastics are the most reliable ones in terms of declared force and overtime degradation.

The introduction of new biomaterials and of the digital workflow deeply changed the way Orthodontics is planned and practiced nowadays. The articles in this Research Topic demonstrated that this is the case and that their use will play an increasing role, havingan even larger impact for the future of the profession.

Author contributions

PC and MT drafted the manuscript, PC and DC revised the manuscript.

Conflict of interest

The authors declare that the research was conducted in the absence of any commercial or financial relationships that could be construed as a potential conflict of interest.

Publisher's note

All claims expressed in this article are solely those of the authors and do not necessarily represent those of their affiliated organizations, or those of the publisher, the editors and the reviewers. Any product that may be evaluated in this article, or claim that may be made by its manufacturer, is not guaranteed or endorsed by the publisher.

frontiers in Dental Medicine

ORIGINAL RESEARCH
published: 18 January 2022
doi: 10.3389/fdmed.2021.748985

Analysis of Class II Intermaxillary Elastics Applied Forces: An *in-vitro* Study

Tommaso Castroflorio[1], Ambra Sedran[1], Francesca Spadaro[1], Gabriele Rossini[1], Giovanni Cugliari[2], Vincenzo Quinzi[3] and Andrea Deregibus[1]*

[1] Department of Surgical Sciences, Specialization School of Orthodontics, Dental School, University of Turin, Turin, Italy, [2] Department of Medical Sciences, University of Turin, Turin, Italy, [3] Department of Life, Health and Environmental Sciences Postgraduate School of Orthodontics, University of L'Aquila, L'Aquila, Italy

Objectives: The aims of this study were: (1) to assess the average inter-arch distances characterizing Class II malocclusions, (2) to analyze the applied forces at those distances by different elastics, and (3) to compare measured forces with those declared by manufacturers, both in dry and wet environments.

Materials and Methods: *Settings and sample population*: Class II models of 167 adult subjects (96 women and 71 men, age: 28 ± 3 years) referred to the Orthodontic Department of the University of Turin, Turin, Italy, between January 2018 and January 2020, were collected. Distances between facial axes (FA) points of upper canines and lower first molars (A), upper first premolar and lower first molar (B), upper second premolar and lower first molar (C), upper canine and lower first premolar (D), and upper canine and lower second premolar (E), were measured using 3Shape Ortho® Viewer program. Different elastics' diameters and forces were tested at those distances. The MTS Insight® Electromechanical Testing System was used to measure the tensile forces of elastics. The applied forces were measured in dry (T0) and wet conditions, after 1 (T1), 6 (T2), and 12 h (T3).

Results: Average distances were calculated: A = 24.64 mm (SD 2.10), B = 16.3 mm (SD 1.94), C = 9.78 mm (SD 1.77), D = 9.8 mm (SD 1.88), and E = 15.99 mm (SD 2.06). Significant differences ($p < 0.05$) were highlighted between the measured force and the force declared by manufacturers, and all elastics had a significant force decay ($p < 0.05$).

Conclusion: The results showed that 3/16" 4.5 oz are the most reliable elastics in terms of applied force with respect to the declared one and in terms of force degradation.

Keywords: class II, adult treatment, elastics, anchorage sites, forces

OPEN ACCESS

Edited by:
Domenico Ciavarella, University of Foggia, Italy

Reviewed by:
Uriel Zapata, EAFIT University, Colombia
Roberta Lione, University of Rome Tor Vergata, Italy
Tarek El-Bialy, University of Alberta, Canada

****Correspondence:***
Tommaso Castroflorio
tommaso.castroflorio@gmail.com

Specialty section:
This article was submitted to Dental Materials, a section of the journal Frontiers in Dental Medicine

Received: *28 July 2021*
Accepted: *13 December 2021*
Published: *18 January 2022*

Citation:
Castroflorio T, Sedran A, Spadaro F, Rossini G, Cugliari G, Quinzi V and Deregibus A (2022) Analysis of Class II Intermaxillary Elastics Applied Forces: An in-vitro Study. Front. Dent. Med. 2:748985. doi: 10.3389/fdmed.2021.748985

INTRODUCTION

Inter-arch elastics are considered one of the most important auxiliaries in orthodontics, supporting the correction of molar relationship, spaces closure, and anchorage management.

Despite the widespread use of elastics in the orthodontic community, there are conflicting data on their mechanical properties. Applied forces are dependent on materials, sizes, and application sites. Anecdotally, the declared force is obtained when the elastic is stretched out three times its original diameter, but evidence supporting this suggestion is still lacking (1–3).

The sizes and declared forces of elastics may vary considerably among manufacturing companies. Ormco® (Sybron Dental Specialties, Glendora, CA, USA), produces 24 different elastics, while there are 19 different elastics produced by American Orthodontics® (Sheboyagan, WI, USA) and 21 by 3M Unitek® (Monrovia, CA, USA).

The weakness of elastics is represented by their rapid deterioration and loss of elasticity into the oral environment (4, 5). A review of the existing literature in the field showed that most of the studies examined the applied force of inter-arch elastics, at standard distances, and in a static environment (6, 7). Only few authors used study models to determine the real elongation distance (8, 9). However, average real inter-arch distances at different anchorage sites obtained from Class II malocclusion patients have not been reported in reducing the validity of force measurements in previous studies.

According to the existing literature, the number of adults seeking orthodontic treatment is rising. The American Association of Orthodontists estimates that 27% of all the United States and Canadian orthodontic patients are adults (10). A similar percentage (26.52%) was obtained from a Brazilian study for patients between 20 and 40 years of age (11). A survey from the British Orthodontic Society indicated the increasing number of adult patients treated by United Kingdom orthodontists (12).

The aims of this study were to assess the average inter-arch distances characterizing Class II malocclusions in adults and to analyze the applied forces at those different distances by Class II inter-arch elastics of different manufacturing companies. Furthermore, the study aimed to compare measured forces with those declared by manufacturers of orthodontic elastics used for the correction of malocclusion class II, both in dry and wet environments.

This study should help clinicians to know the effectively applied forces by elastics, based on average inter-arch distances, to improve the clinical efficiency of Class II treatments.

MATERIALS AND METHODS

Sample Group Selection and Inter-arch Distances Measurements

Study models obtained from intraoral scans (iTero Element, Align Tech., San José, CA, USA) of 167 adult orthodontic patients (100 women 67 men, mean age 29 ± 12.5 years, median 27) were used to determine the stretching distances elastics. The selected patients had Class II malocclusion, according to the objective grading system's occlusal relationship evaluation (13). Other inclusion criteria were: (1) presence of complete permanent dentition, (2) absence of periodontal disease, (3) absence of prosthodontic restorations, (4) no history of craniofacial trauma, and (5) no syndromes. The study was approved by the local ethic committee (Comitato Etico Interaziendale A.O.U. Città della Salute e della Scienza di Torino #157/2020).

The distance between the facial axes (FA) (14) points of the upper canine and the lower first molar was measured on both left and right sides at centric occlusion jaw relationship, using the *"3Shape Ortho Viewer"* software (3Shape A/S, Copenhagen, Denmark). In addition, measurements were detected between the FA points of upper first premolars and lower first molars, between upper second premolars and lower first molars, between upper canines and lower first premolars, and between upper canines and lower second premolars, to test all the possible clinical scenarios in which Class II elastics could be used (**Figure 1**).

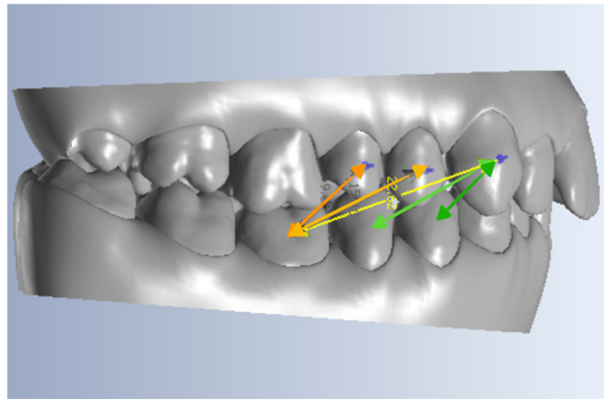

FIGURE 1 | Representation of a subject model, including the five distances considered.

Class II Elastics Mechanical Evaluation

The sample of latex elastics analyzed in the present study was represented by 24 Ormco® (Ormco Corporation, Glendora, CA, USA) elastics, 19 American Orthodontics® (American Orthodontics Corporate, Sheboygan, WI, USA) elastics, and 21 3M Unitek® (3M Oral Care, St. Paul, MN, USA) elastics. In other words, all the inter-arch elastics produced by those three companies were tested. Elastics were provided by the manufacturers in their original sealed plastic bags and were stored accordingly to instructions of manufacturers.

The MTS Insight® Electromechanical Testing System (MTS Systems, Eden Prairie, MN, USA) was used to measure tensile forces of elastics: two hooks were created with 1.5 mm diameter stainless steel wire and located over the support plates of the machine (**Figure 2**). The distance between the two hooks was adjusted to reproduce every considered FA points distance. For each diameter/force combination, five elastics were tested employing a 500 N-load cell to measure the applied force. So, each elastic type was tested five times at every above-mentioned FA points distance and forces data were obtained in Newton.

Artificial saliva was obtained by dissolving chemical compounds in 1 dm^3 of distilled water in the following quantities: NaCl (0.4 g), KCl (0.4 g), NaOH (0.05 g), $CaCl_2 \cdot 2H_20$ (0.22 g), NaH_2PO_4 (0.12 g), and urea (1 g), at a temperature of 37°C. Prior to the tests, all samples were conditioned in 20 ml of artificial saliva.

The applied force of elastic was measured in four different conditions: (1) baseline (T0) when measures were performed on dry elastics (picked up from the sealed bag); (2) after 1-h

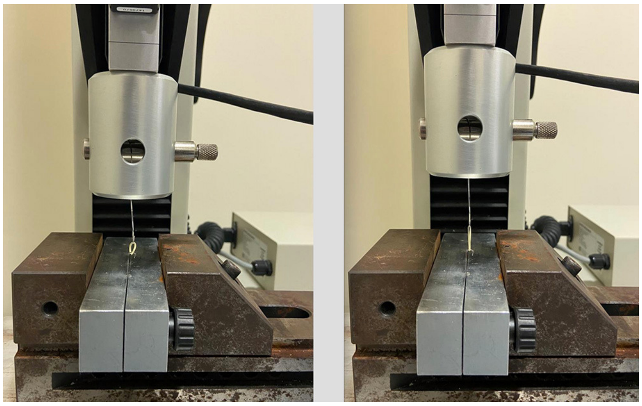

FIGURE 2 | The MTS Insight® Electromechanical Testing System.

artificial saliva (temperature = 37°C, pH = 6.7) immersion (T1), (3) after 6-h artificial saliva immersion (T2), and (4) after 12-h artificial saliva immersion (T3). All tests were performed at room temperature (25°) and dry air condition.

Statistical Analysis

The Shapiro–Wilk test was used to evaluate the normality assumption; homoscedasticity and autocorrelation of the variables were assessed using the Breusch–Pagan and the Durbin–Watson tests. Linear regression analysis was performed to estimate (1) differences between observed and declared force values (declared force values used as reference) and (2) the force variation during artificial saliva immersion follow-up (T0 measurements used as reference).

All the analyses were stratified by elastic type (diameter of the elastic and declared force value). Values are shown as mean ± SD and 95% *CI* is used to test the outcome variability. The level of statistical significance was set at $p < 0.05$.

Statistical analyses were conducted using the R statistical package (version 3.5.3, R Core Team, Foundation for Statistical Computing, Vienna, Austria).

Power Calculation

A priori power analysis was performed to test the difference between groups using T statistic and non-centrality parameter with the aim to detect an effect size ≥ 0.30 and an SD = 1.00 (reference in population). Results showed that a total sample of 167 participants was required to achieve a statistical power of 80% (15).

RESULT

Regarding Class II models, the average distances measured between the considered FA points are as follows (mean ± SD):

- 9.80 mm ± 1.8 between the upper canine and the lower 1st premolar (A).
- 15.99 mm ± 2.0 between the upper canine and the lower 2nd premolar (B).
- 24.64 mm ± 2.1 between the upper canine and the lower 1st molar (C).
- 16.30 mm ± 1.9 between the upper 1st premolar and the lower 1st molar (D).
- 9.78 mm ± 1.7 between the upper 2nd premolar and the lower 1st molar (E).

The force values declared by the manufacturer and the force values measured at T0 (dry elastics), T1, T2, and T3 (respectively, after 1, 6, and 12 h of artificial saliva immersion) for each elastic type and for every FA points distance considered in the study are shown in **Supplementary Table 1**.

Supplementary Table 2 shows the mean deviation (MD) between the manufacturer declared force value and the T0 measured value, for every considered FA points distance. Most of the elastics showed a significant difference between the declared force value and the measured one ($p < 0.05$).

Results of the statistical analysis comparing the force values measured at T0 with those measured after artificial saliva immersion showed significant results. The force released by most of the elastics at T1, T2, and T3 had a significant decay with respect to T0 ($p < 0.05$). **Supplementary Table 3** reports the MD among the force values, for every considered FA points distance.

DISCUSSION

Despite the widespread use of inter-arch elastics in orthodontics, the real force released during their clinical applications is still unknown. In this experimental study, clinical application distances were obtained from 167 Class II patients. During the treatment of this malocclusion, the typical inter-arch elastics configuration is represented by anchoring them on the lower first molar and the upper canine (8, 9).

In the analyzed sample, the average distance between those two force application points was 24.6 mm, which is larger than three times the lumen of either 1/4" (18.7 mm), or 3/16" (14 mm) elastics.

The mean distance from the lower 1st molar to the upper 1st premolar was 16.3 mm, which is slightly lower than the three times the lumen of a 1/4" elastic, and slightly higher than that of a 3/16" elastic. Therefore, it may be advisable to use these reference average measurements to select the proper elastic diameter and force in adult patients requiring the use of Class II elastics. To our knowledge, this is the first study in which similar data are provided.

The existing literature related to Class II treatment with inter-arch elastics highlighted optimal elastics forces ranging from 2 (56.69 g) to 6.5 oz (184.27 g) (3, 7, 16). In the present study, we tested 8 oz (226.79 g) force elastics, considering their spreading in the clinical setting (17).

The mechanical testing was initially performed on dry elastics at room temperature (18). The force values obtained by most of the dry elastics (T0) showed significant differences when compared to the force values declared by the manufacturers. These results are important since the differences were measured for all the possible Class II elastics of the considered

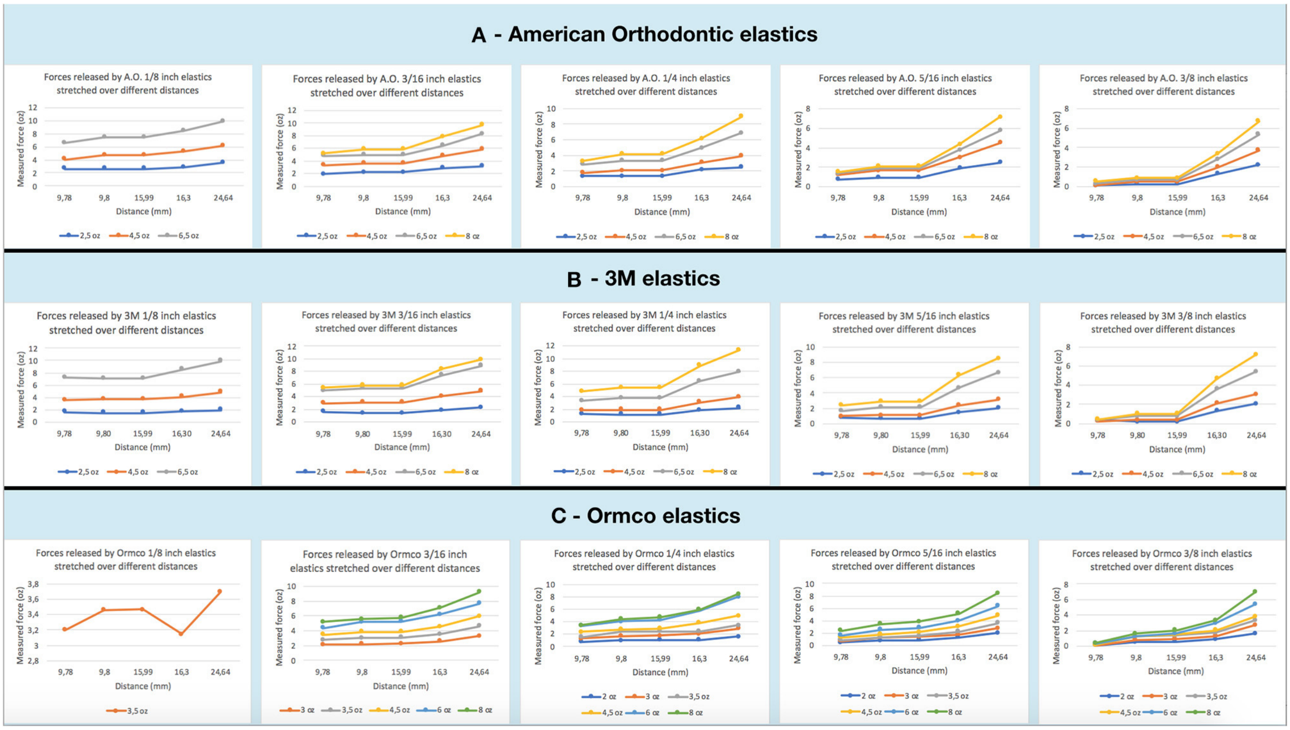

FIGURE 3 | (A) Graphs of forces applied by American Orthodontics elastics stretched over measured distances. **(B)** Graphs of forces applied by 3M elastics stretched over measured distances. **(C)** Graphs of forces applied by Ormco elastics stretched over measured distances.

manufacturers and not only for those suggested by a pool of clinical orthodontists (2, 3, 6, 8, 9, 19).

According to Kersey et al., differences between measured and declared forces, varied from negative to positive values, independent of the application points (18). In the present study, for elastics applied at 24.6 mm distance (upper canine-lower first molar), the observed differences ranged from −169.5 cN (6.1 oz) of the GLORIA 3M® elastics to 36.4 cN (1.3 oz) of the PUMA American Orthodontics® elastics, while for elastics applied at 16.3 mm (upper first premolar-lower first molar) distance, the observed differences ranged from −117.9 cN (4.2 oz) of the GLORIA 3M® elastics to 128.6 cN (4.6 oz) of the PUMA American Orthodontics® elastics. The elastic diameter showing the lowest discrepancy between the tested and declared force is the 3/16”, at a distance of 16.3 mm (upper first premolar-lower first molar). However, for the 3/16” diameter, the lowest discrepancy was observed for the 6.5 oz American Orthodontics elastic band, for the 2 oz 3M® elastic band and for 4.5 oz ORMCO® elastics. So regardless of the brands, it seems advisable to carefully choose the size (inches) of elastics based on the inter-arch distance rather than on the strength needed.

Mansour et al. analyzing 3/16” and 1/4” elastic diameters at a distance of 14.6 mm, revealed no significant differences between tested and declared forces (9). In particular, the ORMCO® 3/16” 4.5 oz showed the minimum discrepancy, as observed in our study.

In contrast, Kanchana et al., comparing elastics with different sizes, extended at a distance of 15 mm, observed that 3/16” Tomy® (Tomy Inc., Tokyo, Japan) 4 oz elastics showed the greatest discrepancy, confirming that manufacturing processes have a huge impact on the applied force (19).

Analyzing the existing literature about inter-arch elastics, many studies focused on testing inter-arch distances >20 mm, to simulate real clinical conditions (5, 9, 16, 18, 19). In previous works, force-extension curves were provided with distances arbitrarily set at 5- or 10-mm intervals from 0 to 60 mm. In this study, we have provided force-extension curves based on real clinical distances, trying to provide more useful information from a clinical perspective. Based on our measurements, the forces exerted by 3/16” ORMCO® elastics (**Figure 3**) showed the best performance. Kanchana et al. obtained the best force-extension curve for 1/4” elastics and their results in terms of measured strength for 3/16” elastics were greater with respect to our observations (18). However, according to Kanchana et al., tests were conducted in 2000 and in the last 20 years, some changes in the structure of the elastomer could explain the performance improvement detected in our study.

As previously reported, salivary pH, oral hygiene conditions, diet, and oral habits influence the elastics behavior in the oral environment (4, 20–22). Force degradation is the greatest disadvantage in using elastics, despite their application is expected to generate constant and optimal force for a specified time period.

In the present study, the wet test was conducted for a period of 12 h simulating a real clinical condition. In agreement with many previous studies, for almost all the elastics, a large force

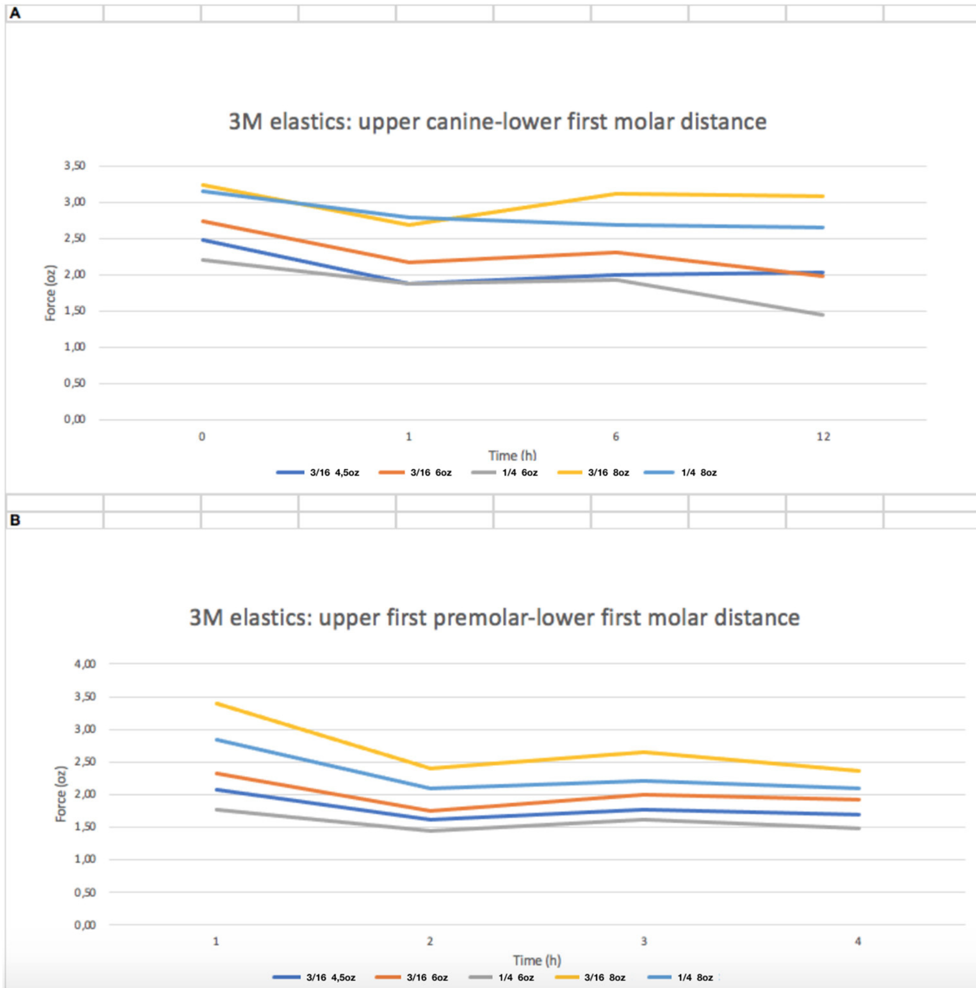

FIGURE 4 | Force decay (oz) over time of 3M 3/16" and 1/4" elastics. **(A)** distance between upper canine and lower first molar; **(B)** distance between upper first premolar and lower first molar.

degradation was observed just after 1 h (3, 5, 23–25) of saliva immersion: at the 24.6 mm distance, the initial force loss of wet elastics was 14.12% for American Orthodontics®, of the 7.92% for 3M®, and of 14.61% for ORMCO®. These data are slightly lower than those reported by Fernandes et al. (15.26–20.72%) that performed the test at a distance of 30 mm (26). Therefore, from a clinical point of view, the percentages reported above could be used to calculate a force level close to the declared one to compensate for the initial force loss of the elastics.

An increase of the force level was observed between the first and the 6th h of artificial saliva immersion, while another force loss was revealed between the 6th and the 12th h.

This trend is particularly evident for 3M® 3/16" and 1/4" elastics, stretched between the upper canine and the lower first molar and between the upper first premolar and lower first molar (**Figure 4**).

A possible cause of this mechanical behavior could be the transitory hardening of the material in saliva immersion (26). Therefore, as suggested by Lopes Nitrini et al. (25), Andreasen and Bishara (27), and Wang et al. (4), elastics do not need to be replaced frequently.

Furthermore, 3/16" elastics showed the lowest discrepancy between the declared and the measured forces and the lowest percentage of force degradation in a wet environment, especially for higher force levels (4.5, 5.5, 6, and 8 oz), confirming the results of previous studies (22). Therefore, in the clinical setting, 3/16" and at least 4.5 oz elastic bands should be used in Class II mechanics.

To our knowledge, only Baty et al. reported a possible clinically significant impact when the difference between the measured and the declared force (ΔF) of elastomeric auxiliaries is >10% (28).

In the present study, almost all the tested elastics had ΔF > 10%.

In conclusion, orthodontists should choose carefully the size and force of the elastics, and this experimental setup provided some suggestions to possibly improve the clinical performances in Class II treatments of adults, using 3/16" and at least 4.5 oz elastics and asking the patients to change them every 6 h.

Limitations of the Study

The most important limitation of this study is the *in vitro* design, which does not make it possible to fully reproduce actual clinical conditions. The simulation of the removal and insertion of elastics after meals or oral hygiene maneuvers was in fact not considered.

However, Liu et al. suggested that after a 1-day interval, the decrease in force values stabilizes, assuming non-significant variation characteristics. For these authors, the stretch variable, due to mouth opening and closing, does not imply a cumulative influence on the material (29).

A comprehensive evaluation of all the possible Class II elastics represented the real aim of the study: however, analyzing only those produced by three of the most important manufacturers in the orthodontic field cannot be considered a shortcut.

As reported by Peck et al., the distance between the maxillary canine and the mandibular first molar would increase during wide opening (16). Therefore, another limitation of the present study is represented by the centric occlusion measurements: however, the present data could be useful to create mathematical models simulating different mandibular positions.

CONCLUSION

- Forces exerted by most of the tested dry and wet elastics were significantly different with respect to the manufacturer's declaration.
- The 3/16" elastics showed the lowest discrepancy between tested and declared forces, at the average distance measured between upper first premolar and lower first molar. Increasing elastic extension, 3/16" diameter elastics showed the lowest increase in force magnitude.
- After 6 h of artificial saliva immersion, force degradation was reduced with respect to the first hour.
- The elastics with high force values showed the lowest percentage of force degradation over time.

DATA AVAILABILITY STATEMENT

The original contributions presented in the study are included in the article/**Supplementary Material**, further inquiries can be directed to the corresponding author/s.

AUTHOR CONTRIBUTIONS

TC and GR contributed to conception and design of the study. FS organized the database. GR performed the statistical analysis. TC and AS wrote the manuscript. GC: substantial contributions to the analysis and interpretation of data for the work, drafting the work for important intellectual content, and agreement to be accountable for all aspects of the work in ensuring that questions related to the accuracy or integrity of any part of the work are appropriately investigated and resolved. All authors contributed to manuscript revision, read, and approved the submitted version.

SUPPLEMENTARY MATERIAL

The Supplementary Material for this article can be found online at: https://www.frontiersin.org/articles/10.3389/fdmed.2021.748985/full#supplementary-material

REFERENCES

1. Proffit WR, Fields HW, Sarver DM. *Contemporary Orthodontics*. Philadelphia: Mosby (2018). p. 276–88.
2. Qodcieh SMA, Al-Khateeb SN, Jaradat ZW, Abu Alhaija ESJ. Force degradation of orthodontic latex elastics: an *in-vivo* study. *Am J Orthod Dentofac Orthop*. (2017) 151:507–12. doi: 10.1016/j.ajodo.2016.08.023
3. Gioka C, Zinelis S, Eliades T, Eliades G. Orthodontic latex elastics: a force relaxation study. *Angle Orthod*. (2006) 76:475–9. doi: 10.1043/0003-3219(2006)076[0475:OLE]2.0.CO;2
4. Wang T, Zhou G, Tan X, Dong Y. Evaluation of force degradation characteristics of orthodontic latex elastics *in vitro* and *in vivo*. *Angle Orthod*. (2007) 77:688–93. doi: 10.2319/022306-76
5. Yang L, Lv C, Yan F, Feng J. Force degradation of orthodontic latex elastics analyzed *in vivo* and *in vitro*. *Am J Orthod Dentofac Orthop*. (2020) 157:313–9. doi: 10.1016/j.ajodo.2019.03.028
6. Kersey ML, Glover KE, Heo G, Raboud D, Major PW. A comparison of dynamic and static testing of latex and nonlatex orthodontic elastics. *Angle Orthod*. (2003) 73:181–6. doi: 10.1043/0003-3219(2003)73<181:ACODAS>2.0.CO;2
7. Bales TR, Chaconas SJ, Caputo AA. Force-extension characteristics of orthodontic elastics. *Am J Orthod*. (1977) 72:296–302. doi: 10.1016/0002-9416(77)90215-9
8. Oesterle LJ, Owens JM, Newman SM, Shellhart WC. Perceived vs measured forces of interarch elastics. *Am J Orthod Dentofac Orthop*. (2012) 141:298–306. doi: 10.1016/j.ajodo.2011.08.027
9. Mansour A. A comparison of orthodontic elastic forces: focus on reduced inventory. *J Orthod Sci*. (2017) 6:136. doi: 10.4103/jos.JOS_58_17
10. Werneck EC, Mattos FS, da Silva MG, do Prado RF, Araújo AM. Evaluation of the increase in orthodontic treatment demand in adults. *Braz Dent Sci*. (2012) 15:47–52. doi: 10.14295/bds.2012.v15i1.738
11. American Association of Orthodontists' "Economics of Orthodontics". *Dental Tribune of America*. (2016). Available online at: https://us.dental-tribune.com/news/adults-are-seeking-orthodontic-treatment-in-record-numbers/ (accessed May 28, 2021).
12. The number of adults seeking orthodontic treatment in the UK continues to rise. *Br Dent*. (2018) 224:847. doi: 10.1038/sj.bdj.2018.455
13. Langlade M. *Optimization of Orthodontic Elastics*. New York: GAC International Ed (2000).
14. O'Neil R, Kau CH. Comparison of dental arch forms created from assessment of teeth, alveolar bone, and the overlying soft tissue. *J Orofac Orthop*. (2021) 82:413–21. doi: 10.1007/s00056-021-00282-6
15. Chow SC, Shao J, Wang H. *Sample Size Calculations in Clinical Research*. 2nd ed. Boca Raton: Chapman and Hall/CRC (2008).
16. Peck CC, Langenbach GEJ, Hannam AG. Dynamic simulation of muscle and articular properties during human wide jaw opening. *Arch Oral Biol*. (2000) 45:963–82. doi: 10.1016/S0003-9969(00)00071-6

17. Kim-Berman H, McNamara JA, Lints JP, McMullen C, Franchi L. Treatment effects of the carrierer motion 2DTM appliance for the correction of class II malocclusion in adolescents. *Angle Orthod.* (2019) 89:839–46. doi: 10.2319/121418-872.1
18. Kersey ML, Glover K, Heo G, Raboud D, Major PW. An *in vitro* comparison of 4 brands of nonlatex orthodontic elastics. *Am J Orthod Dentofac Orthop.* (2003) 123:401–7. doi: 10.1067/mod.2003.22
19. Kanchana P, Godfrey K. Calibration of force extension and force degradation characteristics of orthodontic latex elastics. *Am J Orthod Dentofac Orthop.* (2000) 118:280–7. doi: 10.1067/mod.2000.104493
20. Ash JL, Nikolai RJ. Relaxation of orthodontic elastomeric chains and modules *in vitro* and *in vivo*. *J Dent Res.* (1978) 57:685–90. doi: 10.1177/00220345780570050301
21. De Genova DC, McInnes-Ledoux P, Weinberg R, Shaye R. Force degradation of orthodontic elastomeric chains-A product comparison study. *Am J Orthod.* (1985) 87:377–84. doi: 10.1016/0002-9416(85)90197-6
22. Leão Filho JC, Gallo DB, Santana RM, Guariza-Filho O, Camargo ES, Tanaka OM. Influence of different beverages on the force degradation of intermaxillary elastics: an *in vitro* study. *J Appl Oral Sci.* (2013) 21:145–9. doi: 10.1590/1678-7757201302256
23. Aju Wahju Ardani IG, Susanti B, Djaharu'ddin I. Force degradation trend of latex and nonlatex orthodontic elastics after 48 hours stretching. *Clin Cosmet Investig Dent.* (2018) 10:211–20. doi: 10.2147/CCIDE.S173648
24. De Carvalho Notaroberto DF, Martins E, Martins M, de Andrade Goldner MT, de Moraes Mendes A, Quintão CCA. Force decay evaluation of latex and non-latex orthodontic intraoral elastics: *in vivo* study. *Dental Press J Orthod.* (2018) 23:42–7. doi: 10.1590/2177-6709.23.6.042-047.oar
25. Nitrini ATL, Chagas AS, Freitas KMS, Valarelli FP, Cançado RH, de Oliveira RCG, et al. Comparison of the force released by intermaxillary elastics used for different time periods. *Turk J Orthod.* (2019) 32:190–4. doi: 10.5152/TurkJOrthod.2019.18022
26. Fernandes DJ, Fernandes GMA, Artese F, Elias CN, Mendes AM. Force extension relaxation of medium force orthodontic latex elastics. *Angle Orthod.* (2011) 81:812–9. doi: 10.2319/120810-709.1
27. Andreasen GF, Bishara S. Comparison of elastic chains with elastics involved with intra-arch molar to molar forces. *Angle Orthod.* (1970) 40:151–8. doi: 10.1043/0003-3219(1970)040<0151:COACWE>2.0.CO;2
28. Baty DL, Volz JE, von Fraunhofer JA. Force delivery properties of colored elastomeric modules. *Am J Orthod Dentofac Orthop.* (1994) 106:40–6. doi: 10.1016/S0889-5406(94)70019-2
29. Liu CC, Wataha JC, Craig RG. The effect of repeated stretching on the force decay and compliance of vulcanized cis-polyisoprene ortho-dontic elastics. *Dent Mater.* (1993) 9:37–40. doi: 10.1016/0109-5641(93)90103-W

Conflict of Interest: The authors declare that the research was conducted in the absence of any commercial or financial relationships that could be construed as a potential conflict of interest.

frontiers in Dental Medicine

CORRECTION
published: 15 February 2022
doi: 10.3389/fdmed.2022.859912

Corrigendum: Analysis of Class II Intermaxillary Elastics Applied Forces: An *in-vitro* Study

Tommaso Castroflorio[1], Ambra Sedran[1], Francesca Spadaro[1], Gabriele Rossini[1], Giovanni Cugliari[2], Vincenzo Quinzi[3] and Andrea Deregibus[1]*

[1] *Department of Surgical Sciences, Specialization School of Orthodontics, Dental School, University of Turin, Turin, Italy,* [2] *Department of Medical Sciences, University of Turin, Turin, Italy,* [3] *Department of Life, Health and Environmental Sciences Postgraduate School of Orthodontics, University of L'Aquila, L'Aquila, Italy*

Keywords: class II, adult treatment, elastics, anchorage sites, forces

OPEN ACCESS

Edited and reviewed by:
Domenico Ciavarella,
University of Foggia, Italy
Uriel Zapata,
EAFIT University, Colombia
Roberta Lione,
University of Rome Tor Vergata, Italy
Tarek El-Bialy,
University of Alberta, Canada

****Correspondence:***
Tommaso Castroflorio
tommaso.castroflorio@gmail.com

Specialty section:
This article was submitted to Dental Materials, a section of the journal Frontiers in Dental Medicine

Received: *21 January 2022*
Accepted: *25 January 2022*
Published: *15 February 2022*

Citation:
Castroflorio T, Sedran A, Spadaro F, Rossini G, Cugliari G, Quinzi V and Deregibus A (2022) Corrigendum: Analysis of Class II Intermaxillary Elastics Applied Forces: An in-vitro Study. Front. Dent. Med. 3:859912. doi: 10.3389/fdmed.2022.859912

A Corrigendum on

Corrigendum: Analysis of Class II Intermaxillary Elastics Applied Forces: An *in-vitro* Study
by Castroflorio, T., Sedran, A., Spadaro, F., Rossini, G., Cugliari, G., Quinzi, V., and Deregibus, A. (2022). Front. Dent. Med. 2:748985. doi: 10.3389/fdmed.2021.748985

In the original article, Giovanni Cugliari was not included as an author. The corrected Author Contributions Statement appears below.

All author contribution statement:

- TC: substantial contributions to the design of the work, revising the work critically for important intellectual content, final approval of the version to be published, and agreement to be accountable for all aspects of the work in ensuring that questions related to the accuracy or integrity of any part of the work are appropriately investigated and resolved.
- AS: substantial contributions to the design of the work, drafting the work for important intellectual content, final approval of the version to be published, and agreement to be accountable for all aspects of the work in ensuring that questions related to the accuracy or integrity of any part of the work are appropriately investigated and resolved.
- FS: substantial contributions to the design of the work, drafting the work for important intellectual content, final approval of the version to be published, and agreement to be accountable for all aspects of the work in ensuring that questions related to the accuracy or integrity of any part of the work are appropriately investigated and resolved.
- GR: substantial contributions to the conception of the work, drafting the work and revising it critically for important intellectual content, final approval of the version to be published, and agreement to be accountable for all aspects of the work in ensuring that questions related to the accuracy or integrity of any part of the work are appropriately investigated and resolved.
- VQ: substantial contributions to the design of the work, revising the work critically for important intellectual content, final approval of the version to be published, and agreement to be accountable for all aspects of the work in ensuring that questions related to the accuracy or integrity of any part of the work are appropriately investigated and resolved.

- AD: substantial contributions to the design of the work, revising the work critically for important intellectual content, final approval of the version to be published, and agreement to be accountable for all aspects of the work in ensuring that questions related to the accuracy or integrity of any part of the work are appropriately investigated and resolved.

The authors apologize for this error and state that this does not change the scientific conclusions of the article in any way. The original article has been updated.

AUTHOR CONTRIBUTIONS

TC and GR contributed to conception and design of the study. FS organized the database. GR performed the statistical analysis. TC and AS wrote the manuscript. GC: substantial contributions to the analysis and interpretation of data for the work, drafting the work for important intellectual content, and agreement to be accountable for all aspects of the work in ensuring that questions related to the accuracy or integrity of any part of the work are appropriately investigated and resolved. All authors contributed to manuscript revision, read, and approved the submitted version.

Publisher's Note: All claims expressed in this article are solely those of the authors and do not necessarily represent those of their affiliated organizations, or those of the publisher, the editors and the reviewers. Any product that may be evaluated in this article, or claim that may be made by its manufacturer, is not guaranteed or endorsed by the publisher.

frontiers in Materials

ORIGINAL RESEARCH
published: 28 January 2022
doi: 10.3389/fmats.2021.794536

Potential Application of 4D Technology in Fabrication of Orthodontic Aligners

Tarek M. Elshazly[1*†], *Ludger Keilig*[1,2], *Yasmine Alkabani*[3], *Ahmed Ghoneima*[4], *Moosa Abuzayda*[5], *Wael Talaat*[6,7], *Sameh Talaat*[1,8‡] *and Christoph P. Bourauel*[1‡]

[1]Oral Technology Department, Dental School, University Hospital Bonn, Bonn, Germany, [2]Department of Dental Prosthetics, Propaedeutics and Materials Science, Dental School, University Hospital Bonn, Bonn, Germany, [3]Restorative and Dental Materials Department, National Research Centre, Giza, Egypt, [4]Department of Orthodontics, College of Dental Medicine, MBRU, Dubai, United Arab Emirates, [5]Department of Prosthodontics, College of Dental Medicine, MBRU, Dubai, United Arab Emirates, [6]Department of Oral and Craniofacial Health Sciences, College of Dental Medicine, University of Sharjah, Sharjah, United Arab Emirates, [7]Department of Oral and Maxillofacial Surgery, Faculty of Dentistry, Suez Canal University, Ismailia, Egypt, [8]Department of Orthodontics, Future University in Egypt, Cairo, Egypt

OPEN ACCESS

Edited by:
Paolo M. Cattaneo,
University of Melbourne, Australia

Reviewed by:
Roberto Savignano,
Loma Linda University, United States
Jialiang Wang,
University of Wisconsin-Madison, United States

****Correspondence:***
Tarek M. Elshazly
tarek.m.elshazly@gmail.com
elshazly@uni-bonn.de

†ORCID:
Tarek M. Elshazly
orcid.org/0000-0002-3219-9048

‡These authors have contributed equally to this work and share last authorship

Specialty section:
This article was submitted to Biomaterials, a section of the journal Frontiers in Materials

Received: *13 October 2021*
Accepted: *07 December 2021*
Published: *28 January 2022*

Citation:
Elshazly TM, Keilig L, Alkabani Y, Ghoneima A, Abuzayda M, Talaat W, Talaat S and Bourauel CP (2022) Potential Application of 4D Technology in Fabrication of Orthodontic Aligners. Front. Mater. 8:794536. doi: 10.3389/fmats.2021.794536

Objectives: To investigate and quantify forces generated by three-dimensional-printed aligners made of shape memory polymers (four-dimensional [4D] aligner).

Methods: Clear X v1.1 material was used in this study. On a custom-made typodont model, correction of maxillary central incisor (tooth 21) malposition by 4D aligners with thicknesses of 0.8 and 1.0 mm was measured by superimposition of subsequent scans. Maximum deflection forces generated by foil sheet specimens were measured at different temperatures in three-point bending (3-PB) tests. In a biomechanical system (orthodontic measurement and simulation system [OMSS]), forces generated on movements of tooth 21 by the 4D aligners were measured at different temperatures.

Results: 4D aligners succeeded to achieve a significant tooth movement (2.5 ± 0.5 mm) on the typodont, with insignificant difference between different thicknesses. In the 3-PB test, the maximum deflection forces measured at 20, 30, 37, 45, and 55°C, were 3.8 ± 1.1, 2.5 ± 0.9, 1.7 ± 0.6, 1.0 ± 0.4, and 0.5 ± 0.4 N, respectively. Forces delivered on palatal displacement of tooth 21 at 37, 45, and 55°C by 0.8-mm aligners were 0.3 ± 0.1, 0.2 ± 0.1, and 0.7 ± 0.2 N, respectively, whereas those by 1.0-mm aligners were 0.3 ± 0.1, 0.3 ± 0.1, and 0.6 ± 0.2 N, respectively. A good concordance with movement on the typodont model was shown in OMSS.

Conclusion: An initial study of 4D-printed aligner shows its ability to move a tooth by biocompatible orthodontic forces, after a suitable thermal stimulus within the oral temperature range.

Keywords: clear aligners, shape memory polymers, biomaterial, biomechanics, tooth movement, 4D printing, orthodontics

HIGHLIGHTS

- Rate-limiting staging of conventional aligners consumes time and materials.
- Orthodontic aligners can be made of different polymers.
- Four-dimensional (4D) technology is a three-dimensional printing of polymeric shape memory material.
- Introduction of 4D technology in the field of orthodontic aligners is highly innovative.
- 4D aligners can move teeth by biocompatible forces.

INTRODUCTION

Aesthetics is one of the major demands of patients who seek dental treatment. Major problems facing patients of orthodontic treatment are the bad appearance of metallic orthodontic braces, keeping good oral hygiene, and the long treatment time (Elshazly et al., 2021). In the last decade, treatment by orthodontic aligners has shown growing interest (Ercoli et al., 2014; Ojima and Kau, 2017). The aligners gain great superiority in aesthetic, comfort, and oral hygiene, over fixed braces, even the ceramic and lingual ones, owing to the fact that they are clear and almost invisible, as well as the ability to remove them during eating, brushing, and flossing (Mehta and Mehta, 2014). Additionally, with clear aligners, treatment time and chair time are reduced in nonextraction cases, sometimes by more than the half, compared with fixed braces (Tamer et al., 2019).

Conventional aligners are made from different types of polymers (Ercoli et al., 2014), such as polyvinyl material, polyvinyl chloride, polyethylene terephthalate glycol (Thukral and Gupta, 2015), polypropylene, polyester, and polyurethane (Momtaz, 2016). The functioning principle of such appliances is based on limited movement of each tooth through a programmed deviation between the real tooth position and a setup position. The programmed geometry of the aligner's stent then defines the new tooth position and the amount of movement to be performed (Boyd and Waskalic, 2001). In most of the popular aligner systems in the market, each aligner is designed to move a tooth within the restriction of 0.2 to 0.3 mm for translations and 1° to 3° for rotations, for that it is worn approximately 14 days, and then it should be changed with its successor (Kwon et al., 2008; Thukral and Gupta, 2015; Elkholy et al., 2016). This stepwise staging of conventional aligners leads to time and material consumption and consequently high cost of the treatment (Martorelli et al., 2013; Ercoli et al., 2014; Elshazly et al., 2021).

With the introduction of the technology of digital scanning, three-dimensional (3D) printing, and CAD-CAM, the orthodontic aligner became more precise. Nonetheless, investigators are continuously working on improving the efficiency of the treatment. Many optimizations, innovations, and advances are aiming to facilitate the process and to reduce the time and the cost (Phan and Ling, 2007; Morton et al., 2017; Elshazly et al., 2021). Several researchers are focusing on two main drawbacks: the shortcomings of conventional materials and the biological consideration of tooth movement. Numerous methods have been introduced to biologically accelerate tooth movement (Ojima and Kau, 2017). On the other side, introduction of new aligner material also draws attention (Silverman and Cohen, 1969; Choi and Kim, 2005; Lai and Rule, 2020; Elshazly et al., 2021).

Shape memory polymers (SMPs) are one of the novel materials to be recently introduced into the field of dentistry, particularly for orthodontic applications (Mahmood et al., 2019; Elshazly et al., 2021). They provide great potential for applications in medical materials (Lendlein and Langer, 2002; Zhang et al., 2009; Meng and Li, 2013). In a study by Jung et al. (Jung and Cho, 2010) and another by Nakasima et al. (1991), SMPs were used in fabrication of orthodontic wires. Choi and Kim (2005) registered a patent about a tray-type appliance made of SMPs used for teeth alignment. Also, Lai and Rule (2020) registered another patent about an orthodontic appliance having a continuous shape memory recovery. Through this shape memory property, it can store a large number of geometries throughout the orthodontic treatment. Recently, Elshazly et al. (2021) reported a new orthodontic aligner system based on thermoresponsive shape memory polyurethane-based thermoplastic material, showing the ability of one aligner to recover its shape through three steps of material treatment and consequently conduct stepwise tooth movement in a way that one aligner may be able to replace three subsequent conventional aligners. Despite the mentioned reports, yet, there is lack of data in literature about the application of SMPs in the field of orthodontic aligners.

The technology of four-dimensional printing (4D printing) is based on the 3D printing of shape memory materials. Clearly, 4D-printed parts have the ability to change shape with time (the fourth dimension), upon given environment conditions (Pei et al., 2020). With the continuous development of SMPs, new 4D printing applications within the product design industry are expected to grow (Nam and Pei, 2020). We proposed in our scientific project to introduce the 4D technology in the fabrication of orthodontic aligners.

In this study, on a custom-made typodont model, correction of malposition of tooth 21 by 4D-printed aligners with thicknesses of 0.8 and 1.0 mm was measured by superimposition of obtained and initial scans. Also, forces generated on 2-mm vertical three-point bending (3-PB) tests were measured at different temperatures. Additionally, forces and movements delivered by the 4D aligners were quantified using an orthodontic measurement and simulation system (OMSS).

MATERIALS AND METHODS

Typodont

A custom-made typodont model was fabricated from resin (Technovit 4004; Kulzer, Wehrheim, Germany) and acrylic teeth (Frasaco, Tetnang, Germany). The upper left central incisor (tooth 21) was separated and kept movable by being embedded in pink wax placed in the model, while the other teeth were fixed by the resin (**Figure 1**). The fully aligned model was scanned (scan 0) using a 3D lab scanner (D2000; 3Shape,

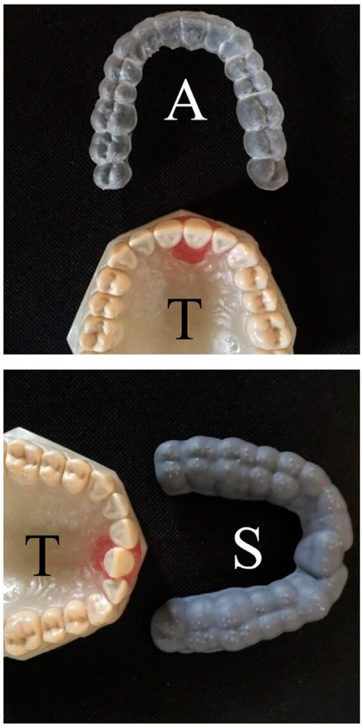

FIGURE 1 | A custom-made typodont (T), a 4D-printed aligner (A), and a gray splint (S).

Copenhagen, Denmark). The model was segmented using an Ortho System software (Ortho Analyzer; 3Shape). Using the appliance designer software (Appliance Designer; 3Shape), two groups of aligners were designed with thicknesses of 0.8 and 1.0 mm and an offset of 0.2 mm, on the fully aligned model. The aligner geometries were then sent for 3D printing, six aligners per each group (n = 6). ClearX v.1.1 3D-printed material (Kline-Europe, Dusseldorf, Germany) was used, reported by the suppliers to have shape memory properties. Afterward, tooth 21 was moved palatally in the software model with a total malalignment of 3 mm. The malaligned model was exported as an STL file and was 3D printed using a 3D-printable resin (Dentona Optiprint model; Dentona AG, Dortmund, Germany). A 3D printer (Asiga Max; SCHEU-DENTAL GmbH, Iserlohn, Germany) was used for the previous printing steps, with 62-µm high-definition print precision.

Three gray splints of thickness 3.0 mm (**Figure 1**) were designed over the malaligned model and were 3D printed (Form 3BL Basic Package; Formlabs, Somerville, MA, USA) using a resin material (Grey Resin 1 L; Formlabs). The first splint was produced over the malaligned model. It was used as an “index” to reposition the typodont (tooth 21) to the exact same malaligned position during testing. The second and third splints were produced over the 3D aligners, one for each different thickness. They were used for reforming and adaptation of the softened aligners to the malaligned models before testing.

The adaptation process was done by immersing the aligner in a hot water bath of 80°C for 30 s to ensure exceeding the glass transition temperature (Tg) of the material, reported by the supplier to be at 30°C, and to ensure enough softening of the material. The aligner was then adapted on the malaligned model by the aid of the corresponding adaptor splint. They were then let together to cool down in a cold water bath of 5°C so that the aligner can maintain its new malaligned shape (malaligned aligner).

The wax around tooth 21 of the typodont model was softened, and the index splint was used to reposition tooth 21 in the typodont model at 3-mm malposition. The typodont was then placed in a 5°C water bath for 10 min to ensure that the wax was no longer soft and could withstand aligner placement without getting distorted. The malaligned typodont model was then scanned (scan 1). Afterward, the malaligned aligner was placed on the malaligned typodont, and both were immersed together for 5 min in a hot water bath of 55°C, which is the activation temperature recommended by the supplier. This initiated the shape memory recovery of the aligner and softened the wax around tooth 21 in the typodont to allow the correction movement of the tooth to happen by the memory recovery of the SMP aligner. Subsequently, they were taken out from the hot water bath and put back in a cold water bath (5°C), so that the wax could get hard at the new position before removing the aligner to avoid distortion. The typodont model was then scanned again (scan 2). Scan 2 was superimposed with scan 1, and the correction was measured by the Ortho Analyzer software (**Figure 2**). The test was repeated six times for each group (0.8 and 1.0 mm), each time new wax and new aligner were used. Using this test, the aligner shape recovery was recorded visually. A schematic diagram illustrating the main steps of ClearX 4D aligner method was added (**Figure 3**).

3-PB Test

The experimental investigation of the force systems generated was performed by a custom-made biomechanical system (OMSS; Drescher et al., 1991) at the University Hospital Bonn in Germany. Six 3D-printed specimens of the 4D ClearX v.1.1 material were produced in dimensions ($50 \times 10 \times 1.0\ mm^3$) and mounted in the biomechanical testing machine (OMSS, **Figure 4**) to perform a 2-mm vertical 3-PB tests under standardized conditions at a rate of 5 mm per minute and at different temperatures of 20°C, 30°C, 35°C, 37°C, 40°C, and 50°C. The force/deflection curves were recorded, and the maximum

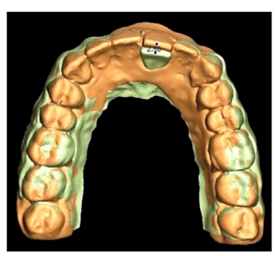

FIGURE 2 | Superimposition of the typodont scans before and after testing of the 4D aligner, scan 1 (before, green) and scan 2 (after, orange).

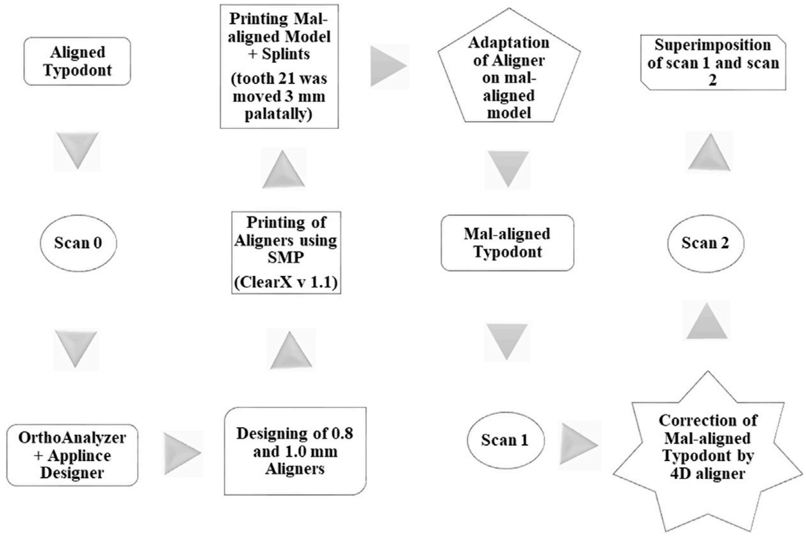

FIGURE 3 | A schematic diagram illustrating the main steps of the ClearX 4D aligner method.

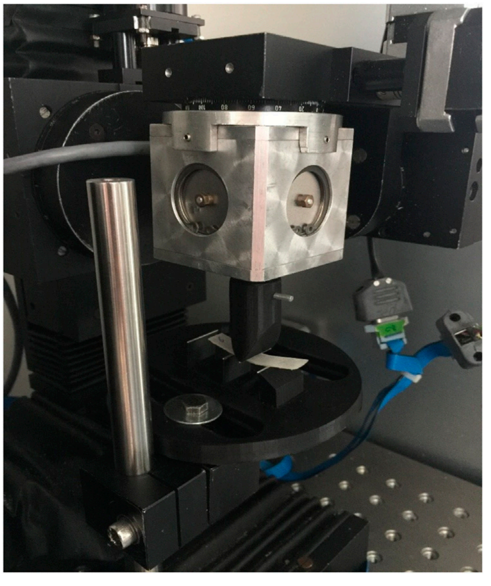

FIGURE 4 | Three-point bending test of a 4D-printed specimen using the orthodontic measurement and simulation system (OMSS) at different temperatures.

generated force was determined. Each cycle was repeated two times with the same specimen.

Experimental Simulation of Tooth Movement

The typodont without the movable tooth 21 was duplicated using Technovit 4004, and tooth 21 was separated. The resin replica was mounted into OMSS (**Figure 5**). In several articles (Drescher et al., 1991; Simon et al., 2014a), more details of the technical specifications and the software running the experiments of OMSS can be found. The OMSS device consists of sensors that can be used for measuring force and moment vectors in three

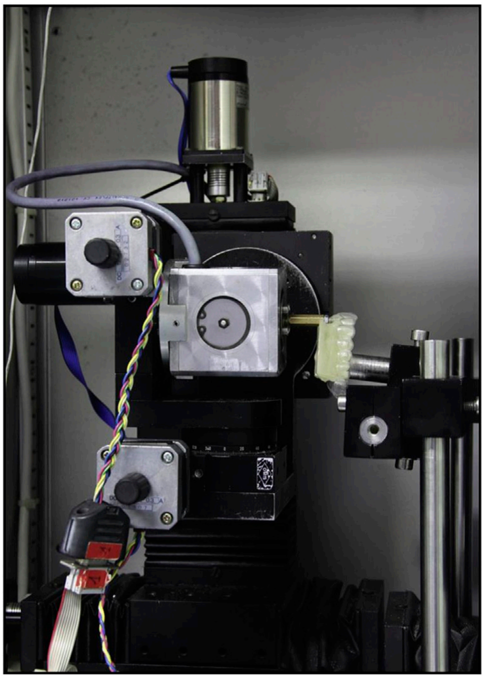

FIGURE 5 | Orthodontic measurement and simulation system (OMSS): a resin replica with a 4D-printed aligner is mounted in the system. Tooth 21 to be analyzed was connected to a computer-controlled 3D sensor. The measured moments and forces are registered, and the motor-driven positioning table simulates the analyzed tooth movement.

TABLE 1 | Mean ± standard deviation (SD) of translation and forces conducted on upper central incisor (tooth 21) by 4D-printed aligners of two thicknesses

	Thickness (mm)	Temperature			*p* value
		37°C	45°C	55°C	
Translation (mean ± SD)	0.8	1.0 ± 0.4^{Ba}	2.4 ± 0.6^{Aa}	2.1 ± 0.5^{Ab}	<0.001*
	1.0	1.1 ± 0.4^{Ba}	1.6 ± 0.2^{Bb}	2.8 ± 0.1^{Aa}	<0.001*
		0.701ns	0.004	0.006	
Force (mean ± SD)	0.8	0.3 ± 0.1^{Ba}	0.2 ± 0.1^{Ba}	0.7 ± 0.2^{Aa}	<0.001*
	1.0	0.3 ± 0.1^{Ba}	0.3 ± 0.1^{Ba}	0.6 ± 0.2^{Aa}	<0.001*
		0.701ns	0.701ns	0.701ns	

Measurement was done at different temperatures in a custom-made biomechanical system (OMSS). Different uppercase and lowercase superscript letters indicate a statistically significant difference within the same horizontal row and vertical columns, respectively.
**Significant (p ≤ 0.05). ns, nonsignificant (p > 0.05).*

dimensions (x, y, and z). Sensors are mounted on a 6-axes motor-driven positioning table, which is able to perform full 3D movements. To describe tooth movements in all three spatial dimensions, a coordinate system was set up. The positive x axis ($+X$) describes extrusive and the negative x axis ($-X$) describes intrusive movements and forces, parallel to the long axis of the tooth. Horizontal forces and movements are described on the y axis and the z axis, where $+Z$ represented the facial movement and force, $-Z$ represented lingual movement and force, $+Y$ represented distal movement and force, and $-Y$ represented mesial movement and force.

The separated tooth 21 was connected to a sensor. Adjustments were made with the index splint so that tooth 21 was passively set in its 3-mm lingual malposition in respect to the other teeth of the resin replica. The whole apparatus was enclosed in a temperature-controlled chamber in order to run the test at different temperatures. Six new aligners for each group of two thicknesses (0.8 and 1.0 mm) were 3D printed on the aligned model. Each aligner was reformed on the malaligned position as described previously at the typodont experiment. The malaligned aligner was mounted on the resin replica, in a way that almost no active forces (zero forces) were transferred to the tooth, whereas the thermal chamber of OMSS is at room temperature (20°C, below Tg). The temperature of the chamber was increased to 37°C, 45°C, and 55°C. By means of continuous measurements of the force systems and simulation of the resulting movement of tooth 21, the force progression generated by an aligner was measured, and the experimentally resulting tooth movement was calculated. For tooth movements in the three dimensions, the measurements were terminated when forces decayed below 0.02 N.

Statistical Analysis

Independent t test was used to compare movement of the typodont tooth with different thicknesses of the aligner. Two-way analysis of variance followed by Bonferroni correction was used to study the effect of different tested variables (temperature and thickness of the aligner) and their interaction on force and translation. The significance level was set at $p \le 0.05$ within all tests. Statistical analysis was performed using IBM SPSS Statistics version 25 for Windows (IBM Company, Endicott, NY, USA).

TABLE 2 | Mean ± standard deviation (SD) of translation of upper central incisor (tooth 21) by 4D-printed aligners of two thicknesses

Translation (mean ± SD)			*p* value (ns)
Thickness	Typodont	OMSS	
0.8 mm	2.2 ± 0.5^{Aa}	2.1 ± 0.5^{Ab}	0.617*
1.0 mm	2.6 ± 0.5^{Aa}	2.8 ± 0.1^{Aa}	0.257*
p value	0.152ns	0.006*	

Measurement was done at temperature of 55°C on a typodont model and in a custom-made biomechanical system (OMSS). Different uppercase and lowercase superscript letters indicate a statistically significant difference within the same horizontal row and vertical columns, respectively.
**Significant (p ≤ 0.05). ns, nonsignificant (p > 0.05).*

RESULTS

On the typodont, 4D-printed aligners succeeded to achieve a significant tooth movement (2.5 ± 0.5 mm), with insignificant difference between the different thicknesses (**Figure 2** and **Table 2**). In 3-PB test, the maximum forces measured at 20°C, 30°C, 37°C, 45°C, and 55°C were 3.8 ± 1.1, 2.5 ± 0.9, 1.7 ± 0.6, 1.0 ± 0.4, and 0.5 ± 0.4 N, respectively (**Figure 6**).

In OMSS simulations, the forces delivered on palatal displacement of tooth 21 at 37°C, 45°C, and 55°C by 0.8-mm aligners were 0.3 ± 0.1, 0.2 ± 0.1, and 0.7 ± 0.2 N, respectively, whereas those by 1.0-mm aligners were 0.3 ± 0.1, 0.3 ± 0.1, and 0.6 ± 0.2 N, respectively (**Figure 7** and **Table 1**). Varying degrees of temperature had a significant effect on the force, whereas the thickness of the aligner along with its interaction with temperature had no significant effect. Pairwise comparison showed that aligner subjected to 55°C conducted a significantly higher force than those subjected to 37°C and 45°C. A good concordance with movement of tooth 21 in the typodont experiment could be shown in OMSS with insignificant difference between them (**Table 2**). At 55°C, there was a higher significant translation by 1.0-mm aligner than the 0.8-mm one (**Tables 1** and **2**).

DISCUSSION

Although orthodontic aligners have been studied in several aspects and great progress was done in orthodontic treatment by aligners (Bowman, 2017), practitioners still report some

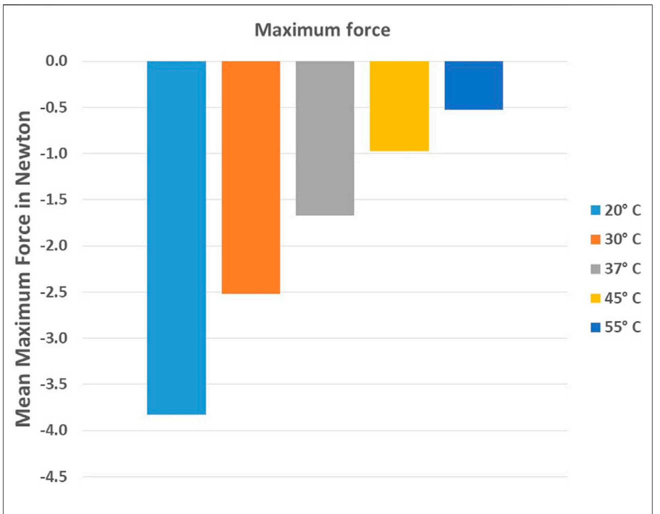

FIGURE 6 | Bar chart showing the mean maximum force generated on a 2-mm vertical three-point bending testing of 3D-printed specimens of ClearX v.1.1 shape memory material at different temperatures.

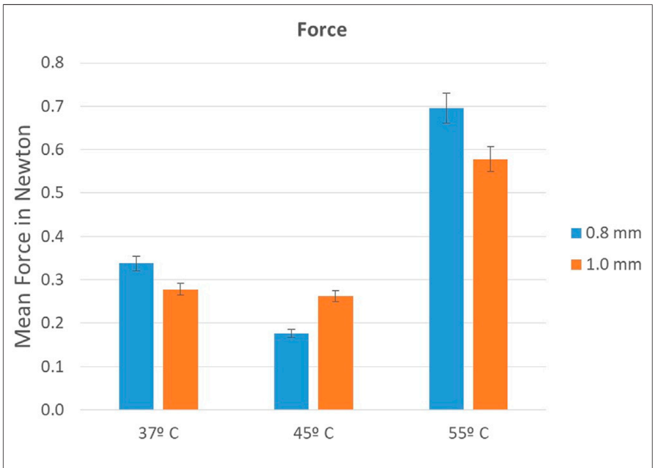

FIGURE 7 | Bar chart showing forces generated by 4D-printed aligners of two different thicknesses; measurement was done at different temperatures in a custom-made biomechanical system (OMSS).

drawbacks to aligner use. On the top of these drawbacks are the limited movement achieved by each single aligner, which leads to use of changing regime through a large series of aligners per treatment (Simon et al., 2014b; Elshazly et al., 2021). Therefore, we believe that if a method could be applied to decrease the number of the aligners per treatment, together with a method to accelerate the biological movement of the teeth, that would be a quantum leap in the field of orthodontics.

The introduction of new aligner materials draws the attention of many researchers. Some of them introduced smart materials, particularly SMPs (Silverman and Cohen, 1969; Choi and Kim, 2005; Lai and Rule, 2020; Elshazly et al., 2021). The idea of clear aligners made of SMPs is aiming to reduce the cost and time of the treatment by using a dynamic aligner that can change its shape intentionally over treatment time, and consequently one shape memory aligner could substitute a series of conventional aligners and overcome the stepwise system. Furthermore, it helps to decrease the plastic consumption by decreasing the number of plastic aligners per treatment plan and thus raise concerns about the ethical responsibility toward the environment (Elshazly et al., 2021). Despite many tryouts mentioned before (Choi and Kim, 2005; Jung and Cho, 2010; Lai and Rule, 2020; Elshazly et al., 2021), still there is a great lack of data in the literature about clear aligners made from SMPs. So far, it is difficult, biomechanical-wise and biocompatibility-wise, to favor an appropriate material.

Thermoresponsive SMPs are a subcategory of smart polymers, which have a novel capacity, to recover their original shape after being deformed, upon specific thermal initiation (Zhang et al., 2009; Meng and Li, 2013). At the molecular level, polymer network-based SMPs consist of at least two different segments, hard and soft, with two different glass transition temperatures (Tg) (Lendlein and Langer, 2002). Shape memory mechanism is attributed to the cooperation of the hard and the soft segments. Phase separation is essential in this mechanism. The separation occurs only above a threshold temperature (transition temperature); prior to it, no phase separation occurs. Soft segments act as a switch (matrix phase) responsible for shape changing, and hard segments act as cross-links responsible for preserving the original shape (Lendlein and Kelch, 2002; Behl and Lendlein, 2007; Zhang et al., 2009). Many of SMPs have a Tg near the body temperature; thus, the body temperature could act as an initiator for shape memory change (Gorna and Gogolewski, 2003). Moreover, many SMPs have the advantage of possessing several inherent properties, such as transparency, low density, and reduced cost (Jung and Cho, 2010). In addition, the shape recovery of some SMPs could last up to approximately 3 months, which might be suitable for orthodontic applications (Small et al., 2010). These advantages may qualify them to be introduced in the fabrication of orthodontic appliances for treatment of initial alignment and leveling of aesthetically concerned patients (Nakasima et al., 1991), as well as the correction of malaligned and severely rotated teeth (Mahmood et al., 2019).

On planning of an orthodontic treatment with an aligner system, it is important to make a biomechanical analysis of the used material and the appliance and know the exact distribution of the forces and moments. The flexure modulus is a mechanical property that relates stress to strain in flexural deformation, and it is an indicator of the material's tendency to resist bending. The developed force is directly proportional to the flexure modulus and to the third order of the thickness in bending direction (Zweben et al., 1979). In orthodontic appliances such as aligners, it is an indicator of the effectiveness for tooth movement (Ryu et al., 2018). The 3-PB test is a method used to determine the flexure modulus and the maximum force delivered upon deflection (Kwon et al., 2008; Min et al., 2010). Additionally, to know the exact force systems of the aligner in all three planes of space, an OMSS was used (Drescher et al., 1991; Bourauel et al., 1992). Moreover, based on the force system, the control program of OMSS calculated the developed tooth movement by using a mathematical model, taking into consideration the center of resistance of the measured tooth (Pedersen et al., 1990).

Optimal force delivery is a must for an ideal orthodontic treatment, in order to achieve a maximum rate of tooth movement without causing irreversible damage to the biological tissues (Kwon et al., 2008). A light continuous force is required for ideal tooth movement. In case of excessive force to a target tooth, indirect bone resorption can occur; accordingly, the speed of tooth movement will be slower, or root resorption may occur. On the contrary, if sufficient force is not delivered to a target tooth, tooth movement will not be obtained (Proffit et al., 2000). Consequently, optimal forces are important for ideal tooth movement. For instance, the optimal forces for tipping movement of a single tooth were reported to be from 0.50 to 0.75 N, for rotation control are 1.00–1.50 N, for torque control are 0.75–1.25 N, and for bodily movement are 0.75–1.25 N (Proffit et al., 2000; Kwon et al., 2008). In conventional aligner systems, the force delivery to a target tooth is generated by the tendency of the plastic material through its resiliency to return to its resting state instead of being deformed 0.25–0.33 mm in some systems (Simon et al., 2014a) or 0.50–1.00 mm in other systems (Sheridan et al., 1993). However, in the 4D-printed aligner system, the aligners are made of SMPs, and the force delivery is obtained from the shape recovery of the material upon appropriate stimulations (Elshazly et al., 2021). Additionally, the 3D printing of the material gives advantage of avoiding the significant decrease of mechanical properties after deep drawing of thermoformed material (Ryu et al., 2018).

The technology of 4D printing is based on the 3D printing of SMPs. In our study, a 3D-printable material (ClearX v.1.1), reported by the supplier to possess thermoresponsive shape memory properties, was used in fabrication of orthodontic clear aligners (4D aligner). A typodont model was used in the study as an initial proof of the movement of the tooth, similar to many other reports (Ishida et al., 2020; Elshazly et al., 2021; Ho et al., 2021). A simple orthodontic case was used in the study, where only a bodily movement of one tooth (maxillary upper incisor, tooth 21) was tested, whereas the other teeth remained fixed in the resin and were used to provide retention to the whole aligner. The maximum forces generated on 2-mm deflection at different temperatures were measured. Furthermore, the forces generated from shape recovery, which should be responsible for the tooth movement, were measured by a custom-made biomechanical system (OMSS).

The results show success of the shape memory aligner to achieve a significant movement of tooth 21 on the typodont, and a congruent movement was also measured in OMSS. The targeted alignment movement (3.00 mm) was not reached; only 2.06–2.82 mm was achieved, which could be referred to the resistance of the wax (in typodont test) and the rigidity of the sensor (in OMSS), in front of the low forces generated by the shape recovery. Nevertheless, the results are satisfactory, and the achieved movement by one shape memory aligner equals nearly the movement that could be achieved by 10 conventional aligners.

In the current study, the force delivery upon deflection of the aligner by bodily movement of tooth 21 for 2 mm needed to be simulated; therefore, the span length in the 3-PB test (distance between the two supports) was set at 24 mm, which was equal to the sum of the average widths of the two maxillary central incisors and one lateral incisor, and the specimen was deflected vertically at its center to a maximum of 2 mm (Kwon et al., 2008). The results of our study (**Figure 7**) show that the range of maximum force delivered on a 2-mm deflection at temperatures from 37°C to 55°C (the activation temperature range of the material) with sheet thickness of 1 mm ranged from 1.20 to 0.50 N. This is located within the acceptable range of orthodontic forces, and it is in the same range of forces generated by conventional aligners upon deflections of 0.20–0.50 mm (Proffit et al., 2000; Kwon et al., 2008). The results show also that the maximum forces are decreasing with increasing the temperature, which can be explained by the fact that the heat in such thermoplastic material leads to a type of softening through debonding of the secondary bonds of the cross-links of the material and therefore weakens the material.

The generated forces at different temperatures (37°C, 45°C, 55°C) measured by OMSS (0.30–0.70 N) are also in the range of acceptable physiological orthodontic forces reported by many studies (Hahn et al., 2010; Simon et al., 2014a; Elkholy et al., 2016; Elkholy et al., 2017; Iliadi et al., 2019). Moreover, these findings are supported by a study by Nakasima et al. (1991), in which it was reported that SMPs are able, at properly controlled oral conditions, to produce light long-lasting forces. They used a stretched orthodontic wire of polynorbornene, a type of SMP, and showed that it could reverse gradually to its original shape upon heating at a temperature of 50°C and generate forces in the physiological range, which could be used to move a human tooth.

In our study, the forces generated at 50°C were higher than the forces generated at 37°C, yet in the accepted range. Interestingly, there was a reduction of forces at 45°C in comparison to the forces at 37°C and 55°C. Explanation of such situation, especially in a viscoelastic material such as the tested material, may need further investigation of the material, such as dynamic thermomechanical analysis and differential scanning calorimetry, in order to get a more clear picture of the phase transition at different temperatures.

Contradicting with previous studies (Kwon et al., 2008; Hahn et al., 2009; Min et al., 2010; Ryu et al., 2018), the current study reported that using thicker aligners has no significant effect on the generated force, except at 55°C in the OMSS. That could be due to inaccuracy of the 3D printing in a way that the aligner thickness is not homogenous, thicker in parts and thinner in others. However, the findings are, from other prospective, generally in agreement with Nam and Pei (2020), who revealed that the shape memory effect of 4D-printed parts is mostly influenced by the recovery temperature and the deformation temperature.

This study still has many limitations. We measured forces for an isolated experimental movement of a single tooth, which is a simplified model that cannot reflect the more complex clinical cases, in which several teeth are included in the treatment plan. Also, we did not fully consider the intraoral conditions such as salivation and humidity, especially that some polymers are sensitive to moisture due to presence of hydrogen bonding between the polymeric chains (Yen et al., 1991; McKiernan et al., 2002). Additionally, the OMSS enables both measurements of the forces of the initial situation and the dynamic force progression during tooth movement; however, in the setup of the present study, sensor and tooth were connected rigidly, with the limitation of simulation of some clinical parameters such as periodontal ligament (PDL), mastication, as well as soft-tissue reactions (Bourauel et al., 1992). Besides, OMSS is based on the hypothesis that there is a linear relationship between the speed of tooth movement and the amount of applied force, which could not really simulate the biomechanical behavior of PDL. Moreover, an ideal center of resistance was used for each tooth (Simon et al., 2014a).

Further studies on the mechanical and physical properties of the used SMP materials should be performed. More clinically oriented simulated models for the force delivery by SMP materials should be developed. Moreover, it is still a challenge to introduce a clinically applicable technique to use the shape memory aligners.

CONCLUSION

Initial investigation of a 3D-printed aligner made of SMPs (4D aligner) shows its capability of moving teeth by biocompatible orthodontic forces after a suitable thermal stimulus within the oral temperature range.

DATA AVAILABILITY STATEMENT

The raw data supporting the conclusion of this article will be made available by the authors, without undue reservation.

AUTHOR CONTRIBUTIONS

Conceptualization: TE. Data curation, analysis, investigation, and methodology: TE and YA. Resources: TE, CB, MA, and AG. Software: TE, CB, and LK. Supervision, validation and visualization: CB, AG, MA, WT, and ST. Writing—original draft: TE. Writing—review and editing: TE, YA, and CB. All authors have read and agreed to the published version of the manuscript.

FUNDING

This work was supported by a grant (MBRU-AlMahmeed Collaborative Research Award 2019) from Mohammed Bin Rashid University of Medicine and Health Sciences (MBRU), Project No: ALM 1931.

REFERENCES

Behl, M., and Lendlein, A. (2007). Shape-memory Polymers. *Mater. Today* 10, 20–28. doi:10.1016/s1369-7021(07)70047-0

Bourauel, C., Drescher, D., and Thier, M. (1992). An Experimental Apparatus for the Simulation of Three-Dimensional Movements in Orthodontics. *J. Biomed. Eng.* 14, 371–378. doi:10.1016/0141-5425(92)90081-u

Bowman, S. J. (2017). Improving the Predictability of clear Aligners. *Semin. Orthod.* 23, 65–75. doi:10.1053/j.sodo.2016.10.005

Boyd, R. L., and Waskalic, V. (2001). Three-dimensional Diagnosis Andorthodontic Treatment of Complex Malocclusions with the Invisalign Appliance. *Semin. Orthod.* 7, 274–293. doi:10.1053/sodo.2001.25414

Choi, Y., and Kim, K.-T. (2005). *Orthodontic Appliance by Using a Shape Memory Polymer*. South Korean Patent No KR100554713B1.

Drescher, D., Bourauel, C., and Thier, M. (1991). Application of the Orthodontic Measurement and Simulation System (OMSS) in Orthodontics. *Eur. J. Orthod.* 13, 169–178. doi:10.1093/ejo/13.3.169

Elkholy, F., Schmidt, F., Jäger, R., and Lapatki, B. G. (2017). Forces and Moments Applied during Derotation of a Maxillary central Incisor with Thinner Aligners: an *In-Vitro* Study. *Am. J. Orthod. Dentofacial Orthopedics* 151, 407–415. doi:10.1016/j.ajodo.2016.08.020

Elkholy, F., Schmidt, F., Jäger, R., and Lapatki, B. G. (2016). Forces and Moments Delivered by Novel, Thinner PET-G Aligners during Labiopalatal Bodily Movement of a Maxillary central Incisor: An *In Vitro* Study. *Angle Orthod.* 86, 883–890. doi:10.2319/011316-37r.1

Elshazly, T. M., Keilig, L., Alkabani, Y., Ghoneima, A., Abuzayda, M., Talaat, S., et al. (2021). Primary Evaluation of Shape Recovery of Orthodontic Aligners Fabricated from Shape Memory Polymer (A Typodont Study). *Dentistry J.* 9 (3), 31. doi:10.3390/dj9030031

Ercoli, F., Tepedino, M., Parziale, V., and Luzi, C. (2014). A Comparative Study of Two Different clear Aligner Systems. *Prog. Orthod.* 15, 31. doi:10.1186/s40510-014-0031-3

Gorna, K., and Gogolewski, S. (2003). The Effect of Gamma Radiation on Molecular Stability and Mechanical Properties of Biodegradable Polyurethanes for Medical Applications. *Polym. Degrad. Stab.* 79, 465–474. doi:10.1016/s0141-3910(02)00362-2

Hahn, W., Dathe, H., Fialka-Fricke, J., Fricke-Zech, S., Zapf, A., Kubein-Meesenburg, D., et al. (2009). Influence of Thermoplastic Appliance Thickness on the Magnitude of Force Delivered to a Maxillary central Incisor during Tipping. *Am. J. Orthod. Dentofacial Orthop.* 136, 12–13. doi:10.1016/j.ajodo.2008.12.015

Hahn, W., Zapf, A., Dathe, H., Fialka-Fricke, J., Fricke-Zech, S., Gruber, R., et al. (2010). Torquing an Upper central Incisor with Aligners-Aacting Forces and Biomechanical Principles. *Eur. J. Orthod.* 32, 607–613. doi:10.1093/ejo/cjq007

Ho, C.-T., Huang, Y.-T., Chao, C.-W., Huang, T.-H., and Kao, C.-T. (2021). Effects of Different Aligner Materials and Attachments on Orthodontic Behavior. *J. Dental Sci.* 16, 1001–1009. doi:10.1016/j.jds.2021.01.011

Iliadi, A., Koletsi, D., and Eliades, T. (2019). Forces and Moments Generated by Aligner-type Appliances for Orthodontic Tooth Movement: A Systematic Review and Meta-analysis. *Orthod. Craniofac. Res.* 22, 248–258. doi:10.1111/ocr.12333

Ishida, Y., Kuwajima, Y., Lee, C., Ogawa, K., Da Silva, J. D., and Ishikawa-Nagai, S. (2020). Effect of Magnet Position on Tipping and Bodily Tooth Movement in Magnetic Force-Driven Orthodontics. *Materials* 13 (16), 3588. doi:10.3390/ma13163588

Jung, Y. C., and Cho, J. W. (2010). Application of Shape Memory Polyurethane in Orthodontic. *J. Mater. Sci. Mater. Med.* 21, 2881–2886. doi:10.1007/s10856-008-3538-7

Kwon, J.-S., Lee, Y.-K., Lim, B.-S., and Lim, Y.-K. (2008). Force Delivery Properties of Thermoplastic Orthodontic Materials. *Am. J. Orthod. Dentofacial Orthopedics* 133, 228–234. doi:10.1016/j.ajodo.2006.03.034

Lai, M.-L., and Rule, J. D. (2020). *Orthodontic Appliance Having Continuous Shape Memory*. US Patent No US20200315747A1.

Lendlein, A., and Kelch, S. (2002). Shape-memory Polymers. *Angew. Chem. Int. Ed.* 41, 2034–2057. doi:10.1002/1521-3773(20020617)41:12<2034:aid-anie2034>3.0.co;2-m

Lendlein, A., and Langer, R. (2002). Biodegradable, Elastic Shape-Memory Polymers for Potential Biomedical Applications. *Science* 296, 1673–1676. doi:10.1126/science.1066102

Mahmood, H. T., Kamal, A. T., Khan, B. N., and Fida, M. (2019). Application of New Biomedical Materials in Orthodontic Appliances. *J. Coll. Physicians Surg. Pak* 29 (7), 654–657. doi:10.29271/jcpsp.2019.07.654

Martorelli, M., Gerbino, S., Giudice, M., and Ausiello, P. (2013). A Comparison between Customized clear and Removable Orthodontic Appliances

Manufactured Using RP and CNC Techniques. *Dental Mater.* 29, e1–e10. doi:10.1016/j.dental.2012.10.011

McKiernan, R. L., Heintz, A. M., Hsu, S. L., Atkins, E. D. T., Penelle, J., and Gido, S. P. (2002). Influence of Hydrogen Bonding on the Crystallization Behavior of Semicrystalline Polyurethanes. *Macromolecules* 35, 6970–6974. doi:10.1021/ma0201274

Mehta, F., and Mehta, S. (2014). Aligners: the Rapidly Growing Trend in Orthodontics Around the World. *Indian J. Basic Appl. Med. Res.* 3, 402–409.

Meng, H., and Li, G. (2013). A Review of Stimuli-Responsive Shape Memory Polymer Composites. *Polymer* 54, 2199–2221. doi:10.1016/j.polymer.2013.02.023

Min, S., Hwang, C.-J., Yu, H.-S., Lee, S.-B., and Cha, J.-Y. (2010). The Effect of Thickness and Deflection of Orthodontic Thermoplastic Materials on its Mechanical Properties. *Korean J. Orthod.* 40, 16–26. doi:10.4041/kjod.2010.40.1.16

Momtaz, P. (2016). The Effect of Attachment Placement and Location on Rotational Control of Conical Teeth Using Clear Aligner Therapy. Master's thesis/dissertation. Las Vegas(USA): University of Nevada).

Morton, J., Derakhshan, M., Kaza, S., and Li, C. (2017). Design of the Invisalign System Performance. *Semin. Orthod.* 23, 3–11. doi:10.1053/j.sodo.2016.10.001

Nakasima, A., Hu, J. R., Ichinose, M., and Shimada, H. (1991). Potential Application of Shape Memory Plastic as Elastic Material in Clinical Orthodontics. *Eur. J. Orthod.* 13, 179–186. doi:10.1093/ejo/13.3.179

Nam, S., and Pei, E. (2020). The Influence of Shape Changing Behaviors from 4D Printing through Material Extrusion Print Patterns and Infill Densities. *Materials* 13 (17), 3754. doi:10.3390/ma13173754

Ojima, K., and Kau, C. H. (2017). A Perspective in Accelerated Orthodontics with Aligner Treatment. *Semin. Orthod.* 23, 76–82. doi:10.1053/j.sodo.2016.10.002

Pedersen, E., Andersen, K., and Gjessing, P. E. (1990). Electronic Determination of Centres of Rotation Produced by Orthodontic Force Systems. *Eur. J. Orthod.* 12, 272–280. doi:10.1093/ejo/12.3.272

Pei, E., Loh, G. H., and Nam, S. (2020). Concepts and Terminologies in 4D Printing. *Appl. Sci.* 10 (13), 4443. doi:10.3390/app10134443

Phan, X., and Ling, P. H. (2007). Clinical Limitations of Invisalign. *J. Can. Dent Assoc.* 73 (3), 263–266.

Proffit, W. R., Fields, H. W., Sarver, D. M., and Ackerman, J. L. (2000). *Contemporary Orthodontics*. St. Louis: Mosby.

Ryu, J.-H., Kwon, J.-S., Jiang, H. B., Cha, J.-Y., and Kim, K.-M. (2018). Effects of Thermoforming on the Physical and Mechanical Properties of Thermoplastic Materials for Transparent Orthodontic Aligners. *Korean J. Orthod.* 48, 316–325. doi:10.4041/kjod.2018.48.5.316

Sheridan, J. J., LeDoux, W., and McMinn, R. (1993). Essix Retainers: Fabrication and Supervision for Permanent Retention. *J. Clin. Orthod.* 27, 37–45.

Silverman, E., and Cohen, M. (1969). *Orthodontic Appliance*. US Patent No US3421221A.

Simon, M., Keilig, L., Schwarze, J., Jung, B. A., and Bourauel, C. (2014). Treatment Outcome and Efficacy of an Aligner Technique-Rregarding Incisor Torque, Premolar Derotation and Molar Distalization. *BMC Oral Health* 14, 1–7. doi:10.1186/1472-6831-14-68

Simon, M., Keilig, L., Schwarze, J., Jung, B. A., and Bourauel, C. (2014). Forces and Moments Generated by Removable Thermoplastic Aligners: Incisor Torque, Premolar Derotation, and Molar Distalization. *Am. J. Orthod. Dentofacial Orthopedics* 145, 728–736. doi:10.1016/j.ajodo.2014.03.015

Small, IV, W., Singhal, P., Wilson, T. S., and Maitland, D. J. (2010). Biomedical Applications of Thermally Activated Shape Memory Polymers. *J. Mater. Chem.* 20, 3356–3366. doi:10.1039/b923717h

Tamer, I., Öztaş, E., Oztas, E., and Marsan, G. (2019). Orthodontic Treatment with Clear Aligners and the Scientific Reality behind Their Marketing: A Literature Review. *Turk J. Orthod.* 32 (4), 241–246. doi:10.5152/turkjorthod.2019.18083

Thukral, R., and Gupta, A. (2015). Invisalign: Invisible Orthodontic Treatment-A Review. *J. Adv. Med. Dent. Sci. Res.* 3 (5), 42–44.

Yen, F.-S., Lin, L.-L., and Hong, J.-L. (1991). Hydrogen-bond Interactions between Urethane- Urethane and Urethane- Ester Linkages in a Liquid Crystalline Poly (Ester- Urethane). *Macromolecules* 32, 3068–3079.

Zhang, H., Wang, H., Zhong, W., and Du, Q. (2009). A Novel Type of Shape Memory Polymer Blend and the Shape Memory Mechanism. *Polymer* 50, 1596–1601. doi:10.1016/j.polymer.2009.01.011

Zweben, C., Smith, W. S., and Wardle, M. W. (1979). "Test Methods for Fiber Tensile Strength, Composite Flexural Modulus, and Properties of Fabric-Reinforced Laminates," in *Composite Materials: Testing and Design (Fifth Conference)*. Editor S. Tsai (West Conshohocken, PA: ASTM International), 228–262.

Conflict of Interest: The authors declare that the research was conducted in the absence of any commercial or financial relationships that could be construed as a potential conflict of interest.

Publisher's Note: All claims expressed in this article are solely those of the authors and do not necessarily represent those of their affiliated organizations, or those of the publisher, the editors and the reviewers. Any product that may be evaluated in this article, or claim that may be made by its manufacturer, is not guaranteed or endorsed by the publisher.

frontiers in Materials

ORIGINAL RESEARCH
published: 04 February 2022
doi: 10.3389/fmats.2021.789143

Comparison Between Different Composite Resins Used for Clear Aligner Attachments: An *In-Vitro* Study

***Francesca Gazzani*[1]*, Denise Bellisario*[2]*, Fabrizio Quadrini*[2]*, Francesca Parrinello*[1]*, Chiara Pavoni*[1,3]*, Paola Cozza*[1,3,4] *and Roberta Lione*[1,3,4]**

[1]Department of Systems Medicine, University of Rome "Tor Vergata", Rome, Italy, [2]Department of Industrial Engineering, University of Rome "Tor Vergata", Rome, Italy, [3]Department of Dentistry, UNSBC, Tirana, Albania, [4]Departmental Faculty of Medicine and Surgery, University of Rome "Unicamillus", Rome, Italy

OPEN ACCESS

Edited by:
Michele Tepedino,
University of L'Aquila, Italy

Reviewed by:
Edoardo Staderini,
Agostino Gemelli University Polyclinic (IRCCS), Italy
Bernardo Souki,
Pontifical Catholic University of Minas Gerais, Brazil

****Correspondence:***
Francesca Gazzani
francescagazzani@hotmail.it

Specialty section:
This article was submitted to Biomaterials, a section of the journal Frontiers in Materials

Received: *04 October 2021*
Accepted: *09 December 2021*
Published: *04 February 2022*

Citation:
Gazzani F, Bellisario D, Quadrini F, Parrinello F, Pavoni C, Cozza P and Lione R (2022) Comparison Between Different Composite Resins Used for Clear Aligner Attachments: An In-Vitro *Study.*
Front. Mater. 8:789143.
doi: 10.3389/fmats.2021.789143

Attachments are specific features of clear aligner treatment designed to ensure the aligner's retention and the predictability of tooth movements. The properties of composite resin used for their reproduction play a relevant role to preserve their integrity and shape over the time. Thus, the aim of the present evaluation was to compare the mechanical properties and the wear performance of two nanocomposite by means of mechanical and tribological tests. Twelve samples for both flowable nanocomposite (FNC) and conventional nanocomposite (CNC) were created. The two nanocomposites differ in terms of filler volume and viscosity of the mixture. The following tests were performed: thermal analysis and burning test; flat instrumented indentation test and a compression stress relaxation test; tribological analysis. Wear evaluation was performed by means of a contact probe surface profiler and a TayMap software for the 3D analysis. A customized step-sliding test was conducted to simulate the clinical application of materials with a polymethyl methacrylate (PMMA) ball used as counterpart. Wear evaluation of both resin surfaces and PMMA ball was performed. No differences were found in terms of polymeric nature and quantity of nanoparticles in the matrix. FNC showed lower density values (1.62 g/cm^3 ± 0.02) and inorganic percentage residue (41%) than the CNC (respectively 1.95 g/cm^3 ± 0.01 and 23%). Significant differences in terms of decrement of stress values, elastic modulus (1,114.12 ± 91.39 MPa), and stress relaxation rate (24.39% ± 3.23) were observed for the CNC when compared to the FNC (respectively, 835.04 ± 184.73 MPa and 40.19% ± 4.65). FNC showed higher values of dynamic friction coefficient (0.72 ± 0.017) and more worn and deeper profiles than the conventional ones. The step-sliding test with a PMMA ball confirmed a higher friction coefficient for FNC and a greater wear of the PMMA surfaces when used against flowable samples. Lower viscosity of FNC ensures a better adaptation during clinical attachment fabrication, whereas it has a negative impact on mechanical properties. CNC showed greater performance and resistance under mechanical stresses than the flowable ones, resulting in being more suitable for clinical needs.

Keywords: nanocomposite resins, attachments, clear aligner treatment, tribological analysis, mechanical properties

INTRODUCTION

Clear aligners treatment (CAT) requires the placement of resin buttons on tooth surfaces to enhance the aligners retention and to create pushing surfaces for a more predictable tooth movement (Morton et al., 2017; D'Anto et al., 2019). In fact, the addition of these auxiliaries, usually referred to as attachments, maximize the contact points and the interaction between the aligner and tooth surfaces. Attachments' position and configuration play a crucial role during the orthodontic treatment since they are strongly related to the force system induced by the aligner. Ideal composite resins suitable for attachment creation need specific esthetic and mechanical properties (Barreda et al., 2017). As for the esthetic aspect, composite resin should be resistant to stain and with similar translucency of the underlying tooth (Feinberg et al., 2016; Barreda et al., 2017). On the other hand, more clinically significant are the mechanical features required. Since they represent needful auxiliary elements for aligners system, their integrity and shapes need to be maintained during the treatment to ensure the functional validity and to not compromise movements' efficiency and aligner fitting (Kravitz et al., 2008; Das et al., 2015; D'Anto et al., 2019; Mantovani et al., 2019). These materials (resin-based dental composite) are widely used in dentistry for dental restorations and orthodontic devices (Aminoroaya et al., 2021). They are usually composed of two phases: an organic resin matrix and an inorganic/organic filler. The organic resin matrix is composed of monomers and light-sensitive initiators, whereas the filler phase consists of different size particles (micro/nano-sized fillers) which determine the material's properties (Fronza et al., 2015; Taheri et al., 2015; Cho et al., 2020; Aminoroaya et al., 2021). The predominant bases monomer used are normally bis-GMA that is sometimes mixed with other dimethacrylates (Ferracane. 2011). Most of the composites contain an activator/initiator system to promote light-activated polymerization of the organic matrix forming cross-linked polymer networks (Nikolaidis. et al., 2019). The most variable contents are represented by the filler particles and their size (Satterthwaite et al., 2009; Satterthwaite et al., 2012). The "nanofill" composites include nanoscale particles characterized by a size range of 1–100 (Ferracane. 2011). Particles' size may range from 20 nm to 5 μm and filler phase overall can represent 70% of the volume (Lang et al., 1992; Barreda et al., 2017). Attachments' creation usually requires conventional (CNC) or flowable (FNC) dental nanocomposite resins (Ferracane 2011; Mantovani et al., 2019) which mainly differ for filler volume and viscosity. Composite viscosity is determined by monomer composition and filler content. CNC is composed of small particle sizes with a high filler volume and high viscosity of the mixture. On the other hand, FNC present the same small particle sizes of conventional composites with a reduced filler volume, increased resin content, and lower viscosity of the mixture (Bayne et al., 1998; Benetti et al., 2015). This composition produces a composite with an easy adaptation to the attachments template, but a negative impact to wear performance and stability (Clelland et al., 2005). In literature, many studies (Feinberg et al., 2016; Barreda et al., 2017; D'Anto et al., 2019; Mantovani et al., 2019) investigated

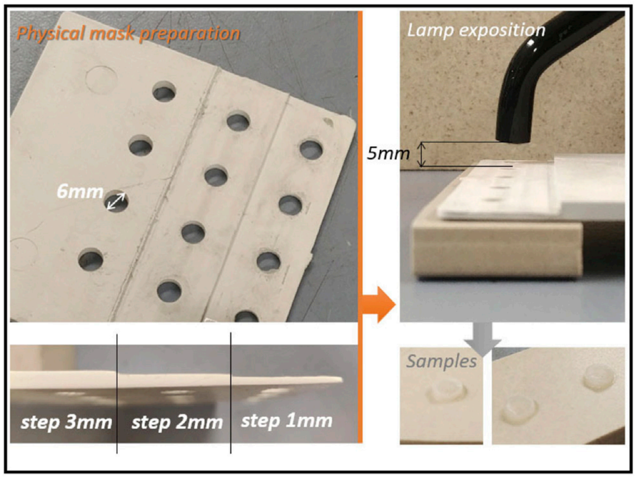

FIGURE 1 | Samples' preparation process: physical mask preparation for sample deposition, lamp exposition, and final samples.

composite resins for this clinical application. D'Anto et al. (2019) demonstrated that composite viscosity does not have any influences on the shape and volume of attachments. However, no data are available on the comparison of mechanical and wear properties of different composite resins available especially when used for attachment. Since the choice of the best material with ideal properties seems to be relevant to ensure the stability and the efficiency of these auxiliary components of CAT, the aim of this study was to analyze the mechanical properties of two nanocomposite resins (CNC vs FNC) with different viscosities and filler volume by means of mechanical and tribological tests.

MATERIALS AND METHODS

A series of 12 samples (6 FNC, 6 CNC) were realized for the experimental analysis. Photocurable thickness limits of about 1 mm for each type of composite were respected and photo-masks with three thickness steps have been manufactured to optimize the deposition and the curing phase. All the masks were machined into a polycarbonate sheet in which five circular seats of 6 mm of diameter have been obtained (**Figure 1**). The diameter of 6 mm has been chosen in order to carry out macroscopic mechanical tests as indentation tests and tribological tests for which a contact surface in the order of 5–10 mm is required as a minimum. An incremental addition of 1 mm of material has been deposited into the mask's seats and then exposed to UV light until reaching 3 mm of total thickness. For each sample, the UV lamp (TPC led curing light 50 N, United States) with an irradiance of 800 mW/cm^2 was positioned at 5 mm of distance and the UV curing time step was set at 25 s. At the end of the curing process, the sample sizes and the weight were measured by means of a digital caliper and a precision balance, and these measures were evaluated as the average dimensions and calculated the density values. The primary endpoints of the present investigation were to evaluate the mechanical properties and the wear behaviour of

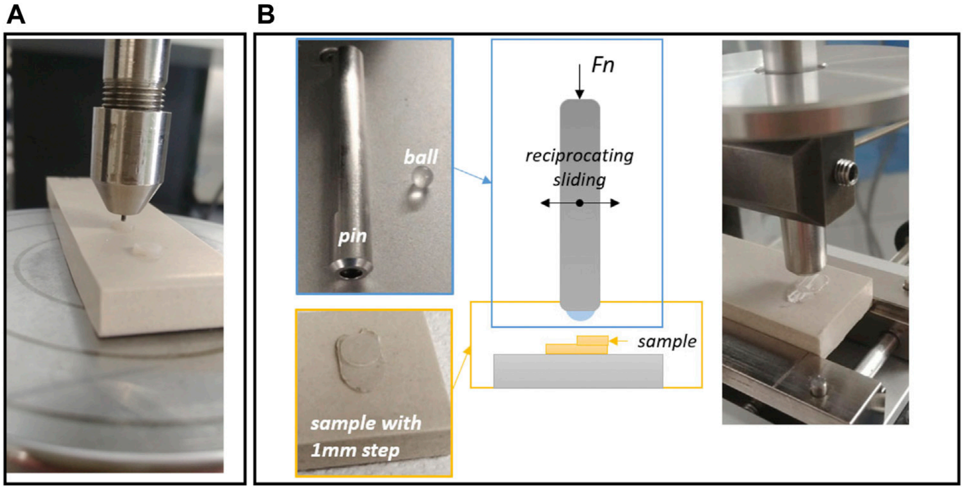

FIGURE 2 | Experimental analysis: **(A)** Flat indentation test. **(B)** Step sliding test.

the two nanocomposites. The secondary endpoints were to analyse their thermal properties and to observe the wear behaviour after the simulation of clinical conditions of use through a step-sliding test in combination with a PMMA.

Thermal Analysis and Burning Test

Given the polymeric nature of the nanocomposite materials, thermal analysis was conducted by differential scanning calorimetry (DSC 7 by Perkin Elmer) in order to evaluate their thermal properties. After samples curing, a small amount (20 mg) of each nanocomposite material was analysed by DSC scanning (range 20–250°C, rate 10 C/min). Considering the amount of inorganic content for both materials analysed, a burning test was realized. Small quantities (150 mg) of nanocomposites were inserted at 600°C for 60 min into a muffle and after that time the unburned residue was evaluated to calculate the percentage of inorganic content.

Mechanical Tests

Evaluation of the mechanical properties were performed through a flat instrumented indentation test (**Figure 2A**) and a compression stress relaxation test. The first analysis was used to assess local mechanical behaviour of nanocomposite samples, while the second test was performed to evaluate the global mechanical properties and the stress relaxation behaviour. The flat indentation tests were carried out on the flat surface of the cylindrical samples, by using a universal material testing machine (Insight/5 by MTS) equipped with an indenter holder. Flat indenter of tungsten carbide was used with a diameter of 1 mm. The tests were performed on 5 samples for each type of material and the indentation was centered with respect to the sample's diameter. The maximum penetration depth imposed was 0.3 mm (10% of total thickness to avoid the influence of the substrate), the rate was 0.1 mm/min, and the pre-load was 1 N. The compression stress relaxation tests were performed by means of a universal testing machine (Alliance/50 by MTS) in compression configuration. Five samples have been compressed up to a maximum of 50 MPa by compression plates and fixing the crosshead position and evaluating the stress decrease for 15 min.

Tribological Tests and Wear Evaluation

Tribological tests with alternative dry-sliding motion were performed on five samples for each type of nanocomposite by a standard tribometer (Linear Reciprocating Tribometer, C.S.M. Instruments, Peseaux, Switzerland) at about 20°C and 40% RH. Tests were performed at 10 N load and with a back-and-forth sliding (stroke length 4 mm, frequency 2.5 Hz, duration 10,000 cycles) of the alumina ball (6 mm diameter). Samples' wear was assessed by contact probe surface profiler (TalySurf CLI 2000; Taylor Hobson, Leicester, United Kingdom). The profilometer was used to rebuild the wear patterns using a 5 μm lateral resolution. The maximum and mean depth, the area, and the volume involved by the action of the counterpart on the surface of the samples were evaluated by using a TayMap software to calculate and qualitatively analyse the 3D wear patterns.

Customized Test and Simulation of Clinical Application

A more targeted test was performed to simulate more specifically the clinical condition of use of materials involved in the investigation. The implementation of materials provides their placement on the tooth in thicknesses of 1 mm to build a step. A step-sliding test has been developed to simulate the insertion and removal of the appliance and the periodic work of the composites in combination with the material of the aligner. A step of each nanocomposite material was created on a ceramic support and a PMMA (polymethyl methacrylate) ball was used as counterpart during step-sliding tests (**Figure 2B**). To assess the type of polymer of the commercial aligner, a thermal analysis by DSC (DSC 7 by Perkin Elmer) was performed. The step-sliding test was performed with a contact length of 10 mm (5 mm above the

TABLE 1 | Measured dimensions and weight of the different fabricated samples.

	H				D			Weight	H_{mean}	D_{mean}	Density
	mm				Mm			g	mm	mm	g/cm^3
CNC1	2.714	2.818	2.824	2.781	5.96	5.97	5.95	0.1508	2.784	5.96	1.94
CNC2	2.661	2.651	2.665	2.656	5.94	5.95	5.94	0.143	2.658	5.94	1.94
CNC3	2.631	2.619	2.629	2.586	5.96	5.97	5.95	0.1436	2.616	5.96	1.97
CNC4	2.656	2.651	2.654	2.659	5.96	5.94	5.97	0.1453	2.655	5.957	1.96
CNC5	2.461	2.465	2.464	2.463	5.96	6.03	5.97	0.1349	2.463	5.987	1.94
CNC6	2.871	2.87	2.868	2.869	5.97	5.98	6.05	0.1585	2.869	6	1.95
FNC1	2.516	2.542	2.558	3	6.12	6.23	6.15	0.1258	2.537	6.167	1.66
FNC2	2.331	2.328	2.327	2.326	6.21	6.16	6.22	0.1128	2.328	6.196667	1.61
FNC3	2.625	2.62	2.617	2.621	6.16	6.25	6.13	0.1287	2.621	6.18	1.64
FNC4	2.803	2.803	2.801	2.804	6.3	6.37	6.33	0.1443	2.802	6.333333	1.63
FNC5	2.688	2.68	2.667	2.673	6.2	6.23	6.17	0.13	2.677	6.2	1.61
FNC6	2.398	2.397	2.403	2.401	6.16	6.12	6.1	0.1135	2.40	6.126667	1.60

mm, millimeters; g: grams; H: height; D: diameter; FNC, flowable nanocomposite; CNC, conventional nanocomposite.

step and 5 mm below the step), a duration of 10,000 cycles, a frequency of 2.5 Hz, and a normal load of 1 N. The wear behaviour of the samples was evaluated by contact profilometer (TalySurf CLI 2000; Taylor Hobson, Leicester, United Kingdom), while the PMMA ball wear was assessed through weight difference before and after the test. The wear values of the nanocomposite samples were also evaluated by 3D maps of the samples' surface at the top of the step.

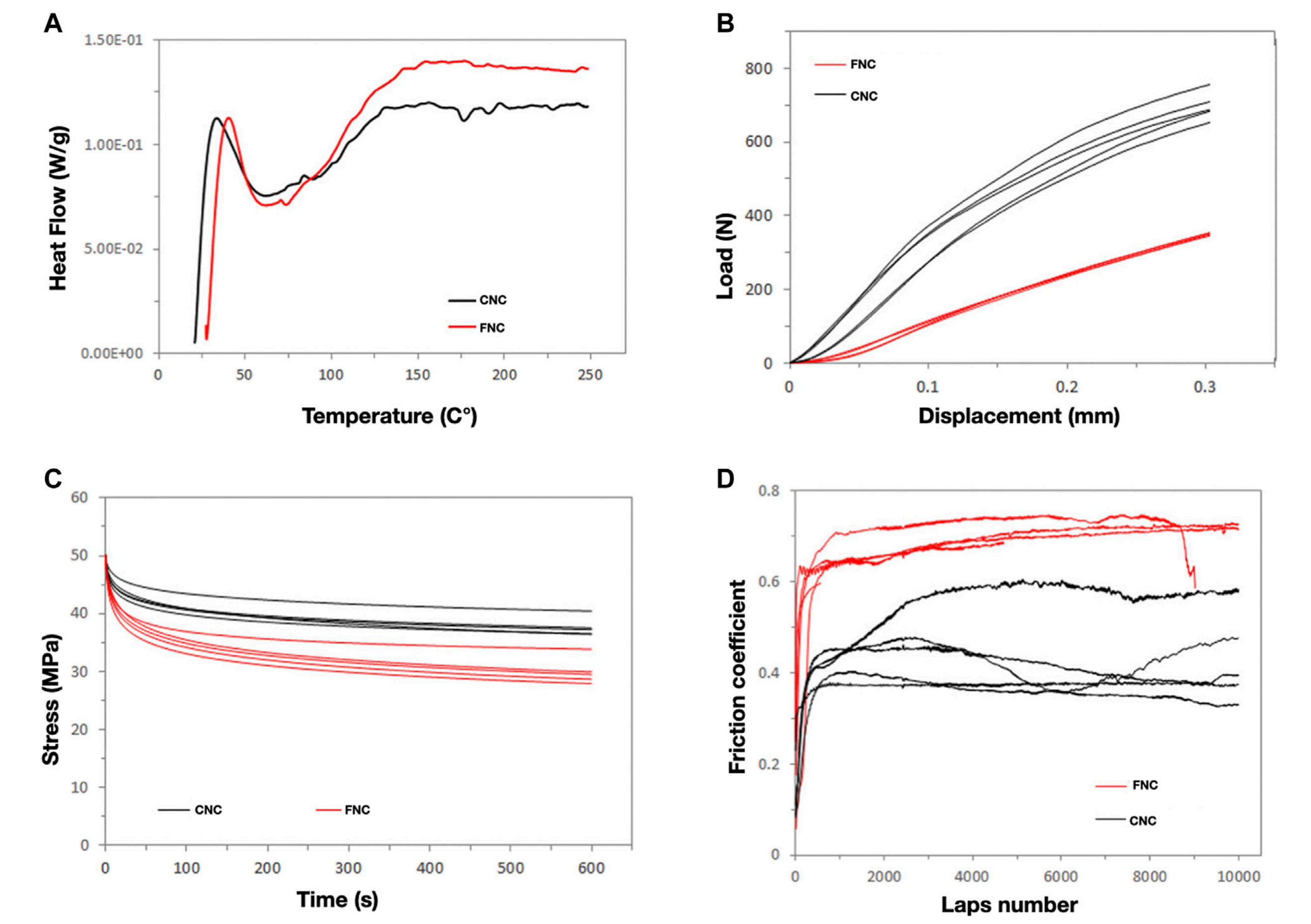

FIGURE 3 | (A) Differential scanning calorimetry curves. **(B)** Flat indentation curves and trend. **(C)** Stress relaxation curves. **(D)** Friction coefficient values monitored during 10,000 laps on the samples' surfaces. The average friction coefficient for each material was evaluated in the range between 6,000 and 8,000 laps at +1 mm from the centred position of linear sliding.

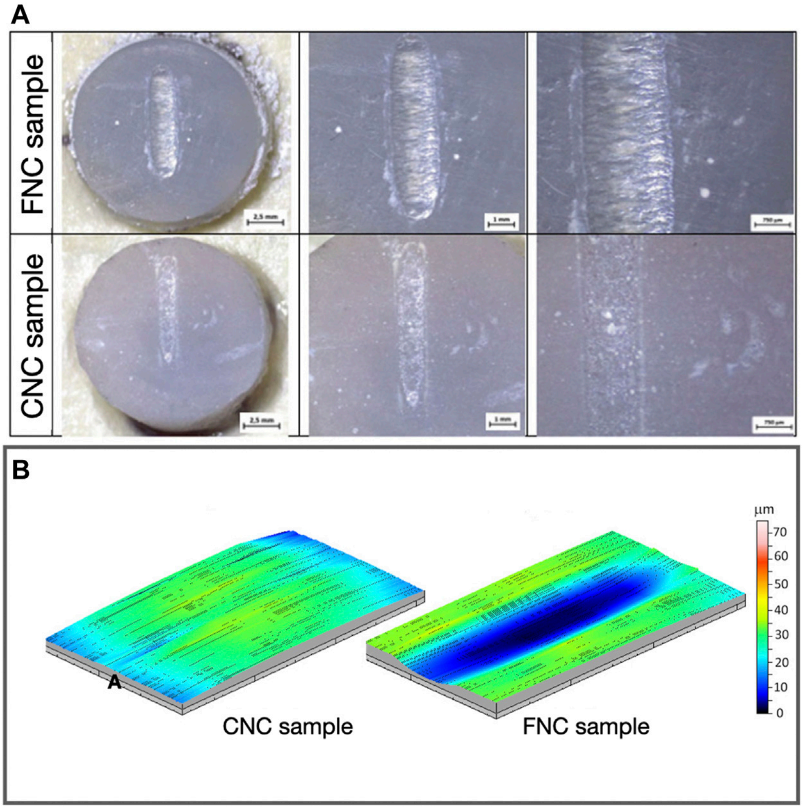

FIGURE 4 | Qualitative evaluation of wear behavior. **(A)** Sample images after tribological tests. **(B)** 3D maps of FNC and CNC worn surfaces after tribological tests.

RESULTS

Table 1 reports the measured dimensions of all fabricated samples in the pilot study and through these values the mean density was evaluated for each type of nanocomposite, in particular 1.62 (g/cm^3) ± 0.02 and of 1.95 (g/cm^3) ± 0.01, respectively for FNC and CNC. Analysing the DSC curves for the two materials, no differences were found in terms of polymeric nature of the composites or substantial changes in the quantity of nanoparticles in the matrix. However, the burning test reported an inorganic percentage residue of 41 and 23%, respectively, for the FNC and for CNC (**Figure 3A**). Form a mechanical point of view, flat indentation tests showed a good repeatability for both materials (**Figure 3B**). The maximum loads reached at a depth of 0.3 mm were 364.94 N ± 27.87 and 723.66 N ± 38.37, respectively, for flowable and conventional samples. Equally significant differences have been found between the two materials in stress relaxation tests. Specifically, a lower decrease of stress value of the CNC material was found in comparison to the FNC (**Figure 3C**). Elastic modulus' evaluations reported greater values observed for the CNC (1,114.12 ± 91.39 MPa) than the FNC (835.04 ± 184.73 MPa). Higher values of stress relaxation were found for the FNC (40.19 ± 4.65) when compared with CNC (24.93 ± 3.23). As for tribological test, some FNC samples did not complete the number of cycles as the maximum limit of tangential force detected by the instrument was reached. Higher values of dynamic friction coefficient for FNC were found (**Figure 3D**). The different wear behaviour of the samples has been also confirmed by the images and 3D maps as shown in **Figure 4**. The comparison of the worn areas showed deeper wear profiles on FNC surfaces than on the conventional ones (**Figures 4, 5A,B**). As reported in **Table 2**, worn surface and volume values for the FNC samples were higher than the CNC, and also as expected the maximum and mean depth of the wear were greater for FNC. The step-sliding test with a PMMA ball showed a higher average friction coefficient for FNC in **Figure 5C**. Also, the PMMA surfaces significantly wore out during the test especially when used against FNC sample. The 3D maps of worn surfaces for both nanocomposites are reported in **Figure 6** Extracted values and volume of the two samples (**Table 3**) showed that the extension of the surface involved is comparable among the two samples, while the worn volume is greater for FNC with a corresponding modification of the PMMA ball geometry.

DISCUSSION

Composite attachments are geometric buttons routinely required for all CAT. These powerful features are essential to control tooth movements and anchorage units, but they also increase aligners' retention (Mantovani et al., 2019). Rossini et al. concluded that all

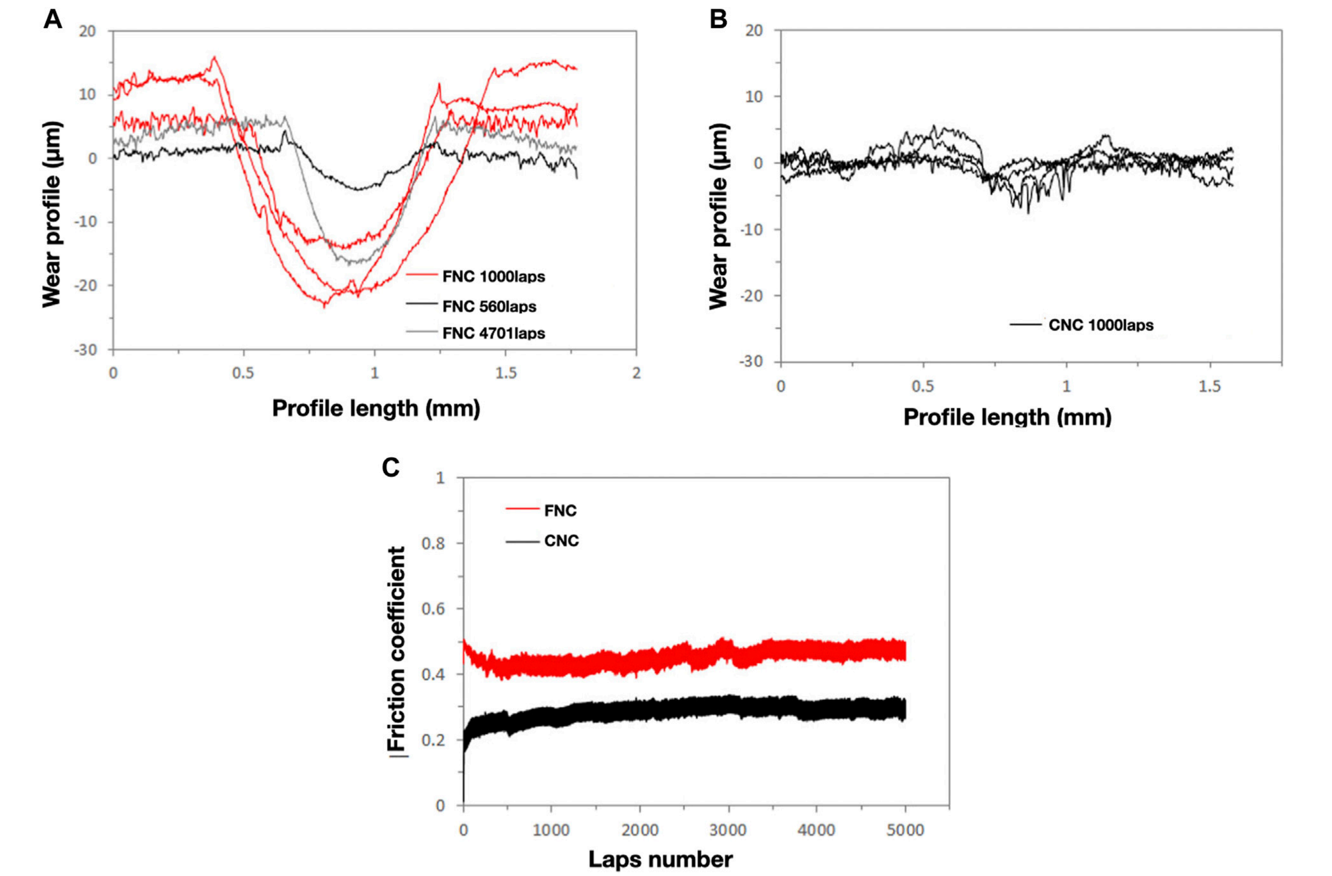

FIGURE 5 | (A) Wear profiles analyses of FNC. **(B)** Wear profiles analyses of CNC. **(C)** Friction coefficient trend during step sliding test. The total number of cycles covered was 5,000, the sliding length was 10 mm. The position at which the friction trends have been evaluated is +2.5 mm compared to the central sliding position (on the top of the step).

TABLE 2 | Evaluated worn surface and volume, and maximum and mean depth for the worn surfaces.

	Worn surface	Worn volume	Max depth	Mean depth
	mm^2	mm^3	µm	µm
FNC	2.158 ± 0.17	0.030 ± 0.014	38.933 ± 15.792	14.867 ± 3.184
CNC	0.901 ± 0.174	0.002 ± 0.001	15.951 ± 5.548	2.193 ± 0.921

mm, millimeters; µm, micrometers; FNC, flowable nanocomposite; CNC, conventional nanocomposite.

kinds of attachments had a great impact on the quality and predictability of the tooth movements (Simon et al., 2014; Rossini et al., 2015). For this reason, the selection of composite resins plays a crucial role for the long-term stability of the attachments' shape and for their structural integrity. The aim of the present investigation was to analyse two composite resins with different viscosity and filler volume in order to compare their mechanical properties and to identify which is more suitable for the attachment's reproduction. Our results showed how a greater degree of wear was observed when the attachment was reproduced with the composite presenting a higher percentage of inorganic particles. As a matter of fact, despite the lower content of inorganic filling content, the CNC resulted denser and it was characterized by a better mechanical resistance (**Figure 3A**). According to our findings, Barreda et al. (2017) compared attachment surfaces made of two composites with different particle size and filler content by means of Scanning Electron Microscopy (SEM). They concluded that the shape of attachments does not change within 6 months. Thus, the movements related would still be effective in this time interval. Additional data suggested that the low viscosity, defined as the measure of a fluid resistance to flow, is related to a greater elastic modulus indicating that the material offers more resistance to the deformation (Simon et al., 2014). On the other hand, once a strain is given to the FNC material, the viscous component gradually "engages" the deformation (**Figure 3C**). Both FNC and CNC demonstrated a stress decrease after a strain application as expected by the material's nature; however, the rate of the decrease was higher for CNC. This underlines how for the CNC the loss of the applied load is faster over time, although the time investigated is relatively short (15 min). As reported by Tanimoto et al. (2006), elastic modulus is not affected by the filler size, but it depends on stress transmission between the filler and

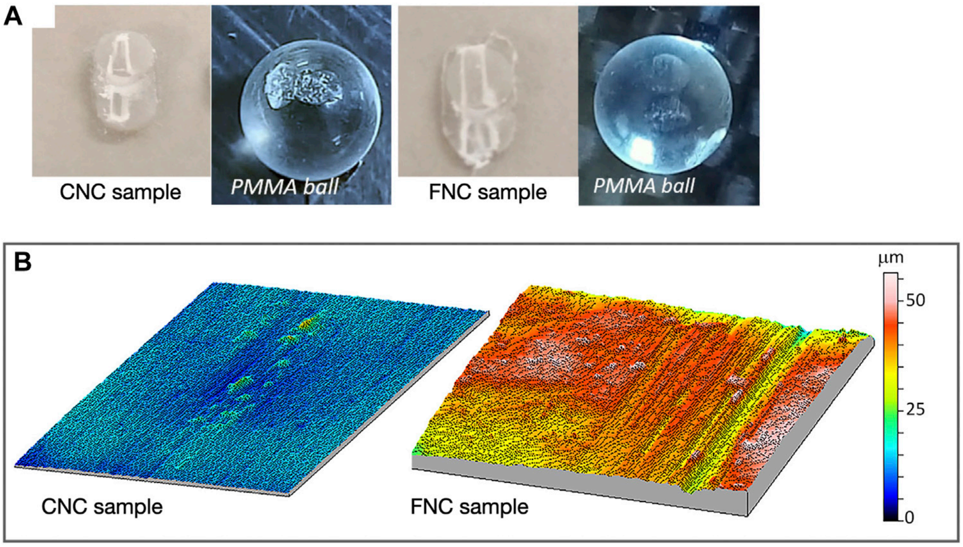

FIGURE 6 | (A) CNC and FNC samples and the respective PMMA balls used after step sliding test. **(B)** 3D maps of the CNC and FNC samples' worn surface s at the top of the sample step.

TABLE 3 | Worn surface and volume and maximum and mean depth of the worn surface of samples after step sliding test.

	Worn surface	Worn volume	Max depth	Mean depth
	mm^2	mm^3	µm	µm
FNC	1.77	0.0038	56	21.6
CNC	1.78	0.0022	7.98	1.26

mm, millimeters; µm, micrometers; FNC, flowable nanocomposite; CNC, conventional nanocomposites.

the matrix. As widely described, resin composites differ from each other in terms of stain resistance, hardness, and wear behaviour (Clelland et al., 2005; Simon et al., 2014; Aminoroaya et al., 2021). In the existing literature (Dasy et al., 2015; Feinberg et al., 2016; Barreda et al., 2017; D'Anto et al., 2019), not many studies analysed the wear behaviour of the composite resins mainly used for attachments reproduction. On the other hand, Barreda et al. (2017) demonstrated that the properties of composites could affect the surface, but not the shape of the attachments during use. More recently, their results have been confirmed by D'Anto et al. (2019) who concluded that viscosity values determine differences in terms of shape and volume. However, the wear behaviour of these materials has not been yet analysed related to their use for attachments reproduction. In this study, the mechanical and wear performances in laboratory tests on the nanocomposites used for the attachments were analysed. In order to carry out such macroscopic evaluations, sample sizes were chosen as small as possible to perform tests under sliding, and as large as possible to have a homogeneous curing under the lamp. Even if the exact clinical conditions are not repeated, at least the single curing step was correctly adopted and it was suitable for the purpose of evaluation and comparison of attachment materials. The tribological test conducted revealed higher values of dynamic friction for the FNC (0.72 ± 0.017) when compared with the CNC (0.41 ± 0.092) with a consequent greater susceptibility to the surface damages (**Figure 3D**). The evaluation of these damages from a morphological point of view were made by 3D maps acquisition by a contact profilometer (**Figures 4**, **5**). In particular, it observed a superficial removal of composite material (worn areas). The qualitative evaluation highlighted deeper grooves and more significant wear traces on FNC samples. The same characteristics have been further confirmed by the step sliding test performed between the nanocomposites and the PMMA ball (**Table 3**). Also in this case, the results obtained revealed significant differences between the two materials, as shown in **Figures 5C**, **6**. A greater wear has been observed when the PMMA ball was used counterpart in the test with FNC samples indicating a larger abrasive damage among the two materials. As for the samples' surfaces, the 3D analysis (**Figure 6**) showed that the extension of the surface involved is comparable among the two samples, while the worn volume results were once again greater for the FNC resin.

STRENGTH AND LIMITATIONS

A strength of the present investigation consisted of having identified the different mechanical and wear properties of the two nanocomposites highlighting the best application of the CNC for attachments reproduction. Wear properties and strength observed during the experimental analysis provide better performance and fitting of aligners, making these materials the best choice for the features design. A limitation of the present study is that although the tests conducted were highly repeatable, they move away from the real conditions of use. Further investigation should be thought to simulate and reproduce the insertion and removal of clear aligners and the periodic work of the composites in combination with their material.

CONCLUSION

CNC resins demonstrated a better mechanical behaviour from a materialistic point of view, and for this reason they seem to be considered the best choice for attachments creation during CAT. Moreover, wear properties in dry conditions and strength observed during the experimental analysis provide better performance and fitting of aligners, making these materials the best choice for the features design.

DATA AVAILABILITY STATEMENT

The original contributions presented in the study are included in the article/Supplementary Material, further inquiries can be directed to the corresponding author.

AUTHOR CONTRIBUTIONS

PC, RL, and FG proposed the research idea and wrote the article. DB and FQ improved the idea and performed the experimental analysis. They also contributed to the writing of the paper. CP and FP assisted the experimental analysis. All authors reviewed the article.

REFERENCES

Aminoroaya, A., Neisiany, R. E., Khorasani, S. N., Panahi, P., Das, O., Madry, H., et al. (2021). A Review of Dental Composites: Challenges, Chemistry Aspects, Filler Influences, and Future Insights. *Composites B: Eng.* 216, 108852. doi:10.1016/j.compositesb.2021.108852

Barreda, G. J., Dzierewianko, E. A., Muñoz, K. A., and Piccoli, G. I. (2017). Surface Wear of Resin Composites Used for Invisalign(R) Attachments. *Acta Odontol. Latinoam.* 30, 90–95.

Bayne, S. C., Thompson, J. Y., Swift, E. J., Jr, Stamatiades, P., and Wilkerson, M. (1998). A Characterization of First-Generation Flowable Composites. *J. Am. Dental Assoc.* 129 (5), 567–577. doi:10.14219/jada.archive.1998.0274

Benetti, A., Havndrup-Pedersen, C., Honoré, D., Pedersen, M., and Pallesen, U. (2015). Bulk-fill Resin Composites: Polymerization Contraction, Depth of Cure, and gap Formation. *Oper. Dent* 40, 190–200. doi:10.2341/13-324-l

Cho, K., Sul, J.-H., Stenzel, M. H., Farrar, P., and Prusty, B. G. (2020). Experimental Cum Computational Investigation on Interfacial and Mechanical Behavior of Short Glass Fiber Reinforced Dental Composites. *Composites Part B: Eng.* 200, 108294. doi:10.1016/j.compositesb.2020.108294

Clelland, N. L., Pagnotto, M. P., Kerby, R. E., and Seghi, R. R. (2005). Relative Wear of Flowable and Highly Filled Composite. *The J. Prosthetic Dentistry* 93, 153–157. doi:10.1016/j.prosdent.2004.11.006

D'Antò, V., Muraglie, S., Castellano, B., Candida, E., Sfondrini, M. F., Scribante, A., et al. (2019). Influence of Dental Composite Viscosity in Attachment Reproduction: An Experimental *In Vitro* Study. *Materials (Basel)* 12 (23), 4001. doi:10.3390/ma12234001

Dasy, H., Dasy, A., Asatrian, G., Rózsa, N., Lee, H.-F., and Kwak, J. H. (2015). Effects of Variable Attachment Shapes and Aligner Material on Aligner Retention. *Angle Orthod.* 85, 934–940. doi:10.2319/091014-637.1

Feinberg, K. B., Souccar, N. M., Kau, C. H., Oster, R. A., and Lawson, N. C. (2016). Translucency, Stain Resistance, and Hardness of Composites Used for Invisalign Attachments. *J. Clin. Orthod.* 50, 170–176.

Ferracane, J. L. (2011). Resin Composite-State of the Art. *Dental Mater.* 27 (1), 29–38. doi:10.1016/j.dental.2010.10.020

Fronza, B. M., Rueggeberg, F. A., Braga, R. R., Mogilevych, B., Soares, L. E. S., Martin, A. A., et al. (2015). Monomer Conversion, Microhardness, Internal Marginal Adaptation, and Shrinkage Stress of Bulk-Fill Resin Composites. *Dental Mater.* 31 (12), 1542–1551. doi:10.1016/j.dental.2015.10.001

Kravitz, N. D., Kusnoto, B., Agran, B., and Viana, G. (2008). Influence of Attachments and Interproximal Reduction on the Accuracy of Canine Rotation with Invisalign. A Prospective Clinical Study. *Angle Orthod.* 78, 682–687. doi:10.2319/0003-3219(2008)078[0682:IOAAIR]2.0.CO;2

Lang, B. R., Jaarda, M., and Wang, R.-F. (1992). Filler Particle Size and Composite Resin Classification Systems. *J. Oral Rehabil.* 19, 569–584. doi:10.1111/j.1365-2842.1992.tb01487.x

Mantovani, E., Castroflorio, E., Rossini, G., Garino, F., Cugliari, G., Deregibus, A., et al. (2019). Scanning Electron Microscopy Analysis of Aligner Fitting on anchorage Attachments. *J. Orofac. Orthop.* 80, 79–87. doi:10.1007/s00056-018-00167-1

Morton, J., Derakhshan, M., Kaza, S., and Li, C. (2017). Design of the Invisalign System Performance. *Semin. Orthod.* 23, 3–11. doi:10.1053/j.sodo.2016.10.001

Nikolaidis, A. K., Koulaouzidou, E. A., Gogos, C., and Achilias, D. S. (2019). Synthesis and Characterization of Dental Nanocomposite Resins Filled with Different Clay Nanoparticles. *Polymers* 11 (4), 730. doi:10.3390/polym11040730

Rossini, G., Parrini, S., Castroflorio, T., Deregibus, A., and Debernardi, C. L. (2015). Efficacy of clear Aligners in Controlling Orthodontic Tooth Movement: A Systematic Review. *Angle Orthod.* 85, 881–889. doi:10.2319/061614-436.1

Satterthwaite, J. D., Maisuria, A., Vogel, K., and Watts, D. C. (2012). Effect of Resin-Composite Filler Particle Size and Shape on Shrinkage-Stress. *Dental Mater.* 28, 609–614. doi:10.1016/j.dental.2012.01.007

Satterthwaite, J. D., Vogel, K., and Watts, D. C. (2009). Effect of Resin-Composite Filler Particle Size and Shape on Shrinkage-Strain. *Dental Mater.* 25, 1612–1615. doi:10.1016/j.dental.2009.08.012

Simon, M., Keilig, L., Schwarze, J., Jung, B. A., and Bourauel, C. (2014). Treatment Outcome and Efficacy of an Aligner Technique - Regarding Incisor Torque, Premolar Derotation and Molar Distalization. *BMC Oral Health* 14, 68. doi:10.1186/1472-6831-14-68

Taheri, M. M., Abdul Kadir, M. R., Shokuhfar, T., Hamlekhan, A., Shirdar, M. R., and Naghizadeh, F. (2015). Fluoridated Hydroxyapatite Nanorods as Novel Fillers for Improving Mechanical Properties of Dental Composite: Synthesis and Application. *Mater. Des.* 82, 119–125. doi:10.1016/j.matdes.2015.05.062

Tanimoto, Y., Kitagawa, T., Aida, M., and Nishiyama, N. (2006). Experimental and Computational Approach for Evaluating the Mechanical Characteristics of Dental Composite Resins with Various Filler Sizes. *Acta Biomater.* 2 (6), 633–639. doi:10.1016/j.actbio.2006.06.006

Conflict of Interest: The authors declare that the research was conducted in the absence of any commercial or financial relationships that could be construed as a potential conflict of interest.

The reviewer BS declared a past collaboration with several of the authors CP, PC, and RL to the handling editor.

frontiers in Materials

REVIEW
published: 11 February 2022
doi: 10.3389/fmats.2022.819121

Clinical Performances and Biological Features of Clear Aligners Materials in Orthodontics

Monica Macrì, Giovanna Murmura, Giuseppe Varvara, Tonino Traini and Felice Festa*

Department of Innovative Technologies in Medicine and Dentistry, University "G. D'Annunzio" of Chieti-Pescara, Chieti, Italy

In recent years, aesthetic concerns regarding orthodontic appliances have significantly increased due to the growing number of adult patients undergoing orthodontic therapy. Clear removable aligners have seen growing popularity as an aesthetic and comfortable alternative to traditional fixed appliances. Clear aligner therapy also appears more respectful of the patient's periodontal health; in fact, clear aligners allow the patients to maintain proper daily oral hygiene thanks to being removable. Among the parameters that affect the clinical efficacy of aligners, the material employed for their manufacturing plays a key role. The present paper aims to review the most used materials in manufacturing clear aligners, focusing on their clinical and mechanical performances, according to the current state of literature. Furthermore, biological features of the different materials are also examined regarding their effects on dental and periodontal tissues, oral mucosa, and potential systemic effects.

Keywords: thermoplastic materials, physical properties, mechanical properties, clear aligner, clinical performances, biocompatibility

OPEN ACCESS

Edited by:
Michele Tepedino, University of L'Aquila, Italy

Reviewed by:
Roberto Savignano, Loma Linda University, United States
Miguel Ángel Garcés-Villalá, Catholic University San Antonio of Murcia, Spain

****Correspondence:***
Monica Macrì
m.macri@unich.it

Specialty section:
This article was submitted to Biomaterials, a section of the journal Frontiers in Materials

Received: *20 November 2021*
Accepted: *03 January 2022*
Published: *11 February 2022*

Citation:
Macrì M, Murmura G, Varvara G, Traini T and Festa F (2022) Clinical Performances and Biological Features of Clear Aligners Materials in Orthodontics. Front. Mater. 9:819121. doi: 10.3389/fmats.2022.819121

1 INTRODUCTION

The idea to employ clear overlay orthodontic appliances to move progressively misaligned teeth was introduced in 1946 by Kesling, who described how consecutive tooth movement is possible by utilising positioners produced from setup models (Kesling, 1945; Kesling, 1946).

In the last decades, thanks to the introduction and spread of CAD/CAM technologies in dentistry, the use of clear removable splints for orthodontic purposes has received a great impulse.

The first digitally designed and manufactured aligners system was the Invisalign system, a series of removable polyurethane aligners launched in 1998 by Align Technology (Santa Clara, CA, United States). In 1999 it was presented at the American Congress of Orthodontists. In 2001 it was introduced in Europe (Galan-Lopez et al., 2019). Currently, it is one of the most used clear aligners systems worldwide (Galan-Lopez et al., 2019; Nemec et al., 2020).

In recent years, the increase of adult patients undergoing orthodontic treatments has led to the widespread clear aligner therapy (CAT), considered a valid alternative to conventional fixed appliances for its aesthetic features and comfort (Rosvall et al., 2009; Fujiyama et al., 2014). Literature has reported various potential advantages correlated to CAT, such as the maintenance of better oral hygiene and periodontal health (Rossini et al., 2015; Lu et al., 2018; Wu et al., 2020), reduction in the amount and incidence of root resorption following orthodontic therapy (Yi et al., 2018; Li et al., 2020), the improvement of TMD-related pain and headache (Festa et al., 2021). Nowadays, clear aligner systems are produced

TABLE 1 | Chemical (molecular) structure of some widely mass-marketed aligners and retainers.

Aligner	Material	Manufacturer
Biolon	PET-G (Polyethylene terephthalate glycol)	Dreve dentamid GmbH. Unna, Germany
Duran	PET	Scheu dental, Iserlohn, Germany
EasyDU	PET (PFb/PFc)	BenQ Co., Taipei, Taiwan
F22	Polyurethane	Sweden-Martina, Due Carrare, PD, Italy
Invisalign	SmartTrack (multi-layer aromatic thermoplastic polyurethane)	Align Technology, Santa Clara, CA, United States
MaxFlex	TPU	Maxflex Co., Taipei, Taiwan
Nuvola	Polyethylene terephthalate glycol (PET-G)	GEO srl, Rome, RM, Italy
Spark	Trugen (multi-layer polyurethane)	Ormco Orange, CA, United States

worldwide by numerous companies, including leading brands in orthodontic products (**Table 1**).

The clinical efficacy of clear aligners can be affected by many factors. Undoubtedly, the properties of materials used to produce clear aligners are among the essential aspects in determining their mechanical and clinical features.

The present paper study reviews the most employed materials in the manufacturing of clear aligners, focusing on their mechanical performances and biological features about their effects on dental and periodontal tissues and oral mucosa.

2 CLEAR ALIGNERS MATERIALS

Materials employed to produce Clear Aligners can affect their clinical performances (Zhang et al., 2011; Lombardo et al., 2017). The type of material used depends on the manufacturing process. Aligners can be produced by moulding the material on physical models, derived from a virtual planning software through 3D printing, or generated directly by 3D printing, without physical models (Tartaglia et al., 2021).

Currently, since no approved photo polymerisable resin is suited for direct printing, only thermoformed aligners are commercialised and clinically employed (Tartaglia et al., 2021).

2.1 Thermoplastic Materials

According to their molecular structure, thermoplastic polymers can be classified into amorphous and semicrystalline polymers. Amorphous polymers have irregularly arranged molecular structures characterised by a low degree of molecular packing. Semicrystalline polymers, instead, contain both areas of uniformly and tightly packed chains (crystalline domains) and irregularly arranged areas (amorphous regions). Crystalline domains can be comparable to fillers in composite materials in these polymers, which confer hardness and rigidity. In general, amorphous polymers are softer, transparent, have low shrinkage, and have better impact resistance. Semicrystalline polymers are hard, opaque or translucent, have good chemical resistance and have a sharp melting point (Chalmers and Meier, 2008; Condò et al., 2021).

The most used polymers, individually or blended, for the production of transparent orthodontic aligners are polyester, polyurethane, and polypropylene (Zhang et al., 2011; Condò et al., 2021).

Among polyesters, polyethylene terephthalate (PET) and polyethylene terephthalate glycol (PETG), a non-crystallising amorphous copolymer of PET, are widely used in the production of clear aligners thanks to their excellent mechanical and optical properties (Dupaix and Boyce, 2005).

Polycarbonate (PC) is also employed for its durability, hardness and transparency (Zhang et al., 2011).

Thermoplastic polyurethane (TPU) an extremely versatile material, featuring several favourable properties such as excellent mechanical and elastomeric characteristics, chemical and abrasion resistance, adhesion properties, simplicity of machining (Frick and Rochman, 2004; Zhang et al., 2011).

Invisalign aligners, were initially produced of a single-layer of polyurethane, Exceed-30 (EX30). In 2013, EX30 was substituted by a new polymer, named Smart Track (LD30) a multilayer aromatic thermoplastic polyurethane/copolyester (Rossini et al., 2015; Li et al., 2020). According to the producer, the new material should provide the aligners with more elasticity and produce more constant forces, improving their clinical efficacy (Lombardo et al., 2017; Condò et al., 2021).

PC, PETG are classified as amorphous (Chen et al., 2011; Demirel et al., 2011). Depending on processing procedures, PET and TPU can have an amorphous or semicrystalline structure (Frick and Rochman, 2004; Condò et al., 2021).

2.2 Polymers Blends

Thermoplastic orthodontic devices should exert continuous and controlled forces to produce correct tooth movements (Zhang et al., 2011).

Mechanical properties of the polymers can be improved by mixing various types of them: polyester, polyurethane, and polypropylene are the most used materials in the polymer blends employed in manufacturing of clear aligners (Zhang et al., 2011; Condò et al., 2021).

Large number of studies on thermoplastic polymer blends has been produced in recent years: (Medellín-Rodríguez et al., 1998; Hwang et al., 1999; Poomali et al., 2008; Zhang et al., 2011; Ma et al., 2016; Seeger et al., 2018). Polymer blending has proven to be a viable way to improve the physical and chemical properties of polymers, thereby enhancing the clinical performances of aligners.

The blending ratio of polymers employed plays an essential role in determining the features of the blend. For example, blending PETG/PC/TPU at the 70/10/20 ratio showed the best mechanical properties compared to other blending ratios, providing sufficient and sustainable orthodontic forces than other commercialised products (Zhang et al., 2011). PETG/PC2858 blend, at 70/30 ratio, expressed the best combination of tensile strength, impact strength and elongation at break (Ma et al., 2016).

2.3 3D Printed Aligners

According to some authors, 3 days printed aligners can offer several advantages compared to thermoformed ones. Direct 3D printing can avoid adverse effects of thermoforming processes, such as alteration of mechanical, dimensional and aesthetic characteristics of the material (Ryu et al., 2018), offering better geometric accuracy and precision, better fit, higher efficacy and mechanical resistance and reproducibility (Maspero and Tartaglia, 2020).

3D printing techniques utilizable to build directly printed aligners can be numerous such as selective laser sintering (SLS), laser sintering melting (SLM), stereolithography (SLA). However, 3D printing by photo-polymerisation of clear liquid resin seems to be the most suitable procedure (Tartaglia et al., 2021).

Material employed through 3D printing in orthodontics can be very different. Among those, we can find acrylonitrile-butadiene-styrene plastic, stereolithography materials (epoxy resins), polylactic acid, polyamide (nylon), glass-filled polyamide, silver, steel, titanium, photopolymers, wax, and polycarbonate (Prasad et al., 2018).

Various studies have investigated mechanical and biological properties of resins suitable for 3D printing of clear aligners (Nakano et al., 2019; Maspero and Tartaglia, 2020); however, at present, no polymerizable material has yet been approved for the production of directly printed aligners (Tartaglia et al., 2021).

3 MECHANICAL AND PHYSICAL PERFORMANCES OF CLEAR ALIGNER MATERIALS

Dental misalignment and malocclusions usually compromise patients' aesthetics and smiles, which negatively impacting oral hygiene and periodontal health. Nowadays, the main reason patients today decide to undergo orthodontic treatment is precisely the improvement of the aesthetics of the face, and in turn, aesthetics play an essential role in the choice of orthodontic treatment. An increasing number of adult and adolescent patients require orthodontic treatment using transparent aligners because it is effective and does not compromise the quality of life because it is invisible (Bucci et al., 2019; Tartaglia et al., 2021).

Another benefit of these aligners is that they are removable, so they do not compromise the patients' oral hygiene, and the result is more comfortable than fixed appliances (Tartaglia et al., 2021).

The treatment is based on a sequence of upper and lower transparent aligners that the patient wears 22 h/day and changes after 14 days (Lombardo et al., 2015).

Thermoplastic materials of the aligners are polymers with different characteristics that respond differently to various types of mechanical stress such as chewing, physical stress such as heat and chemicals stress such as colouring agents, salivary enzymes and mouthwashes (Lombardo et al., 2015; Ma et al., 2016).

The ideal aligner should have excellent transparency, low hardness, resilience, elasticity, resistance to mechanical stress and overtime and biocompatibility. Therefore, to improve the performance of aligners in orthodontic treatment, it is significant to investigate the properties characteristic of the materials and how they respond to various stresses and then develop the more performing ones, for example, combining them (Ma et al., 2016).

3.1 Colour Stability and Transparency of Different Types of Clear Aligners Materials

In light of the patient's aesthetic, the transparency of the aligner should remain stable approximately during the 2 weeks of treatment (Liu et al., 2016). However, the aligners' colour stability and transparency are affected by colouring drinks, ultraviolet radiation, and mouthwashes (Bernard et al., 2020).

The dentists always recommend that patients remove the aligners when eating or drinking anything (except water). Often, many patients ignore the doctor's requests and eat and drink with the aligners, undermining their transparency, which is the essential aesthetic characteristic of the resinous copolymer that composes them (Bernard et al., 2020). It has been found that about 50% of Americans do not remove aligners for eating and drinking (Liu et al., 2016).

Different studies aim to investigate the aligners' colour stability and transparency when exposed to colouring agents and saliva (Liu et al., 2016; Daniele et al., 2020). The materials examined were: multi-layered thermoplastic polyurethane with integrated elastomer (Smart Track); one material based on PET-G (Erkodur), one material of copolyester (Essix ACE), two based on PET (Essix Plastic e Ghost aligner) and resinous polyurethane (Zendura).

Visual inspection about colour stability indicated that all types of aligners showed no colour change after the 12-h, in contact with colouring agent (wine, coffee, black tea, cola and nicotine) except for the Smart Track in coffee and red wine.

With the increase of the time to 7 days, all the aligners showed colour changes slightly, except for the immersion in the coffee solution and black tea, which created an important colour change for all brands after 7 days. show a perceivable colour variation. In this last case, Essix P., Gost Aligner, Essix A and Zendura samples exhibited a slight colour variation;

TABLE 2 | Colour stability.

Time after	Coffee	Red wine	Nicotine	Artificial saliva	Black tea*	Cola*
12h						
Smart track**						
zendura						
erkodur						
Essix ace						
Essix Plastic						
Ghost aligner						
7 gg						
Smart track**						
Zendura						
erkodur						
Essix Ace						
Essix Plastic						
Ghost aligner						
14gg						
Smart Track**						
Zendura						
Erkodur						
Essix Ace**						
Essix Plastic						
Ghost aligner						

Not colored
slight
moderate
strong
Not tested

Grade of extrinsic coloration of aligners
*colouring agents tested only after 12h and 7 days
**materials not tested after 14 days

while the Erkodur and SmartTrack samples display marked colour changes. Regarding the red wine, ST exhibit a substantial colour change after 7-day immersion.

Considering the immersion in the nicotine solution for 14 days, all the samples have only slightly colour changes; when immersed in red wine, they revealed enhanced colour variation, especially for Zendura and Essix P., while the other disks presented only perceivable variations (**Table 2**).

3.2 The Influence of Thermoforming Process

Changes in material performances are made out also by the thermoforming process.

Various studies show how the transparency, hardness and thickness vary before and after the aligner's thermoforming process (Ryu et al., 2018; Bucci et al., 2019).

Ryu et al. study (Ryu et al., 2018) relates the thickness of the materials to the transparency before and after the thermoforming process and shows changes in four types of materials (two copolyester-based: Essix A + and Essix ACE another two pet-g based: Duran and ECligner).

The study has shown that thermoforming affects the material's transparency by decreasing it. After thermoforming, the transparency of the eCligner samples, 0.5 and 0.75 mm thickness, respectively, is remarkably reduced compared to that which characterises the Duran and Essix A + samples of the same thickness.

The Essix ACE sample, 0.75 mm thick, shows an important decrease in transparency compared to eCligner, with a thickness of 0.75 mm.

Furthermore, the transparency of Duran and Essix A + samples (wall thickness) are significantly lower after the thermoforming compared to the pre-forming value, while no significant differences are seen, pre and post thermoforming, for the eCligner and Essix ACE samples.

The solubility in water and its absorption also affects the hardness of the material.

The hardness of all four materials did not show a significant difference compared to controls before thermoforming (Ryu et al., 2018).

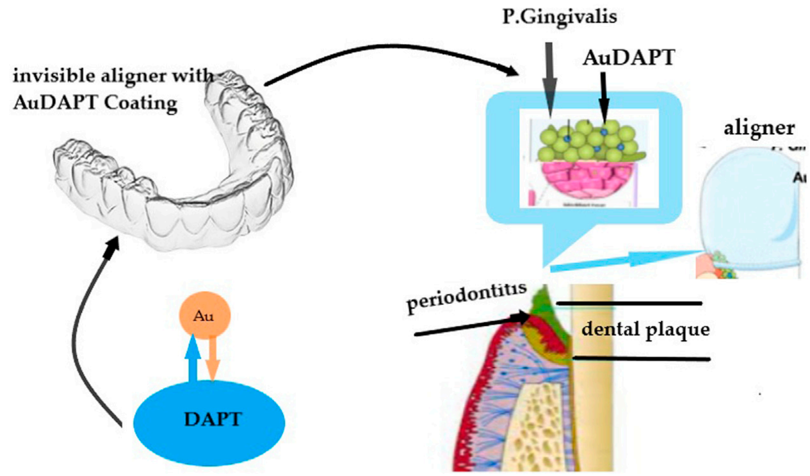

FIGURE 1 | Aligner with AuDAPT Coating.

In all four materials, there is an increase in the absorption ability of water after thermoforming. As for the solubility in water, there is a significant increase for Duran, Essix A + and Essix ACE samples, unlike what happens for eCligner samples.

However, The hardness of essix A and Essix Ace samples was less than the eCligner samples after thermoforming. Essix A + and Essix ACE samples showed higher surface hardness after thermoforming than before thermoforming (Ryu et al., 2018).

It has been seen through another study (Bucci et al., 2019) that investigated two types of aligners, one passive and one active in PET-G 0.75 mm film, that the thermoforming process can make changes in the thickness of the aligners.

After thermoforming, There are different thicknesses throughout the occlusal surface ranging from a minimum value of 0.38 mm to a maximum of 0.69 mm.These values are lower than the 0.75 of the original PET-G sheets before being thermoformed.

Despite this variation, this does not affect the clinical performance of the devices.

Similar results are also obtained in the *in vitro* study of Dalaie et al. (Dalaie et al., 2021).

The study of Dalaie et al. investigated the thermomechanical properties of two PET-G aligners of two different thicknesses, 1 and 0.8 mm, in response to thermoforming; it has been seen that in both types, the hardness decreases by about 7.6% after thermoforming, but there are no significant differences in hardness into the two types of aligners. The reduction of thickness decreases after thermoforming in both types of aligners, which justifies the reduction of flexural modulus (Dalaie et al., 2021). Comparing the flexural modulus of Duran with a thickness of 0.75 and Duran 1mm, the first modulus increases and the second decrease, meaning that with increasing thickness of the Pet-G sheets, the bending modulus decreases (Dalaie et al., 2021).

3.3 The Influence of the Oral Environment

In the oral cavity, the aligners are subject to humidity, salivary enzymes and temperature variations that can alter their shape and properties throughout time. However, they are also subjected to continuous and intermittent forces due to normal oral functions such as chewing, speaking, swallowing and parafunction such as clenching and grinding (Bucci et al., 2019). The temperature of the oral environment can rise to 57° after taking a hot drink, and it can take several minutes to return to its original temperature. Such temperature increases can affect the mechanical properties of thermoplastics (Iijima et al., 2015). As evidence of this, there are several *in vivo* and *in vitro* studies (Ryokawa et al., 2006; Iijima et al., 2015; Bucci et al., 2019; Dalaie et al., 2021).

One *in vitro* study based its results on comparing eight different types of most used materials (PET-G, PC, PP, PUR, A +, C +, PE and EVA) from different manufacturers and placed them in contact with a solution that simulated the oral environment (Ryokawa et al., 2006).

It assessed that the elastic modules of Polycarbonate (PC), PET-G and Essix A + in the intraoral environment exhibited significant increases compared to the original samples; in reverse, those of polypropylene (PP), C +, polyethylene (PE) and Ethylene Vinyl Acetate (EVA)were significantly reduced. No significant changes were observed in the polyurethane (PUR).

On the other hand, an increase in thickness in all materials was also highlighted due to water absorption (Ryokawa et al., 2006).

The *in vitro* study by Dalaie (Dalaie et al., 2021) simulated the temperature variations that occur in the oral environment through intermittent thermocycles, 22 h per day for 14 days and studied how the hardness, thickness and flexural modulus of two aligners (in Pet-G foil with thicknesses of 1 and 0.8 mm) vary in contact of the oral environment.

Significant variations in hardness were highlighted only in the 0.8 mm thick PET-G sheet; in the other 1 mm sheet, there were no significant ones. This increase in hardness can be attributed to changes in the crystalline and amorphous structures or the release of plasticisers after exerting intermittent thermal cycling.

The study aimed to investigate the effects of temperature variations on the shape memory properties of five

TABLE 3 | Cytotoxicity of four of different thermoplastic materials for clear aligners. Cell viability (%) = (optical density of test group/optical density of cellular control group) × 100. Cytotoxicity scored according to the classification of Ahrari et al. (from Martina et al., modified) (Ahrari et al., 2010; Martina et al., 2019).

Brand	Composition	Cell viability (%)	Cytotoxicity
Biolon	Polyethylene terephthalate glycol (PETG)	64.6 ± 3.31	Slight
Zendura	Polyurethane resin	74.4 ± 2.34	Slight
SmartTrack	Multilayer aromatic thermoplastic polyurethane	78.8 ± 6.35	Slight
Duran	Polyethylene terephthalate glycol (PETG)	84.6 ± 4.02	Slight

thermoplastic materials with different glass transition temperatures and different crystalline structures (Iijima et al., 2015). The materials selected are PET-G (Duran), polypropylene (Hardcast), polyurethane polymers (PU1 PU2 PU3) with three different glass transition temperatures.

The mechanical properties for each material were significantly reduced after 2,500 thermocycles, and a significant decrease is observed in Hardcast material (crystal plastic) with the highest Tg (155.5°) and PU 1 (crystalline or semicrystalline plastic) with the lower Tg (29.6°C). Duran (73.3°), PU 2 (56.5°) and PU3(80.7°), with intermediate Tg, exhibited more stable mechanical properties. Polyurethane polymers exhibited excellent shape memory undergoing the range of intraoral temperature variations.

The orthodontic strength produced by thermoplastic devices decreased for all materials with the gradual temperature change.

The *in vivo* study (Bucci et al., 2019) plays an essential role in the orthodontic history of materials because it considers the oral cavity's temperature variations and all the oral functions and parafunction to which the aligners are subjected.

A series of passive and active aligners formed by PET-G foil is used in this study, and patients were instructed to wear them 10 days for 22 h per day, and it was seen how their thickness changes after this time.

It was found that there were small reductions in the thickness of the aligner after 10 days but not significant as to affect the therapeutic performance, so the sheets of PeT-G have good stability in contact with the oral environment (Bucci et al., 2019).

3.4 The Influence of Mechanical Stress and the Phenomenon of Stress Relaxation

The aligners have an essential characteristic; they are viscoelastic, so they are in the middle between the properties of viscous and elastic materials. This means that their behaviour can vary significantly over time under load, even when inserted first and before any tooth movement.

Under constant loads, the deflection of the viscoelastic material increases over time, while at constant deflection, the loads decrease, and this phenomenon is called self-relaxation (Lombardo et al., 2017).

As already mentioned, the aligners placed in the oral cavity are subject to various stresses and intermittent loads in the long and short term. The phenomenon of stress relaxation reduces the forces exerted by the aligner placed in the mouth, at constant deflection and before the tooth begins to move. However, this depends on the characteristics of the material of aligners and the magnitude of the applied loads. It is essential to consider this reduction and quantify it to ensure that tooth movement occurs.

To examine the different mechanical characteristics of the materials, the study (Lombardo et al., 2017) investigated four types of materials, two single-layer materials based on PET-G and polyurethane and two multilayers.

After an initial resistance test, the samples were subjected to a constant load for 24 h in a humid environment and at a constant temperature, and the stress relaxation of the various materials was measured; the test was performed three times.

The monolayered aligners showed significant resistance to absolute stress and stress relaxation speed; the multi-layered ones instead showed a constant stress relaxation but an absolute stress resistance four times lower than the monolayered ones. In general, all the materials tested showed a significant relaxation to rapid stress in the first 8 h, but 24 h, it tended to plateau for some materials; for others, it decreased. The polyurethane-based monolayer aligner produced higher initial stress values and a high decay rate, the other one based on Pet-g showed the most significant stress relaxation rate during 24 h. Multilayers showed lower stress relaxation rates and lowered initial stress values than monolayers (Lombardo et al., 2017).

4 BIOCOMPATIBILITY OF MATERIALS USED AS ORTHODONTIC ALIGNERS

According to a retrospective analysis by FDA (Food and Drug Administration) (Allareddy et al., 2017), the adverse clinical events reported during the use of active aligners were analysed. During a 10-years observation period, the most frequently reported adverse events are difficult breathing, sore throat, swollen throat, swollen tongue, hives and itchiness, anaphylaxis (Allareddy et al., 2017) adverse events during use of Invisalign Technology.

4.1 Cytotoxicity of Materials

The lack of scientific literature due to the few studies available and the contradictory results have kept the debate open about the existence of toxic effects related to the use of invisible aligners. Moreover, the increasing introduction of the new aligners has provided the need to test the cytotoxicity of the materials used by various manufacturers.

In vitro studies have evaluated the potential toxicity of thermoplastic materials used by different brands. Four different materials used for the aligners were evaluated: Duran (Germany), Biolon (Germany), Zendura (United States) and

SmartTrack (United States). Human Gingival Fibroblasts (HGFs) are the cell lines often used to verify the biocompatibility of dental materials. Their use *in vitro* is recommended by the International Standards Organization (ISO) (Martina et al., 2019) because they constitute the main cell line present in the oral tissues and are the most exposed to the toxic effects of the materials of the aligners as they are in intimate contact with the periodontal tissues when they are in placeAmong the four tested materials, Biolon showed the highest toxic action on HGFs, followed by Zendura, SmartTrack, and finally, Duran proved to have the lowest toxic activity. In this study, it appears that all tested materials exhibit low *in vitro* toxicity on the tested cells. (**Table 3** (Ahrari et al., 2010; Martina et al., 2019))

On the other hand, there are only two previous studies in which the cytotoxicity of clear aligner materials is tested. Eliades et al. evaluated the potential release of Bisphenol-A (BPA) from the materials used by the Invisalign technology (Eliades et al., 2009). The study shows the non-existence of estrogenic and toxic effects on HGFs, in contrast to the slight toxicity that emerged from the current study.

It has been shown that the chemical composition of thermoplastic Invisalign materials does not have the elements necessary to release BPA. Isocyanate and not BPS is the component that could develop potentially harmful effects on health (Alexandropoulos et al., 2015). Premaraj et al. (2014) found that the isocyanate in Invisalign aligners can trigger oral health effects. Allergic contact reactions have been reported following exposure to isocyanate. After contact with oral tissues, isocyanates react by rapidly binding to proteins and biomolecules, creating an immunogenic event that leads to a sensitization reaction in humans. These experiments have shown that the contact of the gingival epithelial cells with the plastic material in a saline-based environment determines an interruption of the membrane integrity, reduced metabolism and reduced cell-cell contact capacity. These Phenomena did not occur in artificial saliva. The results can play a protective role and reduce the effects of the plastic material of the allineators.

4.2 Gold Nanoparticle-Modified Dental Aligner Used as Periodontal Therapy

The correlation between the gingival pocket depth, gingival bleeding, periodontal disease and the presence of a type of bacteria in periodontal pockets have been widely demonstrated (De Iuliis et al., 2016). Appreciable changes in the oral microbiome, with higher anaerobic and facultative anaerobic bacteria, have been detected in patients wearing fixed orthodontic appliances (Kado et al., 2020). This effect is attributed to the fact that fixed appliances make dental hygiene procedures more difficult due to brackets and archwires. Conversely, the use of removable appliances may allow orthodontic patients to maintain adequate oral hygiene by allowing the standard procedures of brushing and flossing, which can be performed by easily removing the splint. Even though causing a significant change in the composition of the subgingival microbiome, CAT has shown to produce no changes in the relative presence of periodontal pathogens, at least in the first 3 months of therapy (Guo et al., 2018).

Several studies, referring to periodontal indexes such as plaque index, gingival index, probing depth, have reported that patients undergoing CAT have better periodontal health than those treated with fixed orthodontic appliances (Rossini et al., 2015; Lu et al., 2018; Wu et al., 2020).

A recent study showed that the aligners coated with gold nanoparticles (Zhang et al., 2020) determine favourable antibacterial activity against P. gingivalis, one of the bacteria responsible for the onset of periodontal disease and other systemic diseases such as Alzheimer's disease. P. gigivalis has recently been identified in the brains of patients with Alzheimer's disease (Kaye et al., 2010; Dominy et al., 2019). This finding could lead to considerations of using aligners as a means of long-term drug delivery in patients with P. gingivalis infection. The antibacterial action of gold nanoparticles (NPs) has opened up new research fields. Studies indicate the gold NPs exert their antibacterial action in different ways, such as reducing membrane potential, inhibiting ATPase activity, inhibiting the binding of ribosomes to tRNA. To evaluate the biocompatibility of AuDAPT, the haemolytic properties on mouse erythrocytes were tested. The results highlighted the absence of harmful irritative effects on the oral mucosa. Thus, AuDAPT can be applied for oral applications (**Figure 1**).

In conclusion, we can state that AuDAPT-coated aligners can perform antibacterial activity on P. gingivalis. Aligners coated with AuDAPT could slow biofilm formation showing favourable biocompatibility. This system could be used for the treatment of systemic infections related to periodontal disease.

5 DISCUSSION

In general, ideal properties of active components of orthodontic devices are considered large spring back, low stiffness, good formability, high stored energy, biocompatibility, and environmental stability (Kapila and Sachdeva, 1989). Even for clear aligners, the main features to be sought, in addition to high transparency and aesthetic stability, should be low hardness, good elasticity and resilience, resistance to ageing (Zhang et al., 2011; Ma et al., 2016). Physical and chemical characteristics of materials employed in the manufacturing of aligners are crucial in determining such features.

Nowadays, the material used to manufacture the aligners are polyethylene terephthalate glycol (PeT-G), polypropylene (PP), polycarbonate (PC), thermoplastic polyurethanes (TPU), ethylene-vinyl acetate (EVA) and many more (Lombardo et al., 2015).

This article investigates the performance of materials used in thermoplastic aligners, such as polyethylene terephthalate glycol (PeT-G), thermoplastic polyurethanes (TPU), polyethylene terephthalate PET.

Regarding aesthetic performances associated with colour stability and transparency, several studies show that the Ghost aligner based on pet-g material is more stable than the other in contact with colouring agents, especially coffee and red wine, after 7 days.

Colour stability and transparency of the aligner should remain stable approximately during the 2 weeks of treatment, but the studies and results are limited in this range of time.

Changes in material performances are made out also by the thermoforming process.

The thickness and hardness of aligners are significant; play a role in the magnitude of the forces delivered on the tooth by the device and, therefore, the performance of the aligners in orthodontic treatment.

The negative results of the thermoplastic process marked changes in the material's properties in response to the generation of heat used during thermoforming.

Ryu et al. (2018) show that the transparency decreases in all the samples after the thermoforming process, and the samples of Essix Ace copolyester-based (0.75 thickness) displays less transparency than the other samples after thermoforming of the same thickness.

After the thermoforming process, lower transparency values are recorded in the samples that had less thickness; for example, the transparency of Duran and Essix A + samples (0.5 mm thickness) is significantly lower after the thermoforming compared to the pre-forming value, so this means that after thermoforming, the transparency decreases with decreasing thickness, since the thermoplastic material is deformed, resulting in a decrease in transparency, without compromise the aesthetics of the aligners themselves.

This finding contrasts with a previous study an increase in transparency with decreased thickness (Azhikannickal et al., 2012).

Regarding the hardness and water solubility, all thermoplastic materials show an increase in water absorption capacity following thermoforming and water solubility, except for the eCligner sample. (Ryu et al., 2018).

The hardness of the thermoplastic materials tested in this study increased after thermoforming. At the same time, the samples of Essix a and Essix Ace show a significant increase of hardness after thermoforming in the other samples is not so different from before thermoforming process. This means that the mechanical properties of the thermoplastic materials used for the production of CA should be studied for their clinical application, thinking to the thermoforming process.

This study contrasts with Delaie's study (Dalaie et al., 2021), which investigates the thermomechanical properties of two PET-G aligners of two different thicknesses, 1 and 0.8 mm, in response to seeing in both types, the hardness decreases by about 7.6% after thermoforming.

In the oral cavity, the aligners are subject to humidity, salivary enzymes and temperature variations that can alter their shape and properties throughout time. However, they are also subjected to continuous and intermittent forces due to normal oral functions such as chewing, speaking, swallowing and para functions such as clenching and grinding. (Bucci et al., 2019).

However, few *in vivo* studies can reproduce the natural oral environment in light of those facts. (Iijima et al., 2015). From this *in vitro* study (Ryokawa et al., 2006), the elastic modules of PC, PETG and A + in the intraoral environment showed significant increases compared to the original sample; in reverse, those of PP, C +, PE, and EVA were significantly reduced. No significant changes were observed in the PUR.

On the other hand, increased thickness in all materials was also highlighted due to water absorption.

The temperature variations that occur in the oral environment is replicated through intermittent thermocycles, 22 h per day for 14 days, and this study show how the hardness, thickness, and flexural modulus of two aligners based on PET-G of 1 and 0.8 mm of thickness vary in contact with this temperature variations (Dalaie et al., 2021).

Significant variations in hardness were highlighted only in the 0.8 mm thick PET-G sheet; in the other 1 mm sheet, there were no significant ones. The changes in the crystalline and amorphous structures or the release of plasticisers probably are linked to the increase in hardness after exerting thermal cycling (Dalaie et al., 2021).

Temperature variations linked to the oral environment also influenced the mechanical performance of materials, depending on different glass transitions (Iijima et al., 2015).

The materials such as Hardcast (polypropylene) with the highest Tg (155.5°) and PU 1 (crystalline or semicrystalline plastic) with the lower Tg (29.6°C) were significantly decreased in mechanical properties after 2,500 thermo cycles, on the other hand, Duran, PU2 and PU3 which had intermediate Tg (75.3°C for Duran, 56.5°C for PU 2 and 80.7°C for PU 3) showed stable mechanical properties (Iijima et al., 2015).

The orthodontic strength produced by devices decreased for all materials with the gradual temperature variation. (Ryokawa et al., 2006; Iijima et al., 2015; Bucci et al., 2019; Dalaie et al., 2021).

In the "*in Vivo*" study (Bucci et al., 2019), a series of passive and active aligners formed by PET-G foil was used, and patients were instructed to wear them 10 days for 22 h per day, and it was seen how their thickness changes after this time.

Ten days is a limited time, and usually in agreement with the doctor, it is decided to have them worn 14 days, the increase in the time they have to stay in the mouth can affect the loss of thickness.

Within the study's limits, the results show that there were small reductions in the thickness of the aligners after 10 days, but not significant as to affect the therapeutic performance, so the sheets of PeT-G have good stability in contact with the environment. (Bucci et al., 2019).

As already mentioned, the aligners placed in the oral cavity are subject to various stresses and intermittent loads in the long and short term. (Bucci et al., 2019).

To examine the different mechanical characteristics of the materials and their resistance to absolute stress and stress relaxation speed, a study investigates four types of materials, two single-layer materials based on PET-G and polyurethane and two multilayers in contact with a humid environment from 8 to 24 h (Lombardo et al., 2017).

The monolayered aligners showed significant resistance to absolute stress and stress relaxation speed; the multi-layered ones instead showed a constant stress relaxation but an absolute stress resistance four times lower than the monolayered ones. In general, all the materials tested showed a significant relaxation to rapid stress in the first 8 hours, but 24 h tended to plateau for some materials; for others, it decreased. (Lombardo et al., 2017).

The biocompatibility of clear aligners is still an open research field due to the lack of scientific literature and the few studies performed. The analysed studies evaluated *in vitro* toxicity of different thermoplastic materials used by the different brands. According to the experimental studies performed, all clear aligner materials exhibited mild cytotoxicity (Martina et al., 2019). Exposure of gingival epithelial cells to aligner plastics in a saline environment resulted in a reduction in membrane integrity, reduction in metabolic activity, and reduced intercellular contact of cell-cell junctions. The same effects were not found in artificial saliva. The results show how the plastic effects of active aligners can be neutralised or reduced in the presence of artificial saliva. Saliva could play an essential role in maintaining the integrity of epithelial cells (Premaraj et al., 2014).

It is essential to consider that it is difficult to compare the effects obtained *in vitro* with an *in vivo* environment, so we still do not have certainty regarding the absence of harmful effects for oral epithelium. In conclusion, we can state that the clear aligner materials showed only a low level of cytotoxicity, and the clinical use could be considered safe. Literature studies reveal that the use of clear aligners guarantees better maintenance of periodontal health than fixed appliances. The oral microbioma changes during orthodontic treatment with fixed appliances, increasing anaerobic bacteria and periodontal pathogens. This change is responsible for the transition from oral health to periodontitis (Kado et al., 2020). The qualitative and quantitative evaluation of plaque showed that periodontal health during treatment with CAT is better than treatment with fixed appliances. There is a significant decrease in periodontal indices (GI, PBI, BoP, PPD) (Rossini et al., 2015). The studies demonstrated that the periodontal status during orthodontic treatment with CAT is much superior to conventional fixed appliances (Wu et al., 2020).

Nanomaterials have recently been reported to exhibit antimicrobial activities above all gold, (NP) nanoparticles. Both *in vitro* and *in vivo* experiments were performed to evaluate the biocompatibility of the basis of AuDAPT. The antibacterial action of gold NPs is currently an active research field. Aligners coated with AuDAPT demonstrated favourable biocompatibility and an ability to slow biofilm formation (Zhang et al., 2020). It is thought that this method could be used to treat systemic infections related to periodontal disease. However, further information is needed because the microorganisms present in the oral cavity are more complex than a single type of bacterium. Investigation should be conducted in the future to simulate the biological environment and develop suitable methods for treating bacterial-related oral diseases through dental devices.

AUTHOR CONTRIBUTIONS

MM wrote the article. MM, FF, GM, TT, and GV researched the articles for the review and selected the appropriate studies. MM, GM, TT, GV, and FF analysed the studies for the review. All the authors read and approved the final manuscript.

REFERENCES

Ahrari, F., Afshari, J. T., Poosti, M., and Brook, A. (2010). Cytotoxicity of Orthodontic Bonding Adhesive Resins on Human Oral Fibroblasts. *Eur. J. Orthod.* 32 (6), 688–692. doi:10.1093/ejo/cjq019

Alexandropoulos, A., Al Jabbari, Y. S., Zinelis, S., and Eliades, T. (2015). Chemical and Mechanical Characteristics of Contemporary Thermoplastic Orthodontic Materials. *Aust. Orthod. J.* 31 (2), 165–170.

Allareddy, V., Nalliah, R., Lee, M. K., Rampa, S., and Allareddy, V. (2017). Adverse Clinical Events Reported during Invisalign Treatment: Analysis of the MAUDE Database. *Am. J. Orthod. Dentofacial Orthopedics* 152 (5), 706–710. doi:10.1016/j.ajodo.2017.06.014

Azhikannickal, E., Bates, P. J., and Zak, G. (2012). Laser Light Transmission through Thermoplastics as a Function of Thickness and Laser Incidence Angle: Experimental and Modeling. *J. Manuf Sci. Eng.* 134 (6). doi:10.1115/1.4007619

Bernard, G., Rompré, P., Tavares, J. R., and Montpetit, A. (2020). Colorimetric and Spectrophotometric Measurements of Orthodontic Thermoplastic Aligners Exposed to Various Staining Sources and Cleaning Methods. *Head Face Med.* 16 (1), 2. doi:10.1186/s13005-020-00218-2

Bucci, R., Rongo, R., Levatè, C., Michelotti, A., Barone, S., Razionale, A. V., et al. (2019). Thickness of Orthodontic clear Aligners after Thermoforming and after 10 Days of Intraoral Exposure: a Prospective Clinical Study. *Prog. Orthod.* 20 (1), 36. doi:10.1186/s40510-019-0289-6

Chalmers, J. M., and Meier, R. J. (2008). *Molecular Characterization and Analysis of Polymers*. Amsterdam: Elsevier.

Chen, L., Zhang, X.-l., Li, H.-y., Li, B., Wang, K., Zhang, Q., et al. (2011). Superior Tensile Extensibility of PETG/PC Amorphous Blends Induced via Uniaxial Stretching. *Chin. J. Polym. Sci.* 29 (1), 125–132. doi:10.1007/s10118-010-1006-6

Condò, R., Mampieri, G., Giancotti, A., Cerroni, L., Pasquantonio, G., Divizia, A., et al. (2021). SEM Characterization and Ageing Analysis on Two Generation of Invisible Aligners. *BMC Oral Health* 21 (1), 316. doi:10.1186/s12903-021-01676-z

Dalaie, K., Fatemi, S. M., and Ghaffari, S. (2021). Dynamic Mechanical and thermal Properties of clear Aligners after Thermoforming and Aging. *Prog. Orthod.* 22 (1), 15. doi:10.1186/s40510-021-00362-8

Daniele, V., Macera, L., Taglieri, G., Di Giambattista, A., Spagnoli, G., Massaria, A., et al. (2020). Thermoplastic Disks Used for Commercial Orthodontic Aligners: Complete Physicochemical and Mechanical Characterization. *Materials* 13 (10), 2386. doi:10.3390/ma13102386

De Iuliis, V., Ursi, S., Di Tommaso, L. M., Caruso, M., Marino, A., D'Ercole, S., et al. (2016). Comparative Molecular Analysis of Bacterial Species Associated with Periodontal Disease. *J. Biol. Regul. Homeost Agents* 30 (4), 1209–1215.

Demirel, B., Yaraş, A., and Elçiçek, H. (2011). Crystallization Behavior of PET Materials. *Baü Fen Bil. Enst. Dergisi Cilt* 13 (1), 26–35.

Dominy, S. S., Lynch, C., Ermini, F., Benedyk, M., Marczyk, A., Konradi, A., et al. (2019). Porphyromonas Gingivalis in Alzheimer's Disease Brains: Evidence for Disease Causation and Treatment with Small-Molecule Inhibitors. *Sci. Adv.* 5 (1), eaau3333. doi:10.1126/sciadv.aau3333

Dupaix, R. B., and Boyce, M. C. (2005). Finite Strain Behavior of Poly(ethylene Terephthalate) (PET) and Poly(ethylene Terephthalate)-Glycol (PETG). *Polymer* 46, 4827–4838. doi:10.1016/j.polymer.2005.03.083

Eliades, T., Pratsinis, H., Athanasiou, A. E., Eliades, G., and Kletsas, D. (2009). Cytotoxicity and Estrogenicity of Invisalign Appliances. *Am. J. Orthod. Dentofacial Orthopedics* 136, 100–103. doi:10.1016/j.ajodo.2009.03.006

Festa, F., Rotelli, C., Scarano, A., Navarra, R., Caulo, M., and Macrì, M. (2021). Functional Magnetic Resonance Connectivity in Patients with

Temporomadibular Joint Disorders. *Front. Neurol.* 12, 629211. doi:10.3389/fneur.2021.629211

Frick, A., and Rochman, A. (2004). Characterization of TPU-Elastomers by thermal Analysis (DSC). *Polym. Test.* 23, 413–417. doi:10.1016/j.polymertesting.2003.09.013

Fujiyama, K., Honjo, T., Suzuki, M., Matsuoka, S., and Deguchi, T. (2014). Analysis of Pain Level in Cases Treated with Invisalign Aligner: Comparison with Fixed Edgewise Appliance Therapy. *Prog. Orthod.* 15 (1), 64. doi:10.1186/s40510-014-0064-7

Galan-Lopez, L., Barcia-Gonzalez, J., and Plasencia, E. (2019). A Systematic Review of the Accuracy and Efficiency of Dental Movements with Invisalign®. *Korean J. Orthod.* 49 (3):140–149.doi:10.4041/kjod.2019.49.3.140

Guo, R., Zheng, Y., Liu, H., Li, X., Jia, L., and Li, W. (2018). Profiling of Subgingival Plaque Biofilm Microbiota in Female Adult Patients with clear Aligners: a Three-Month Prospective Study. *PeerJ* 6, e4207. doi:10.7717/peerj.4207

Hwang, S.-H., Jeong, K.-S., and Jung, J.-C. (1999). Thermal and Mechanical Properties of Amorphous Copolyester (PETG)/LCP Blends. *Eur. Polym. J.* 35 (8), 1439–1443. doi:10.1016/s0014-3057(98)00235-3

Iijima, M., Kohda, N., Kawaguchi, K., Muguruma, T., Ohta, M., Naganishi, A., et al. (2015). Effects of Temperature Changes and Stress Loading on the Mechanical and Shape Memory Properties of Thermoplastic Materials with Different Glass Transition Behaviours and crystal Structures. *Eortho* 37 (6), 665–670. doi:10.1093/ejo/cjv013

Kado, I., Hisatsune, J., Tsuruda, K., Tanimoto, K., and Sugai, M. (2020). The Impact of Fixed Orthodontic Appliances on Oral Microbiome Dynamics in Japanese Patients. *Sci. Rep.* 10 (1), 21989. doi:10.1038/s41598-020-78971-2

Kapila, S., and Sachdeva, R. (1989). Mechanical Properties and Clinical Applications of Orthodontic Wires. *Am. J. Orthod. Dentofacial Orthopedics* 96 (2), 100–109. doi:10.1016/0889-5406(89)90251-5

Kaye, E. K., Valencia, A., Baba, N., Spiro, A., 3rd, Dietrich, T., and Garcia, R. I. (2010). Tooth Loss and Periodontal Disease Predict Poor Cognitive Function in Older Men. *J. Am. Geriatr. Soc.* 58 (4), 713–718. doi:10.1111/j.1532-5415.2010.02788.x

Kesling, H. D. (1946). Coordinating the Predetermined Pattern and Tooth Positioner with Conventional Treatment. *Am. J. Orthod. Oral Surg.* 32, 285–293. doi:10.1016/0096-6347(46)90053-1

Kesling, H. D. (1945). The Philosophy of the Tooth Positioning Appliance. *Am. J. Orthod. Oral Surg.* 31 (6), 297–304. doi:10.1016/0096-6347(45)90101-3

Li, Y., Deng, S., Mei, L., Li, Z., Zhang, X., Yang, C., et al. (2020). Prevalence and Severity of Apical Root Resorption during Orthodontic Treatment with clear Aligners and Fixed Appliances: a Cone Beam Computed Tomography Study. *Prog. Orthod.* 21 (1), 1. doi:10.1186/s40510-019-0301-1

Liu, C.-L., Sun, W.-T., Liao, W., Lu, W.-X., Li, Q.-W., Jeong, Y., et al. (2016). Colour Stabilities of Three Types of Orthodontic clear Aligners Exposed to Staining Agents. *Int. J. Oral Sci.* 8 (4), 246–253. doi:10.1038/ijos.2016.25

Lombardo, L., Martines, E., Mazzanti, V., Arreghini, A., Mollica, F., and Siciliani, G. (2017). Stress Relaxation Properties of Four Orthodontic Aligner Materials: A 24-hour *In Vitro* Study. *Angle Orthod.* 87 (1), 11–18. doi:10.2319/113015-813.1

Lombardo, L., Arreghini, A., Maccarrone, R., Bianchi, A., Scalia, S., and Siciliani, G. (2015). Optical Properties of Orthodontic Aligners-Spectrophotometry Analysis of Three Types before and after Aging. *Prog. Orthod.* 16, 41. doi:10.1186/s40510-015-0111-z

Lu, H., Tang, H., Zhou, T., and Kang, N. (2018). Assessment of the Periodontal Health Status in Patients Undergoing Orthodontic Treatment with Fixed Appliances and Invisalign System. *Medicine (Baltimore)* 97 (13), e0248. doi:10.1097/md.0000000000010248

Ma, Y. S., Fang, D. Y., Zhang, N., Ding, X. J., Zhang, K. Y., and Bai, Y. X. (2016). Mechanical Properties of Orthodontic Thermoplastics PETG/PC2858 after Blending. *Chin. J. Dent Res.* 19 (1), 43–48. doi:10.3290/j.cjdr.a35696

Martina, S., Rongo, R., Bucci, R., Razionale, A. V., Valletta, R., and D'Antò, V. (2019). *In Vitro* cytotoxicity of Different Thermoplastic Materials for clear Aligners. *Angle Orthod.* 89 (6), 942–945. doi:10.2319/091718-674.1

Maspero, C., and Tartaglia, G. M. (2020). 3D Printing of Clear Orthodontic Aligners: Where We Are and where We Are Going. *Materials* 13 (22), 5204. doi:10.3390/ma13225204

Medellín-Rodríguez, F. J., Phillips, P. J., Lin, J. S., and Avila-Orta, C. A. (1998). Triple Melting Behavior of Poly(ethylene Terephthalate Co-1,4-cyclohexylene Dimethylene Terephthalate) Random Copolyesters. *J. Polym. Sci,part B:polym Phys.* 36, 763–781. doi:10.1002/(sici)1099-0488(19980415)36:5<763:aid-polb4>3.0.co;2-m

Nakano, H., Kato, R., Kakami, C., Okamoto, H., Mamada, K., and Maki, K. (2019). Development of Biocompatible Resins for 3D Printing of Direct Aligners. *J. Photopol. Sci. Technol.* 32 (2), 209–216. doi:10.2494/photopolymer.32.209

Nemec, M., Bartholomaeus, H. M., H. Bertl, M., Behm, C., Ali Shokoohi-Tabrizi, H., Jonke, E., et al. (2020) Behaviour of Human Oral Epithelial Cells Grown on Invisalign SmartTrack Material® *Materials* 13 (23), 5311.doi:10.3390/ma13235311

Poomali, S., Sureshac, B., and Lee, J. H. (2008). Mechanical and Three-Body Abrasive Wear Behaviour of PMMA/TPU Blends. *Mater. Sci. Eng. A* 492 (1-2), 486–490. doi:10.1016/j.msea.2008.03.018

Prasad, S., Kader, N. A., Sujatha, G., Raj, T., and Patil, S. (2018). 3D Printing in Dentistry. *J. 3D Printing Med.* 2 (3), 89–91. doi:10.2217/3dp-2018-0012

Premaraj, T., Simet, S., Beatty, M., and Premaraj, S. (2014). Oral Epithelial Cell Reaction after Exposure to Invisalign Plastic Material. *Am. J. Orthod. Dentofacial Orthopedics* 145 (1), 64–71. doi:10.1016/j.ajodo.2013.09.011

Rossini, G., Parrini, S., Castroflorio, T., Deregibus, A., and Debernardi, C. L. (2015). Periodontal Health during clear Aligners Treatment: a Systematic Review. *Eortho* 37 (5), 539–543. doi:10.1093/ejo/cju083

Rosvall, M. D., Fields, H. W., Ziuchkovski, J., Rosenstiel, S. F., and Johnston, W. M. (2009). Attractiveness, Acceptability, and Value of Orthodontic Appliances. *Am. J. Orthod. Dentofacial Orthopedics* 135, 276–277. e1–276.e12; discussion 276–277. doi:10.1016/j.ajodo.2008.09.020

Ryokawa, H., Miyazaki, Y., Fujishima, A., Miyazaki, T., and Maki, K. (2006). The Mechanical Properties of Dental Thermoplastic Materials in a Simulated Intraoral Environment. *Orthod. waves* 65 (2), 64–72. doi:10.1016/j.odw.2006.03.003

Ryu, J.-H., Kwon, J.-S., Jiang, H. B., Cha, J.-Y., and Kim, K.-M. (2018). Effects of Thermoforming on the Physical and Mechanical Properties of Thermoplastic Materials for Transparent Orthodontic Aligners. *Korean J. Orthod.* 48 (5), 316–325. doi:10.4041/kjod.2018.48.5.316

Seeger, P., Ratfisch, R., Moneke, M., and Burkhart, T. (2018). Addition of Thermo-Plastic Polyurethane (TPU) to Poly(methyl Methacrylate) (PMMA) to Improve its Impact Strength and to Change its Scratch Behavior. *Wear* 406-407, 68–74. doi:10.1016/j.wear.2017.11.024

Tartaglia, G. M., Mapelli, A., Maspero, C., Santaniello, T., Serafin, M., Farronato, M., et al. (2021). Direct 3D Printing of Clear Orthodontic Aligners: Current State and Future Possibilities. *Materials* 14 (7), 1799. doi:10.3390/ma14071799

Wu, Y., Cao, L., and Cong, J. (2020). The Periodontal Status of Removable Appliances vs Fixed Appliances. *Medicine (Baltimore)* 99 (50), e23165. doi:10.1097/md.0000000000023165

Yi, J., Xiao, J., Li, Y., Li, X., and Zhao, Z. (2018). External Apical Root Resorption in Non-extraction Cases after clear Aligner Therapy or Fixed Orthodontic Treatment. *J. Dental Sci.* 13 (1), 48–53. doi:10.1016/j.jds.2017.09.007

Zhang, M., Liu, X., Xie, Y., Zhang, Q., Zhang, W., Jiang, X., et al. (2020). Biological Safe Gold Nanoparticle-Modified Dental Aligner Prevents the Porphyromonas Gingivalis Biofilm Formation. *ACS Omega* 5 (30), 18685–18692. doi:10.1021/acsomega.0c01532

Zhang, N., Bai, Y., Ding, X., and Zhang, Y. (2011). Preparation and Characterization of Thermoplastic Materials for Invisible Orthodontics. *Dent. Mater. J.* 30 (6), 954–959. doi:10.4012/dmj.2011-120

Conflicts of Interest: The authors declare that the research was conducted in the absence of any commercial or financial relationships that could be construed as a potential conflict of interest.

Publisher's Note: All claims expressed in this article are solely those of the authors and do not necessarily represent those of their affiliated organizations, or those of the publisher, the editors and the reviewers. Any product that may be evaluated in this article, or claim that may be made by its manufacturer, is not guaranteed or endorsed by the publisher.

frontiers in Dental Medicine

ORIGINAL RESEARCH
published: 07 March 2022
doi: 10.3389/fdmed.2022.768103

Accuracy of Sterile and Non-Sterile CAD/CAM Insertion Guides for Orthodontic Mini-Implants

Björn Ludwig[1], Luisa Krause[1] and Adith Venugopal[2,3]*

[1] Department of Orthodontics, University of Homburg/Saar, Traben-Trarbach, Germany, [2] Department of Orthodontics, Saveetha Dental College and Hospitals, Saveetha Institute of Medical and Technical Sciences, Saveetha University, Chennai, India, [3] Department of Orthodontics, University of Puthisastra, Phnom Penh, Cambodia

Aim: The aim of this study was to measure the transfer accuracy of computer-aided design/computer-aided manufacturing (CAD/CAM) insertion guides using mini-implants. The target value is the virtual planned position (100%). It is also clinically mandatory to use sterilised surgical guides (autoclaved at 137°C). The results obtained using sterilised and non-sterilised insertion guides were compared. In addition, the actual position of the mini-implants, as implemented, was compared with the digitally planned positions.

Materials and Methods: Following CAD/CAM planning and production of 60 insertion guides made from synthetic resins that had been previously tested for suitability, 120 mini-implants were inserted in pairs and in blocks of the bone of the substitute material. Half of the insertion guides were sterilised, while the other half were non-sterilised. Compared with the position of the mini-implants in the digital plans, deviations in the apical and coronal distances between the mini-implants and insertion depth, as well as the included angle of the mini-implants to one another and to the surface of the bone substitute material, were determined.

Results: In post-sterilisation, the dimensional and material changes were observed. When compared, the deviations to the virtual planned position were achieved when the performed insertion using sterilised insertion guides were lower than those achieved when using non-sterilised insertion guides. The heat treatment during the sterilisation process improved the accuracy of the insertion guides. When comparing sterile insertion guides to the digital planned position (100%), the mean coronal deviation was 0.057 mm (0.81%), the apical deviation was 0.428 mm (6.11%), and insertion depth mean deviation at the right side was 0.15 mm (2.15%), while that on the left was 0.073 mm (1.04%).

Conclusion: The CAD/CAM TAD insertion guide could not achieve 100% accuracy in translating the digitally planned position into the real anatomic location. Deviations to the ideal position between 0.81 and 6.11% were observed. Clinically, for appliances that fit post-mini-implant insertion, the coronal distance of the mid-mini-implant head is the most important. At this point, the mean deviation to the planned positions is 0.81%, which is clinically acceptable and most likely reproducible by using CAD/CAM insertion guides.

Keywords: CAD/CAM, TAD, 3D printing, mini-implants, palate, insertion guides

OPEN ACCESS

Edited by:
Paolo M. Cattaneo,
University of Melbourne, Australia

Reviewed by:
Satoshi Yamaguchi,
Osaka University, Japan
Gabriele Di Carlo,
Sapienza University of Rome, Italy

****Correspondence:***
Björn Ludwig
bludwig@kieferorthopaedie-mosel.de

Specialty section:
This article was submitted to
Dental Materials,
a section of the journal
Frontiers in Dental Medicine

Received: *31 August 2021*
Accepted: *24 January 2022*
Published: *07 March 2022*

Citation:
Ludwig B, Krause L and Venugopal A (2022) Accuracy of Sterile and Non-Sterile CAD/CAM Insertion Guides for Orthodontic Mini-Implants. Front. Dent. Med. 3:768103. doi: 10.3389/fdmed.2022.768103

BACKGROUND

Mini-implants used in orthodontics have proved themselves over the last few decades as means of achieving maximum anchorage due to high success rates and a wide range of possible applications (1–4). The area of the jaw that is best suited for the insertion of mini-implants is the anterior palate (5–7) due to a large amount of the available bones and the minimal risk of damaging vital anatomical structures (8), such as tooth roots, blood vessels, and nerves. Many studies have shown that this region provides sufficient vertical bone height for secure placement of mini-implants (9). Baumgaertel et al. (10) reported a bone height of 8.68 ± 3.68 mm at the level between the first and second premolars. According to Hourfar et al. (11), the third pair of palatal rugae is considered an anatomical landmark. The precise planning of the position of the mini-implants was, on one hand, carried out using an analysis of an intraoral scan or plaster model and, on the other hand, by means of X-ray (lateral cephalogram or CBCT) (12, 13).

Insertion guides in dental implantology were developed to minimise the risk of damaging the anatomical structures and, at the same time, make ideal use of the available bone material (14). There are a multitude of factors that adversely affect the success of mini-implants. Some of these factors such as an incorrect insertion angle (15), incorrect insertion depth (16), and clinician inexperience (17) can be reduced by precise planning of the position and by the perioperative guidance of the insertion blade using an insertion guide (18). For this study, digitally manufactured CAD/CAM insertion guides that have already been described in the literature were used (14, 18, 19). According to various studies, the insertion depth can be well-controlled by using CAD/CAM-manufactured insertion guides (20, 21).

A central aspect that optimises treatment management is the preoperative preparation of the bone-borne orthodontic appliances (sliders, rapid palatal expanders, etc.) (20). These appliances can be designed and manufactured based on the digitally planned position of the mini-implant and enable a one-visit insertion of the mini-implant and appliance (**Figure 1**). Therefore, an accurate transfer of the digital planned position to the real anatomic location is essential.

The values of the following parameters are important for an optimal fit:

- Coronal distance
- Insertion depth
- Apical distance between the mini-implants
- An angle of the two mini-implants to one another
- An angle of the individual mini-implants to the surface.

This study aimed at measuring the transfer accuracy of CAD/CAM insertion guides using mini-implants. The target value is the virtual planned position (100%). It is also clinically mandatory to use sterilised surgical guides (autoclaved at 137°C). The results obtained using sterilised and non-sterilised insertion guides were compared. The actual position of the mini-implants, as implemented, was compared with the digitally planned positions.

MATERIALS AND METHODS

Preliminary Material Testing

As part of this study, CAD/CAM-planned insertion guides were produced using an STL dataset and a 3D printer (Formlabs, Form 2) (**Figure 2**).

First, three variants made of three different materials (white resin, dental LT clear resin, and dental SG resin: Formlabs) were printed, cured (Formcure UV, Formlabs, 60°C, 20 min), and autoclaved (Vakuclav 41 B, Melag, 135°C, 18.23 min; **Figure 3**). Only one material (Dental SG resin) exhibited a suitable behaviour for use in further tests.

Laboratory Work

Sixty identical insertion guides were produced from the above materials (**Figure 4**). As previously mentioned, they were cured in a curing chamber under UV light and further divided into two groups, with 30 insertion guides each. Random allocation using RandList-software was performed between the non-sterile and sterile groups.

Group 1: the "non-sterile group" and Group 2: the "sterile group." Accordingly, only the insertion guides in the second group were sterilised, and those in the first group remained non-sterile.

The insertion guides were fixed at 60 identical solid-rigid-foam bone substitute blocks (SawBones Europe AB, Malmö, Sweden), with a bone density of 40 PCF using screws

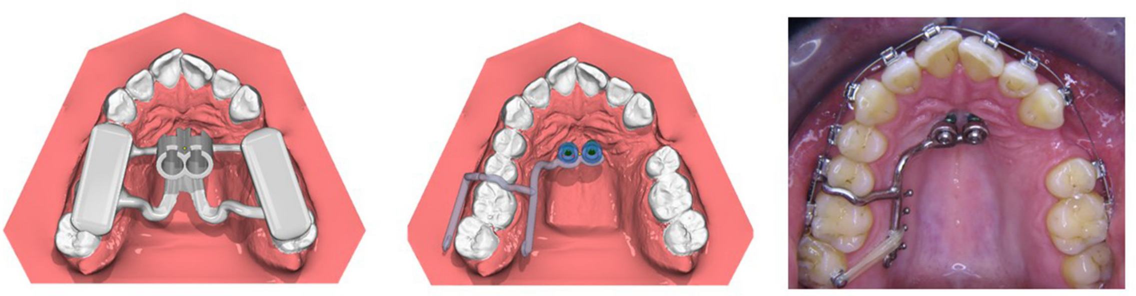

FIGURE 1 | CAD/CAM one-visit planning of mini-implant and orthodontic appliance insertion.

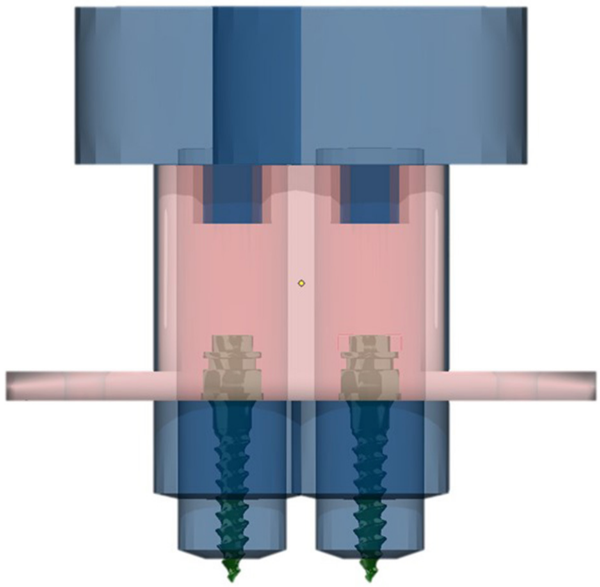

FIGURE 2 | CAD/CAM planning of the insertion guide using Onyxceph (Image Instruments, Chemnitz, Germany).

(Connex, 10 mm). Since these mini-implants (OrthoEasy Pal Pins, Forestadent, 1.7 × 8 mm) were used in pairs, 120 mini-implants were needed.

Clinical Implementation of the Insertion

Since the thread of the OrthoEasy Pal pin is a self-drilling type, no pre-drilling is necessary. Implantation was performed using a standard angled, double-green contra-angle hand piece using a ProFeel+ dental unit (Dentsply Sirona, Germany). The following device settings were defined: no torque limitation and a rotational speed of 60 rotations/min. All 120 insertions were performed by the same clinician. After every 10 mini-implants, a new insertion blade was utilised.

X-Rays and Data Acquisition

A steel strip was attached between the insertion guides and bone blocks to create a radiopaque layer for subsequent Cone-beam computed tomography (CBCT) images. These X-ray images were obtained using the Orthophos SL 3D X-ray device from Sirona (program VOL 2, 6 mA, 14.4 s). The scans were saved in the DICOM format.

Evaluation and Statistical Analysis

The scans were analysed using the OnyxCeph software (Image Instruments, Chemnitz, Germany). Four measurement points were determined for the tips (points 3 and 4) and heads (points 1 and 2) of the mini-implants in each case. The following angles and distances were partly determined directly in the OnyxCeph program and partly calculated using SPSS for Windows (Statistics 21, SPSS Inc., USA) (**Figure 5**, **Table 1**).

The determined values were then compared with the target value (CAD/CAM planned position), and the associated deviations were ascertained.

RESULTS

Preliminary tests showed that only the Dental SG resin was suitable for further use in this study. In case of the other two materials, post-sterilisation dimensional imbalances and material changes occurred, rendering them unsuitable for further use. The results of this analysis are summarised in **Table 1**. Post-sterilisation, dimensional, and material changes were observed. When compared, the achieved deviations to the virtually planned position when performing the insertion using sterilised insertion guides were lower than those achieved when using non-sterilised insertion guides. Heat treatment during the sterilisation process improved the accuracy of the insertion guides. When comparing sterile insertion guides to the digitally planned position (100%), the mean coronal deviation was 0.057 mm (0.81%), the apical deviation was 0.428 mm (6.11%), and insertion depth mean deviation at the right side was 0.15 mm (2.15%), while that at the left was 0.073 mm (1.04%) (**Table 1**, **Figure 6**).

DISCUSSION

The aim of this study was to evaluate the level of accuracy when implementing a digitally planned mini-implant position using sterilised and non-sterilised CAD/CAM insertion guides. For this purpose, mini-implants were inserted into a bone-substitute material, and their positioning was examined three-dimensionally and compared with the associated target tolerance values.

The results showed that all mean values were outliers to the target values. On comparing the mean deviations achieved, the studies revealed similar results. Möhlhenrich et al. (14), for example, compared the transfer accuracy of gingiva-borne (GBG) and tooth-borne (TBG) surgical guides made of silicone. He examined the parameters of lateral and vertical deviations as well as deviations in angulations. The values he determined were 0.8, 2.34 mm, and 3.6° for the lateral deviation, vertical deviation (TGB), and angulation (TGB), respectively. Compared with these results, smaller deviations were observed in the present study. Unlike Möhlhenrich et al., Cassetta et al. used CAD/CAM insertion guides (18) and examined the accuracy of the positioning of palatal mini-implants. They documented a deviation of 1.38, 1.73 mm, and 4.60° (1) for the coronal position, apical position, and angulation, respectively.

The deviations between the non-sterile and sterile groups recorded for each examined parameter showed that the sterilisation process had an impact on the material properties of the insertion guides. The accuracy is increased when sterilised insertion guides are used. To date, the material behaviour of synthetic resin insertion guides in the sterilisation process has not been examined in any comparative study. Most Class 1 and Class 2 resins need a temperature elevation during post-curing to fully achieve final polymerisation and ideal mechanical properties. The sterilisation process at 137°C seems to improve the polymerisation according to Bayarsaikhan et al. (22).

The use of insertion guides, made from a wide variety of materials, has been extensively described in literature (18–21, 23, 24). There are various options for materials, such as silicone,

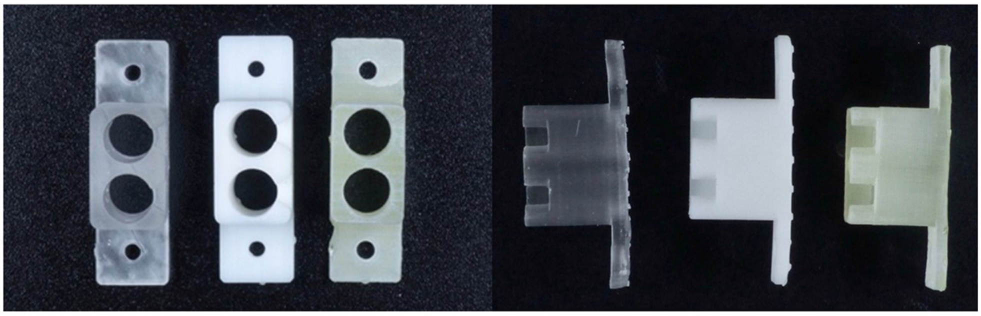

FIGURE 3 | Three different materials (white resin, dental LT clear resin, dental SG resin: Formlabs) were printed, cured (Formcure UV, Formlabs, 60°C, 20 min), and then autoclaved (Vakuclav 41B, Melag, 135°C, 18.23 min).

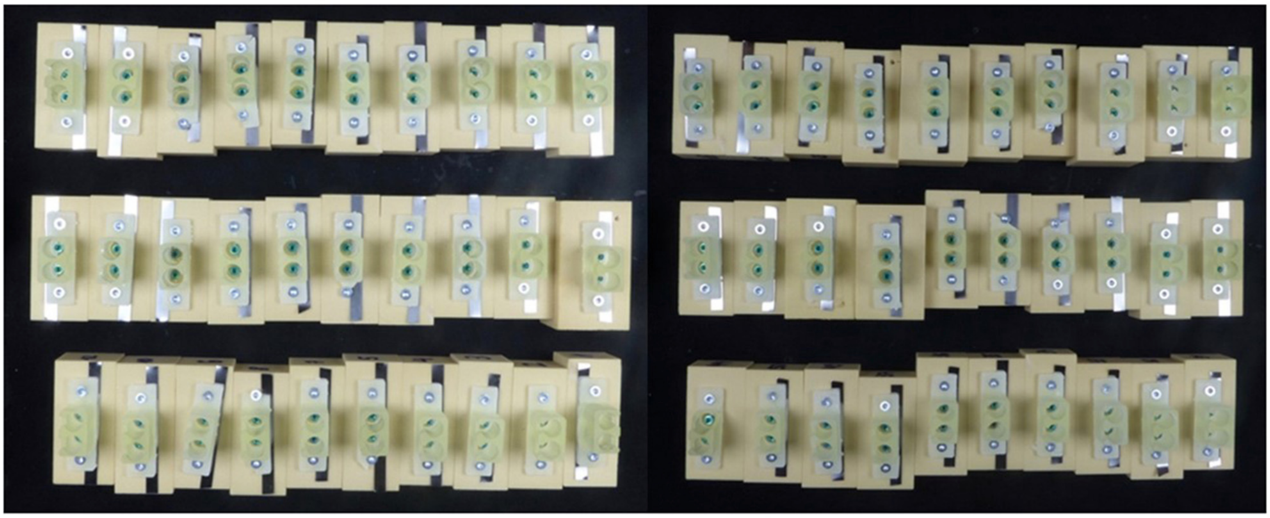

FIGURE 4 | Sixty identical insertion guides were produced and divided into two groups, with 30 insertion guides each.

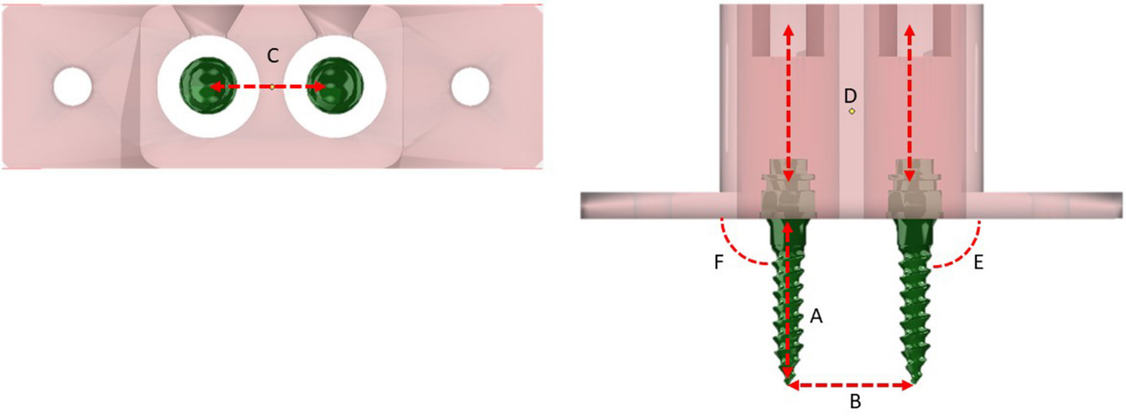

FIGURE 5 | Measurements post insertion. **(A)** Insertion depth of the mini-implants. **(B)** Apical distance between the mini-implants. **(C)** Coronal distance between the mini-implants. **(D)** An angle of the mini-implants to one another. **(E,F)** An angle of the mini-implants to the surface of the bone substitute material.

TABLE 1 | Results of the analysis of post insertion position of the mini-implants and deviation in % to the virtually planned position.

		Mean value	Mean deviation	Deviation in % to virtual planned position
Insertion depth, R (mm)	Non-sterile	8.192	0.208	2.98
	Sterile	8.385	0.15	2.14
Insertion depth, L (mm)	Non-sterile	7.942	0.458	6.54
	Sterile	8.327	0.073	1.04
Apical distance (mm)	Non-sterile	6.365	0.535	7.64
	Sterile	6.472	0.428	6.11
Coronal distance (mm)	Non-sterile	6.785	0.115	1.64
	Sterile	6.843	0.057	0.81
Angle of the mini-implants to one another (°)	Non-sterile	5.283	2.283	0.63
	Sterile	2.992	0.011	0.003
Angle of the mini-implants to the surface, R (°)	Non-sterile	6.552	3.552	0.99
	Sterile	3.927	0.927	0.26
Angle of the mini-implants to the surface, L (°)	Non-sterile	7.24	4.24	1.18
	Sterile	4.43	1.43	0.40

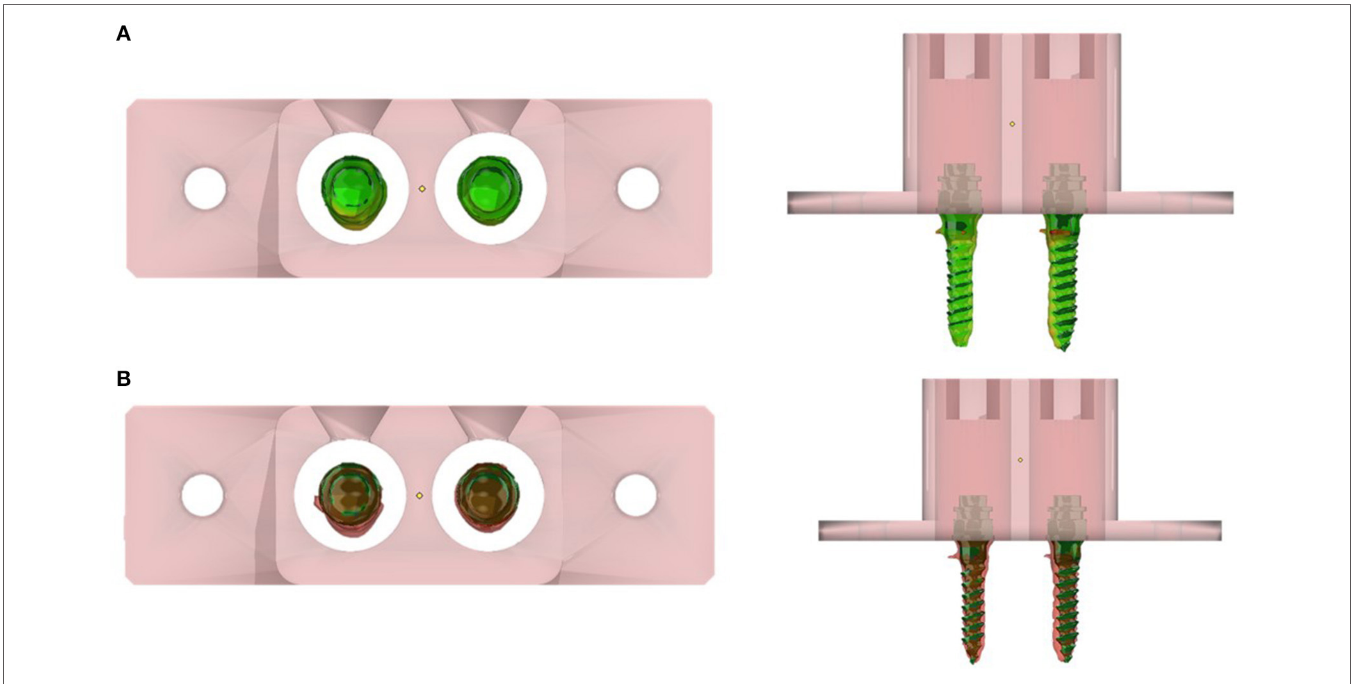

FIGURE 6 | 3D colour-coded matching/superimposition of inserted mini-implants and digitally planned position: **(A)** at 0.1-mm deviation, and **(B)** 0.5-mm deviation.

synthetic resin, or thermoforming films. Möhlhenrich et al. (14) believed that the elastic properties of silicone can lead to inaccuracies in the achieved insertion depth. There are no consistent results in the literature that shows that one system is superior to the other. In this study, CAD/CAM insertion guides made of a synthetic resin were used. According to the manufacturer (Formlabs), the material used is approved for use in dentistry and is also suitable for sterilisation. Similar results were documented with conventional dental implants in an *in vitro* study by Soares et al. (25). The angular deviation was 2.16 ± 0.92°. Overall, the authors rated the positions as promisingly precise. Similar results were observed in a meta-analysis by Van Assche et al. (26) who also evaluated the positional accuracy of dental implants. In that study, mean deviations of 0.99 mm in the coronal direction and 1.24 mm in the apical direction were documented. The angular deviation was 3.81°. These values were consistent with the results of our study.

Tatakis et al. (27) addressed the possible sources of errors that cause inaccuracies in the final implant position. They cited the gap between the guide unit of the insertion guides and the blade of the system in question as a possible cause. Their study showed that the effects on accuracy are proportional to the difference between the inner diameter of the guide sleeve and the outer diameter of the blade. However, Laederach et al. (28) noted that one cannot refrain from using a minimal gap as large mechanical frictional forces may arise. Another cause cited by Tatakis et al. (27) is the experience of the clinician, because, despite a guided insertion, it is possible to improve the implant positioning when the implantation is performed by an experienced clinician. These potential sources of error may be considered similar for dental implants as well as for orthodontic mini-implants.

CONCLUSION

- The CAD/CAM insertion guides were unable to implement a digitally planned position with 100% accuracy.
- Clinically, for appliances that fit post-mini-implant insertion, the coronal distance of the mid-mini-implant head is the most important. At this point, the mean deviation to the planned positions is 0.81%, which is clinically acceptable and most likely reproducible by using CAD/CAM insertion guides.
- The results obtained showed a similar level of accuracy compared with studies on dental implants.
- Heat treatment for mandatory clinical sterilisation improved the accuracy of the CAD/CAM insertion guide.

DATA AVAILABILITY STATEMENT

The raw data supporting the conclusions of this article will be made available by the authors, without undue reservation.

AUTHOR CONTRIBUTIONS

LK conceived the project, gathered and processed the data, created the material presented (tables, electronic images, references, et cetera), and drafted the manuscript. BL translated and critically revised the manuscript. AV reviewed the process and critically revised the manuscript. All authors read and approved the final manuscript.

REFERENCES

1. Sherman AJ. Bone reaction to orthodontic forces on vitreous carbon dental implants. *Am J Orthod*. (1978) 74:79–87. doi: 10.1016/0002-9416(78)90047-7
2. Hourfar J, Bister D, Kanavakis G, Lisson JA, Ludwig B. Influence of interradicular and palatal placement of orthodontic mini-implants on the success (survival) rate. *Head Face Med.* (2017) 13:14. doi: 10.1186/s13005-017-0147-z
3. Leung MT, Lee TC, Rabie AB, Wong RW. Use of miniscrews and miniplates in orthodontics. *J Oral Maxillofac Surg*. (2008) 66:1461–6. doi: 10.1016/j.joms.2007.12.029
4. Lee KJ, Joo E, Kim KD, Lee JS, Park YC, Yu HS. Computed tomographic analysis of tooth-bearing alveolar bone for orthodontic miniscrew placement. *Am J Orthod Dentofacial Orthop*. (2009) 135:486–94. doi: 10.1016/j.ajodo.2007.05.019
5. Ludwig B, Glasl B, Bowman SJ, Wilmes B, Kinzinger GS, Lisson JA. Anatomical guidelines for miniscrew insertion: palatal sites. *J Clin Orthod.* (2011) 45:433–41; quiz: 467.
6. Hourfar J, Bister D, Lisson JA, Ludwig B. Incidence of pulp sensibility loss of anterior teeth after paramedian insertion of orthodontic mini-implants in the anterior maxilla (acccepted). *Head Face Med.* (2016) 13:1. doi: 10.1186/s13005-016-0134-9
7. Ludwig B, Baumgaertel S, Bowman JS. *Mini-Implants in Orthodontics. Innovative Anchorage Concepts.* London: Quintessence Publishing Co Ltd. (2008).
8. Hourfar J, Ludwig B, Bister D, Braun A, Kanavakis G. The most distal palatal ruga for placement of orthodontic mini-implants. *Eur J Orthod.* (2015) 37:373–8. doi: 10.1093/ejo/cju056
9. Winsauer H, Vlachojannis C, Bumann A, Vlachojannis J, Chrubasik S. Paramedian vertical palatal bone height for mini-implant insertion: a systematic review. *Eur J Orthod.* (2014) 36:541–9. doi: 10.1093/ejo/cjs068
10. Baumgaertel S. Quantitative investigation of palatal bone depth and cortical bone thickness for mini-implant placement in adults. *Am J Orthod Dentofacial Orthop*. (2009) 136:104–8. doi: 10.1016/j.ajodo.2008.11.020
11. Hourfar J, Kanavakis G, Bister D, Schatzle M, Awad L, Nienkemper M, et al. Three dimensional anatomical exploration of the anterior hard palate at the level of the third ruga for the placement of mini-implants–a cone-beam CT study. *Eur J Orthod.* (2015) 37:589–95. doi: 10.1093/ejo/cju093
12. Jung BA, Wehrbein H, Wagner W, Kunkel M. Preoperative diagnostic for palatal implants: is CT or CBCT necessary? *Clin Implant Dent Relat Res.* (2012) 14:400–5. doi: 10.1111/j.1708-8208.2009.00259.x
13. Baumgaertel S, Palomo JM, Palomo L, Hans MG. Reliability and accuracy of cone-beam computed tomography dental measurements. *Am J Orthod Dentofacial Orthop.* (2009) 136:19–25; discussion: 25–8. doi: 10.1016/j.ajodo.2007.09.016
14. Möhlhenrich SC, Brandt M, Kniha K, Prescher A, Hölzle F, Modabber A, et al. Accuracy of orthodontic mini-implants placed at the anterior palate by tooth-borne or gingiva-borne guide support: a cadaveric study. *Clin Oral Invest.* (2019) 23:4425–31. doi: 10.1007/s00784-019-02885-1
15. Kuroda S, Tanaka E. Risks and complications of miniscrew anchorage in clinical orthodontics. *Jpn Dent Sci Rev.* (2014) 50:79–85. doi: 10.1016/j.jdsr.2014.05.001
16. Tsaousidis G, Bauss O. Einfluss der insertionsstelle auf die misserfolgsraten kieferorthopädischer verankerungsschrauben. *J Orofac Orthop.* (2008) 69:349–56. doi: 10.1007/s00056-008-0809-3
17. Park HS, Jeong SH, Kwon OW. Factors affecting the clinical success of screw implants used as orthodontic anchorage. *Am J Orthod Dentofacial Orthop.* (2006) 130:18–25. doi: 10.1016/j.ajodo.2004.11.032
18. Cassetta M, Altieri F, R. Di Giorgio, Barbato E. Palatal orthodontic miniscrew insertion using a CAD-CAM surgical guide: description of a technique. *Int J Oral Maxillofac Surg.* (2018) 47:1195–8. doi: 10.1016/j.ijom.2018.03.018
19. Liu H, Liu DX, Wang G, Wang CL, Zhao Z. Accuracy of surgical positioning of orthodontic miniscrews with a computer-aided design and manufacturing template. *Am J Orthod Dentofacial Orthop*. (2010) 137:728.e1–10; discussion: 728–9. doi: 10.1016/j.ajodo.2009.12.025
20. Gabriele O, Dallatana G, Riva R, Vasudavan S, Wilmes B. The easy driver for placement of palatal mini-implants and a maxillary expander in a single appointment. *J Clin Orthodont.* (2017) 51:728–37.
21. Maino BG, Paoletto E, Lombardo L III, Siciliani G. A Three-dimensional digital insertion guide for palatal miniscrew placement. *J Clin Orthod.* (2016) 50:12–22.
22. Bayarsaikhan E, Lim J-H, Shin S-H, Park K-H, Park Y-B, Lee J-H, et al. Effects of Postcuring Temperature on the Mechanical Properties and Biocompatibility of Three-Dimensional Printed Dental Resin Material. *Polymers.* (2021) 13:1180. doi: 10.3390/polym13081180
23. Tosun T, Keles A, Erverdi N. Method for the placement of palatal implants. *Int J Oral Maxillofac Implants*. (2002) 17:95–100.
24. Morea C, Hayek JE, Oleskovicz C, Dominguez GC, Chilvarquer I. Precise insertion of orthodontic miniscrews with a stereolithographic surgical guide based on cone beam computed tomography data: a pilot study. *Int J Oral Maxillofac Implants.* (2011) 26:860–5.

25. Soares MM, Harari ND, Cardoso ES, Manso MC, Conz MB, Vidigal GM Jr. An *in vitro* model to evaluate the accuracy of guided surgery systems. *Int J Oral Maxillofac Implants*. (2012) 27:824–31.
26. Van Assche N, Vercruyssen M, Coucke W, Teughels W, Jacobs R, Quirynen M. Accuracy of computer-aided implant placement. *Clin Oral Implants Res*. (2012) 23(Suppl 6):112–23. doi: 10.1111/j.1600-0501.2012.02552.x
27. Tatakis DN, Chien HH, Parashis AO. Guided implant surgery risks and their prevention. *Periodontol 2000*. (2019) 811:194–208. doi: 10.1111/prd.12292
28. Laederach V, Mukaddam K, Payer M, Filippi A, Kühl S. Deviations of different systems for guided implant surgery. *Clin Oral Implants Res*. (2017) 28:1147–51. doi: 10.1111/clr.12930

Conflict of Interest: The authors declare that the research was conducted in the absence of any commercial or financial relationships that could be construed as a potential conflict of interest.

Publisher's Note: All claims expressed in this article are solely those of the authors and do not necessarily represent those of their affiliated organizations, or those of the publisher, the editors and the reviewers. Any product that may be evaluated in this article, or claim that may be made by its manufacturer, is not guaranteed or endorsed by the publisher.

frontiers in Bioengineering and Biotechnology

ORIGINAL RESEARCH
published: 16 March 2022
doi: 10.3389/fbioe.2022.840622

In Vitro Comparison of Different Invisalign® and 3Shape® Attachment Shapes to Control Premolar Rotation

Nikolaos Ferlias[1]†, Michel Dalstra[1]†, Marie A. Cornelis[2]† and Paolo M. Cattaneo[2]†*

[1]Section of Orthodontics, Department of Dentistry and Oral Health, Aarhus University, Aarhus, Denmark, [2]Melbourne Dental School, Faculty of Medicine, Dentistry and Health Sciences, The University of Melbourne, Melbourne, VIC, Australia

OPEN ACCESS

Edited by:
Yin Fang,
Nanyang Technological University,
Singapore

Reviewed by:
Gianluca Tartaglia,
University of Milan, Italy
Yongliang Ni,
Lam Research, United States

****Correspondence:***
Nikolaos Ferlias
nferlias@gmail.com

†ORCID:
Nikolaos Ferlias
orcid.org/0000-0003-4995-1934
Michel Dalstra
orcid.org/0000-0001-5526-4415
Marie A. Cornelis
orcid.org/0000-0001-8050-2868
Paolo M. Cattaneo
orcid.org/0000-0001-7604-3259

Specialty section:
This article was submitted to Biomaterials, a section of the journal Frontiers in Bioengineering and Biotechnology

Received: *21 December 2021*
Accepted: *02 February 2022*
Published: *16 March 2022*

Citation:
Ferlias N, Dalstra M, Cornelis MA and Cattaneo PM (2022) In Vitro Comparison of Different Invisalign® and 3Shape® Attachment Shapes to Control Premolar Rotation. Front. Bioeng. Biotechnol. 10:840622. doi: 10.3389/fbioe.2022.840622

Aim: To evaluate *in vitro* the differences of various Invisalign® attachments in their effectiveness during derotation of an upper second premolar in terms of forces and moments created and compare them to the 3Shape® box attachment as well as to no attachment at all.

Materials and Methods: A Force System Identification (FSI) machine, comprising two load sensors, was used in this study. Sensor 1 was connected to the test tooth (i.e. upper second premolar) carrying a different attachment design, and the fixed sensor (Sensor 2) was connected to the base model. Once the corresponding aligner was passively seated on the teeth, 12 different setups (i.e. 11 different attachments and one setup with no attachment at all) were tested by rotating the test tooth 4.5° mesially and 4.5° distally, in increments of 0.45°.

Results: The vertical rectangular attachments were able to generate the highest derotational moment on both mesial and distal rotations but also received the most side effects (intrusive force, torque, and tipping). The no-attachment setup performed least favorably in terms of derotational ability but exhibited the least side effects. In the *y*-axis, all attachments received a buccal root torque with a lingual force during disto-rotation and a lingual root torque with a buccal force during mesio-rotation.

Conclusion: Attachments are necessary for derotating an upper second premolar. An aligner incremental change of more than 1° derotation can generate high moments. The vertical rectangular attachments perform best in derotations; however, they exhibit the most side effects. Finally, despite presenting the least side effects, derotation of a premolar with no attachment is not as efficient.

Keywords: orthodontics, clear aligners, biomechanics, tooth movement, 3D printing

INTRODUCTION

Clear aligner therapy has been an alternative treatment modality to conventional orthodontic fixed appliances to clinicians for almost 20 years, despite the concept having been introduced almost half a century ago (Kesling, 1945). However, the initial limitations of the aligners' clinical applications kept the orthodontic community quite skeptical in the beginning. These were most commonly the lack of finishing control with imprecise final detailing and the lack of rotational control and poor aligner fit due to lack of compliance (Sheridan, 2004). In the rapid evolutionary process that followed, orthodontists came to acknowledge clear aligner therapy as a valid alternative to conventional multi-bracket systems. Patients played an important role in this change, as a significant number of them find metal or ceramic fixed appliances unattractive and unacceptable (Rosvall et al., 2009). This evolution, however, may have come with inadequate evidence, with the research community in general not being able to keep up with the aligners' fast-growing pace, thus leading to a technology bypass.

It is true that compliance is the most important factor in clear aligner therapy, yet retention of the aligner is equally crucial if we want to apply the necessary forces to achieve the desired tooth movements. There are certain movements that prove to be quite challenging in every day clinical practice; these are mainly the torque and root angulation, extrusion as well as rotation, especially of those more rounded teeth, like the canines and premolars (Rossini et al., 2015; Bowman, 2017). In fact, Kravitz et al. (Kravitz et al., 2009) report that derotation of a lower canine is the least accurate movement when compared to all other teeth. In addition, the mean accuracy of tooth movement with clear aligners is as low as 41% with the extrusion being the least accurate (Kravitz et al., 2009).

The company that created the market, Invisalign® (Align Technology, San Jose, CA, USA), developed rapidly since its appearance 2 decades ago and added attachments and auxiliaries in order to improve aligner retention and achieve more complex orthodontic tooth movements, in an attempt to apply bio-mechanical principles. Different attachment shapes have been introduced since by Invisalign® and are being used in almost all aligner treatments. These seem to have improved the overall treatment accuracy (Haouili et al., 2020). However, there is lack of evidence regarding the differences in performance between the different types of attachments in achieving certain kinds of orthodontic tooth movement (Dasy et al., 2015). As a consequence, the boundaries between marketing claims and evidence-based clinical reality can be quite blurred.

In a recent retrospective study, the efficacy of different Invisalign® attachments was investigated and no difference was found between conventional and optimized attachment designs (Karras et al., 2021). The movement investigated was rotation of canines and premolars as well as extrusion of anterior teeth which is more challenging to achieve predictably with Invisalign® (Papadimitriou et al., 2018). With the present evolution of 3D printing and the rapid development of in-house aligners, investigating the clinical differences of various attachment shapes can have implications for the clinician in their treatment approach and efficacy.

Therefore, the aim of this study was to evaluate, *in vitro*, the differences of various Invisalign® attachment designs in their effectiveness to derotate of an upper second premolar in terms of forces and moments transmitted to the tooth, and compare those to the 3Shape® box attachment (3Shape®, Copenhagen, Denmark) as well as when no attachment at all is used.

MATERIALS AND METHODS

Design and 3D Printing

First, an intraoral scan of an upper jaw with fairly aligned teeth was taken using the TRIOS intraoral scanner by 3Shape® (Copenhagen, Denmark). The various attachments (full description in the next paragraph) were then virtually placed in the middle of the crown (middle of the mesio-distal and apico-occlusal dimensions) using Orthoanalyzer® (3Shape®). The STL files created were then imported into the Dental System®

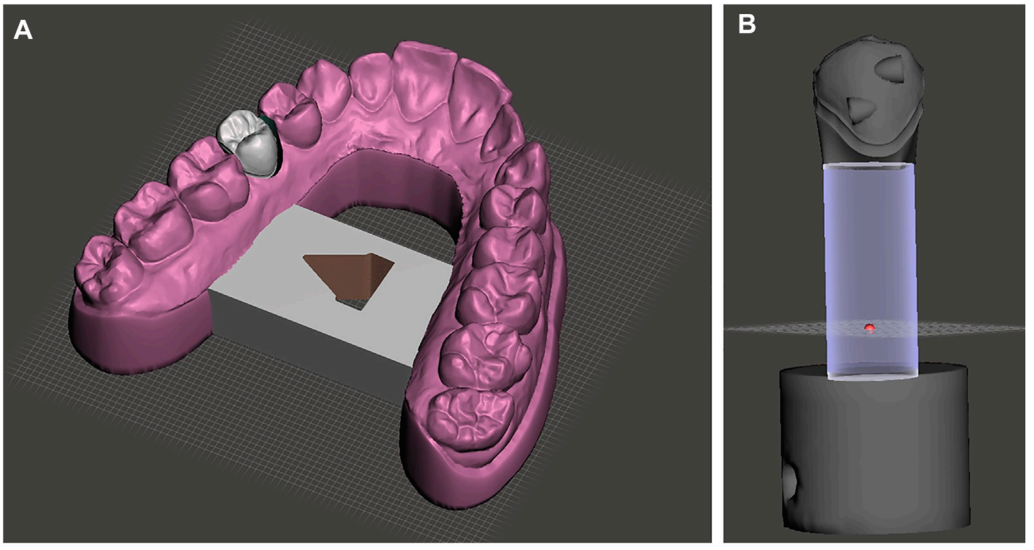

FIGURE 1 | 3D design of the set up. **(A)**. Model base used for all tests (in purple) and the test tooth 15 fitted with the various attachments (grey). Please, note the clearance around test tooth 15, which allowed for free rotation around the tooth long axis, without any interference. **(B)**. All the setups of tooth 15 with the different types of attachments were built on the same base tooth model and had the same cylindrical base. Here, the ElliPair attachment (consisting of two hemi-elliptical attachments, HemiElliR and HemiElliL) are depicted.

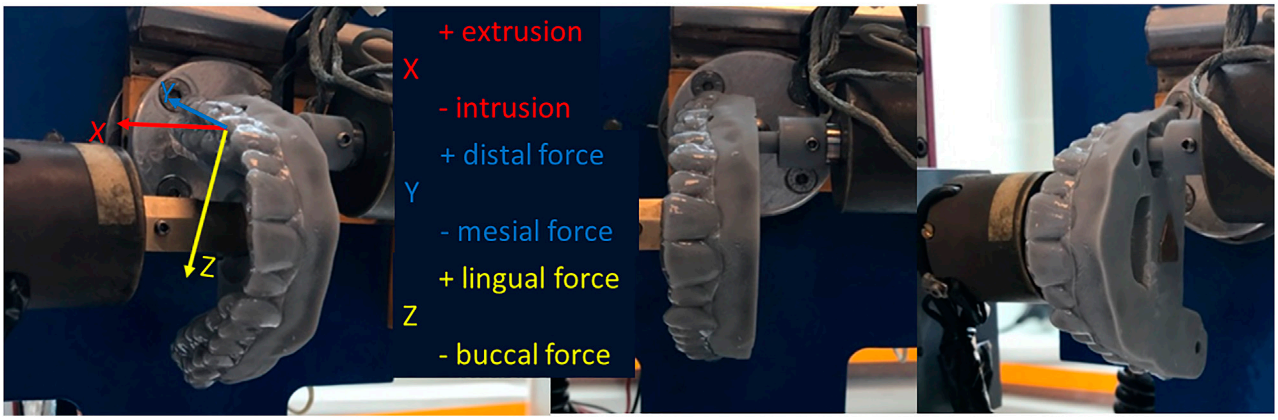

FIGURE 2 | Overview of the testing set-up. Sensor 1 (rotating tooth carrying different attachment design, seen on the right) and Sensor 2 (stable base model, left) in action. Each aligner corresponding to the specific attachment was mounted in the "test position" which was reproduced for all tests by the same FSI software coordinates. The three axes: X: long axis of the tooth; Y: mesio-distal axis; and Z: bucco-lingual axis are represented for intelligibility.

(3Shape®). A new order was then created for a single coping using the Model Builder® workflow. Then, the upper right second premolar with the particular attachment was separated as a single die, and both parts, the model and the die, were then saved and exported as STL files. Finally, these files were imported into Meshmixer (Autodesk®, San Rafael, CA, United States) for the final preparation so that the die and the model could be mounted on the FSI sensors. During this preparation, the same cylindrical base parallel to the long axis of the tooth and with the same dimensions was used for all the different attachment setups (**Figure 1**).

As far as the 3D printing procedure is concerned, all models as well as the single premolar teeth with the various attachments were printed in a Nextdent 5100® 3D printer (Vertex-Dental, Soesterberg, Netherlands) using the Model 2.0® printing material produced by the same company. The aligners were manually fabricated once all the 12 initial models were printed using the Taglus® aligner foils (Laxmi Dental, Mumbai, India) with a thickness of 0.762 mm.

Setup

The setup of this study consisted of a dental model that was divided into two separate parts, each one connected to a sensor measuring the forces and moments (F/M) created, using the Force System Identification (FSI) machine, which was developed for the Department of Orthodontics, Aarhus University, Denmark. The first part in the setup was the base model carrying all the upper teeth except tooth 15, at which place a hole was drilled in the model (**Figures 1**, **2**). This part was attached to Sensor 2 of the FSI machine and was kept fixed throughout the whole testing procedure. The second part, connected to Sensor 1 of the FSI machine, was tooth 15 carrying the different attachment at each test. The tooth 15 part was replicated 12 times, each one characterized by 11 different types of attachment and one where no attachment was present. The attachments tested (abbreviation and dimensions in parenthesis) were the Invisalign® "Bevelled" (Bevelled, 3.5 × 1.5 × 1 mm), "Horizontal Ellipsoid" (HEllipsoid, 3 × 2 × 1 mm), "Vertical Ellipsoid" (VEllipsoid 3 × 2 × 1 mm), "Elliptical Pair" (ElliPair, 2 × 2 × 1 mm/each), "Hemi-elliptical Right" (HemiEllipR, 2 × 2 × 1 mm), "Hemi-elliptical Left" (HemiEllipL, 2 × 2 × 1 mm), "Horizontal Rectangular Left" (HRecL, 3.5 × 1.5 × 1 mm), "Horizontal Rectangular Right" (HRecR, 3.5 × 1.5 × 1 mm), "Vertical Rectangular Down" (VRecDOWN, 3.5 × 1.5 × 1 mm), and "Vertical Rectangular Up" (VRecUp, 3.5 × 1.5 × 1 mm). In addition, the regular "3Shape® Box" (3Shape, 3.5 × 1.5 × 1 mm) attachment was also tested, as well as a tooth 15 with "No Attachment" (NoAtt) at all (**Figures 3**, **4**).

The mounting was completed on a reproducible position with saved coordinates (neutral position) and controlled by the FSI computer software.

Once both parts were mounted on the sensors, position two (test position) was reproduced using the FSI's "test-position" coordinates. The specific aligner corresponding to the particular attachment was then placed on the teeth. Prior to placement, the inside of the aligner was lubricated with a saliva substitute using a squirt on every tooth (GUM® Hydral®, Etoy Switzerland). Then, Sensor 1 was automatically rotated, in steps of 0.45°, up to 4.5° mesial and back to neutral position. Prior to the distal rotation, the aligner was removed and seated again on the teeth and then it was rotated the other direction, 4.5° distal and back to neutral again (**Figure 2**).

For descriptive reasons, the attachments were arranged in five main groups according to their orientation and shape. Group 1, "Rectangular Vertical" included two rectangular shape attachments with a vertical orientation (i.e. "VRecUp" and "VRecDOWN"). Group 2, "Rectangular Horizontal" included four rectangular shape attachments with a horizontal orientation (i.e. "HRecR"; "HRecL"; "3Shape"; "Bevelled"). Group 3 included one ellipsoid attachment with a vertical orientation (i.e. the "VEllipsoid"). Group 4 consisted of four ellipsoid attachments with a horizontal orientation (i.e., "HEllipsoid"; "HemiEllipR"; "HemiEllipL"). Finally,

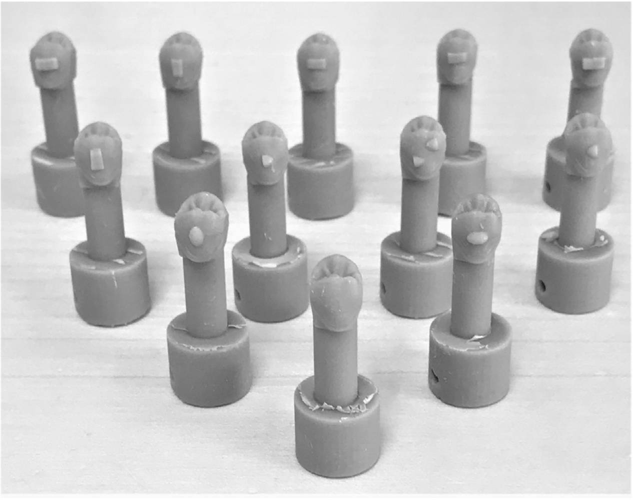

FIGURE 3 | Twelve different setups were tested consisting of eleven Invisalign® attachments, the 3Shape® Box attachment and one setup with no attachment at all serving as control.

Group 5 was comprised of twin semi-ellipsoid attachment (i.e., "ElliPair") and the no-attachment configuration (i.e., "NoAtt").

In our setup, the *x*-axis coincided with the long axis of the tooth with positive force values (F_x) corresponding to "extrusion" and negative values corresponding to "intrusion" (**Figure 2**; **Table 1**). Similarly, positive values in *x*-axis moments (M_x) indicated "distal rotation," while negative values indicated "mesial rotation." The *y*-axis was the mesio-distal axis, with positive force (F_y) values indicating "distal" direction and negative values indicating "mesial" direction. When the moments in the *y*-axis (M_y) were positive, they corresponded to "lingual root torque" and negative to "buccal root torque." Finally, the *z*-axis was the bucco-lingual axis, where positive values represented the "lingual" direction and the "negative" values a "buccal" force direction (F_z). The moments in the *z*-axis (M_z) indicated "distal tipping" when positive and "mesial tipping" when negative.

Statistics

All measurements were repeated after a minimum of 2 week interval between them. For the error of the method, the intraclass correlation coefficient (ICC) was used to compare the two rounds of measurements. The number of attachments used in the present study was determined purely on the availability of the most commonly used attachment designs.

RESULTS

The ICC showed excellent reliability (>0.91) for all measurements, except for the HemiEllipR and HEllipsoid, where the ICC was 0.83 and 0.81, respectively.

During the measurements, complete disengagement of the aligner did not occur, although disengagement to some minor extent occurred with some attachment setups. All results for the forces and moments at the end positions (4.5° mesial and 4.5° distal rotation) are summarized in **Tables 1**, **2** (1.35° mesial and distal rotation).

x-Axis

As far as the *x*-axis is concerned (long axis of the tooth), when 15 was mesially rotated, the attachment producing the highest force was the 3Shape, generating an intrusive force of 177cN. At the other side of the range, the tooth with NoAtt received the least amount of vertical force. When the tooth was rotated distally, most attachments again received an intrusive force, while the

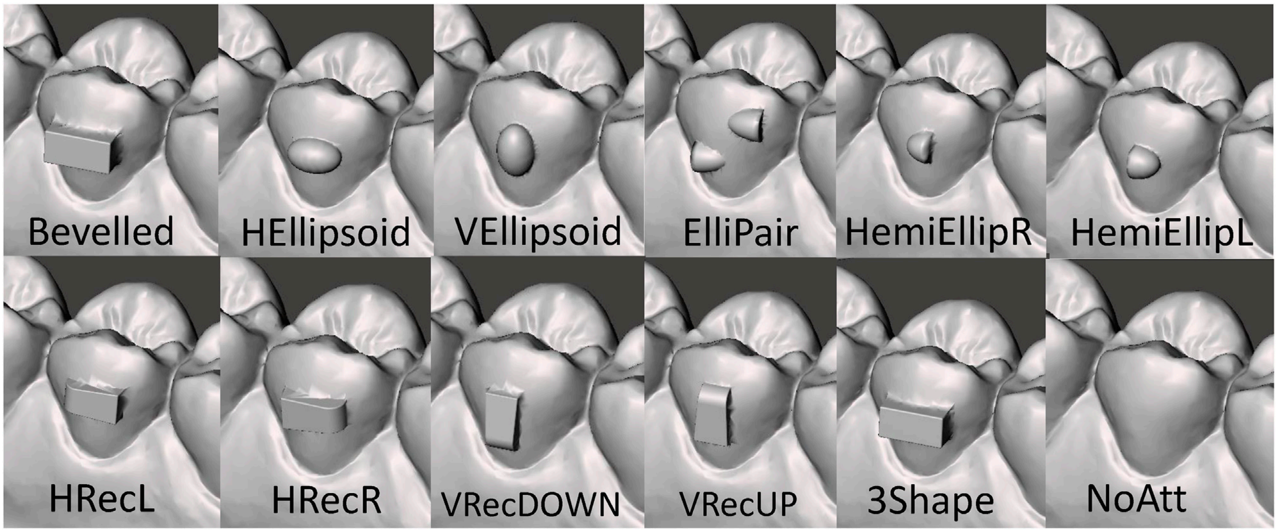

FIGURE 4 | Details of the attachments reported in **Figure 3** are presented with the names 411 used throughout the article.

Research Topics

Advanced use of materials in orthodontics

Edited by
Domenico Ciavarella, Michele Tepedino and Paolo M. Cattaneo

Published in
Frontiers in Materials
Frontiers in Bioengineering and Biotechnology
Frontiers in Dental Medicine

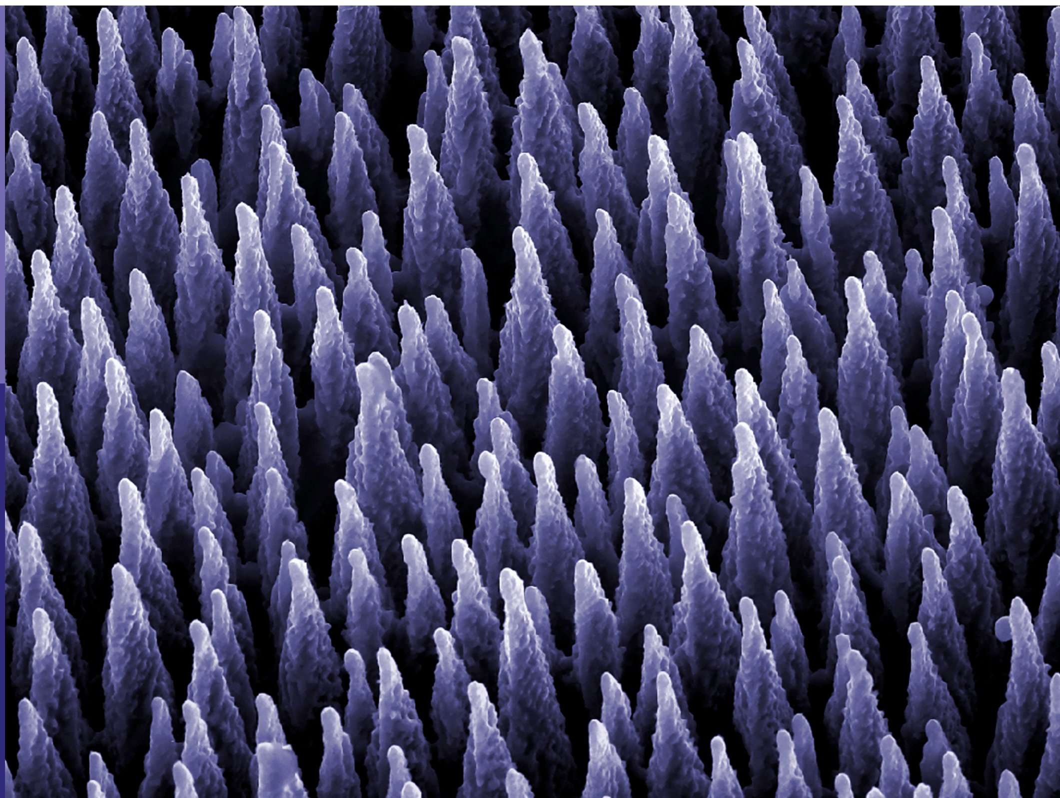

TABLE 2 | Forces (F, in cN) and moments (M, in cNmm) in all three axes at 1.35 mesial and 1.35 distal rotations. When the test tooth is 1.35 mesial rotated, forces and moments are created to disto-rotate the tooth (Mx positive).

	Attachment	*x*-Axis				*y*-Axis				*z*-Axis			
		Fx		Mx		Fy		My		Fz		Mz	
		+ (extrusion) /– (intrusion)		+ (distal rotation) /– (mesial rotation)		+ (distal) /– (mesial)		+ (lingual root torque) /– (buccal root torque)		+ (lingual) /– (buccal)		+ (distal tipping) /– (mesial tipping)	
Tooth Rotation		1.35° Mesial	1.35° Distal	1.35° Mesial	1.35° Distal	1.35° Mesial	1.35° Distal	1.35° Mesial	1.35° Distal	1.35° Mesial	1.35° Distal	1.35° Mesial	1.35° Distal
Group 1: “Rectangular Vertical”	VRecUp	–32	–22	2,535	–2,870	4	–15	–2,372	1,212	80	–37	602	–573
	VRecDOWN	–12	–19	1775	–2,984	–22	–53	–693	1,634	19	–57	–281	–1,304
Group 2: “Rectangular Horizontal”	HRecR	–45	18	2,661	–2,507	0	–6	–1,475	955	51	–17	420	–937
	HRecL	2	–10	1,108	–1,354	12	–13	–849	–316	23	14	339	–442
	3Shape® Box	–44	22	2020	–1707	–5	0	–462	38	–17	5	129	–140
	Bevelled	–12	3	646	–2,705	–5	–13	581	461	–23	–16	–88	–278
Group 3: “Ellipsoid Vertical”	Vellipsoid	–22	7	1,254	–1,463	6	–22	–572	972	16	–29	224	–728
Group 4: “Ellipsoid Horizontal”	Hellipsoid	–42	–5	1,623	–819	8	–9	–897	23	36	3	478	–256
	HemiEllipR	–24	35	1779	–1,228	13	5	–575	166	15	–11	504	–99
	HemiEllipL	–48	22	2,594	-1702	13	–19	–1,693	499	64	–19	756	–700
Group 5: “Other”	ElliPair	1	–8	1,560	–2,643	–3	–27	–351	729	11	–26	–23	–731
	NoAtt	–2	–23	828	–862	11	–10	–416	785	14	–24	517	–254
	= highest												
	= lowest												

3Shape attachment displayed an extrusive force of 52cN. The NoAtt tooth received the largest intrusive force of 137cN, whereas the least force was applied to the HRecR and HEllipsoid, and this was extrusive and intrusive, respectively.

When it comes to the moment created around the *X*-axis (derotation moment), for the mesially rotated tooth, the largest moments were encountered when the HemiEllipL was tested, followed by the vertical rectangular attachments of Group 1, VRecUP and VRecDOWN. Similarly, for the distal rotation, the largest moments were observed for the vertical rectangular attachments (VRecUP and VRecDOWN). For both mesial and distal rotation, the tooth with no attachment exhibited the least de-rotating moment (**Figure 5**).

y-Axis

In the *y*-axis, when the tooth was rotated mesially 4.5°, the largest amount of force (73 cN), distal in this case, was when the VEllipsoid attachment was used and the least (5 cN) when the VRecDOWN was used, although this force had a mesial direction. For the distal rotation, all teeth received a mesial force with the VRecDOWN exhibiting the highest amount, at 216cN and the NoAtt setup the smallest, with around 10 cN.

Regarding the moment created around the *Y*-axis, when the tooth was rotated mesially, all setups received a buccal root torque with the highest seen with the VRecUP attachment and the smallest with the Bevelled. In the other direction, for the distally rotated tooth, a moment of lingual root torque was observed in all setups. The highest (7,704 cNmm) was seen in the VRecDOWN setup, whereas the Hellipsoid and NoAtt setups exhibited the lowest moments.

z-Axis

Regarding the *z*-axis, again the vertical rectangular attachments (VRecUP and VRecDOWN) received the most amount of force. This had a lingual direction when the tooth was rotated mesial and was smallest in the Bevelled and in the NoAtt setup, whereas for the distally rotated tooth, this was directed buccally and was again smallest in the NoAtt tooth at around 60cN.

Regarding the moments, for the mesial rotation, the Bevelled attachment exhibited the smallest amount of moment (distal tipping), whereas the highest was encountered in the HemiEllipL and VRecUp setups. Finally, for the distal rotation, the highest moment (mesial tipping) was seen in the VRecDOWN setup (5,402 cNmm) and the lowest in the NoAtt setup (96 cNmm).

DISCUSSION

The results clearly demonstrate the variability between the different shapes and types of attachments used in aligner treatment. In the present study, there is a great range of moments, in all three axes of orientation and especially in the

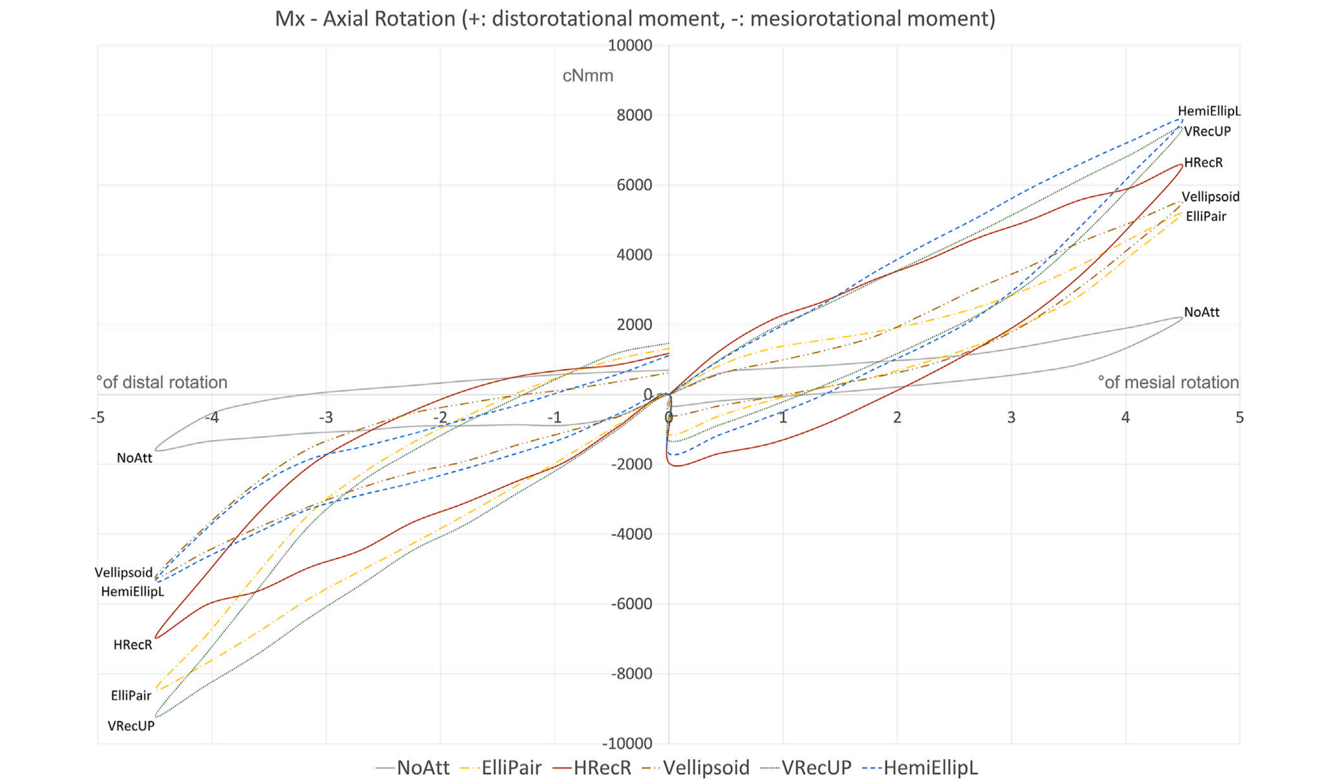

FIGURE 5 | Best performing attachment from each of the five groups and the "NoAtt" setup. Vertical Rectangular attachments performed best on both mesial and distal rotations. HemiEllipL performed best on disto-rotation but not on mesio-rotation. Worth noticing the high moments created after only 1° of rotation and also the small degree of permanent deformation and fatigue in the aligner when looking at the de-activation part of the hysteresis loop. The time needed to reach 4.5° rotation either side (0°–4.5°) was 64°s, time that clinically translates to an instance when snapping the aligner in place.

x-axis (mesio-/disto-rotation) of around 8,000 cNmm. Most importantly, this shows that a rotation of 4.5° in the aligner creates high moments at a level that most likely exceeds the moments needed for effective derotation. Although we do not know what the success criteria for the attachments are, and given that it is hard to find strict values to compare to in the literature, according to Proffit, the optimal force level for derotation was reported to be in the range 35–60 cN (Proffit et al., 2013). In addition, it is known that a challenging movement like lower molar uprighting requires moments in the range 1,200–1,800 cNmm (Raveli et al., 2017; Viecilli et al., 2009). Subsequently, these high moments could increase the risk of root resorption (Roscoe et al., 2015; Theodorou et al., 2019). The setup used in the present study reveals that already at 1° of mesial or distal rotation, the moments created should suffice for achieving an effective derotation (**Figure 5**). Therefore, it would make sense to not exceed 1° or 1.5° of derotation per step in aligner staging. Besides, it has been shown that the efficacy of tooth movement decreases significantly with a staging larger than 1.5°/aligner (Simon et al., 2014). This is probably the reason why Invisalign® decided that the derotation provided by one stage never exceeds 2° (Align Technology, 2015).

In addition, in the absence of occlusal forces, our setup was "forgiving" as the aligners could be pushed in the occlusal direction and thus slightly disengage. One would assume that in the presence of function, the occlusal forces re-engage the aligner into position and the moments and forces created could potentially reach even higher levels. On the other hand, occlusion is happening only for a fraction of the 24 h (Proffit et al., 2013). Nevertheless, in a study with a comparable setup, but with an aligner-retention device where the aligner engagement was secured throughout testing, the rotational moments at 5° were smaller (Elkholy et al., 2019).

Derotation moment, M_x

If we focus purely on the amount of moment created to derotate the tooth (M_x), our results show that the vertical rectangular attachments outperformed the others by creating the largest moments when the tooth was rotated either mesial or distal. This trend was seen in the smaller rotations of 1°, 2°, or 3° as well. To explain this, we should look at the design of these attachments where there is a large mesial and distal "flat" surface (3.5 × 1 mm), where the aligner can apply the needed derotational force. Also, it seems like the placement of the bevelled end of the vertical

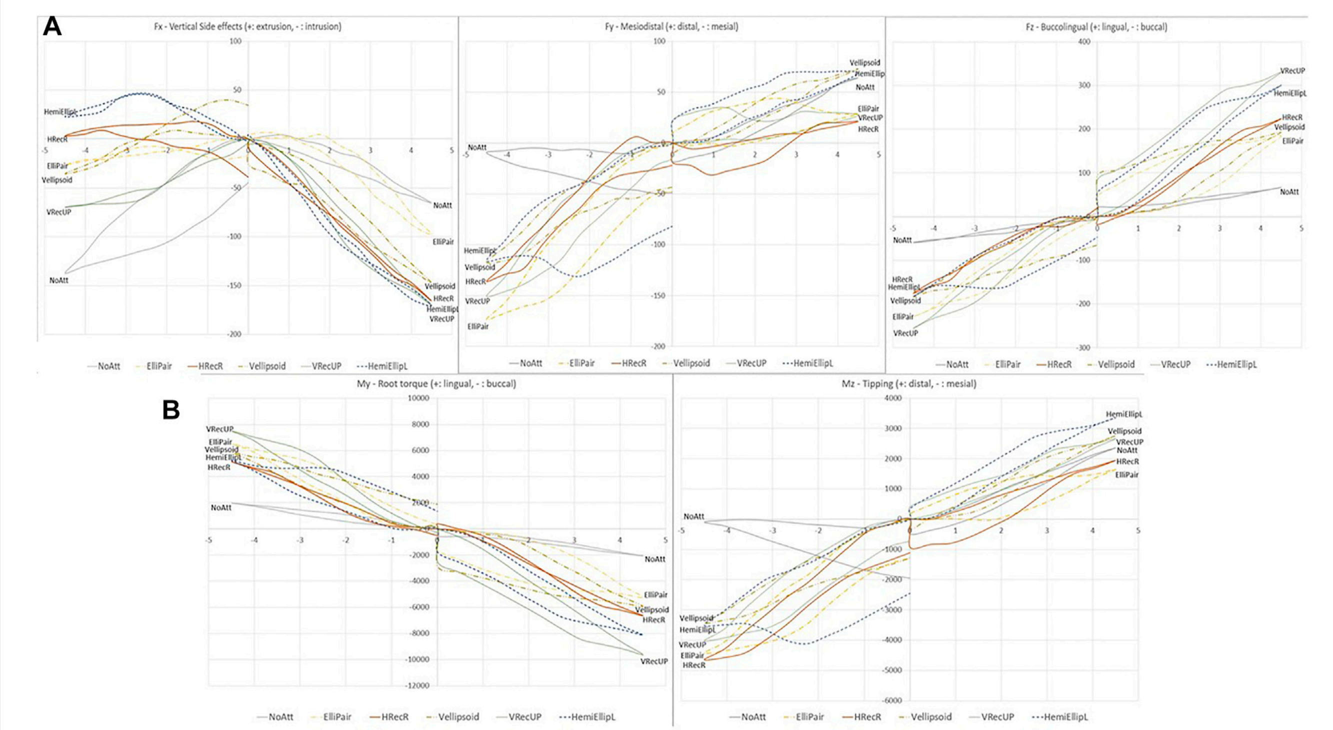

FIGURE 6 | Side effects observed in all three planes of space for the best performing attachments of each group in terms of **(A)**. Forces and **(B)**. Moments. Note that the NoAtt setup exhibits the least amount of side effects in most charts.

rectangular attachment (either up or down) does not play a significant role as both VRecUP and VRecDOWN created moments at comparable levels. Interestingly, the HemiElliL attachment created the highest moment but only when the tooth was rotated mesial (disto-rotation). This means that the flat surface of the attachment (located mesial) was more efficient in creating the needed force system to derotate the tooth compared to the bevelled end when the tooth was rotated distal. It seems that the flat end of the attachment works better as an active surface where a force is more easily applied.

Furthermore, our NoAtt setup exhibited the least amount of derotational moment (M_x) for both mesial and distal rotations. These results demonstrate the need for auxiliaries like attachments in order to perform certain orthodontic tooth movements. This need has been previously reported for certain kinds of movement, as for the extrusion of an upper central incisor or derotation of a lower canine (Bowman, 2017; Elkholy et al., 2019; Savignano et al., 2019). Our results come in agreement with this, which most likely is due to lack of proper "grip" of the tooth by the aligner. It does make sense to think that attempting to reliably rotate a "round" tooth like a premolar requires some sort of a "handle" (Bowman, 2017; Cortona et al., 2020).

It was also interesting to observe that the ElliPair generated almost twice as much derotational moment, when the tooth was rotated distal compared to the opposite direction. To explain this, we need to consider the attachment's design which consists of two hemi-elliptical shapes, the distal one positioned in the occlusal third of the crown, and the mesial one in the gingival third (**Figure 4**). It seems that during mesio-rotation, the attachment positioned more occlusal (here the distal one) is able to generate almost twice the amount of moment compared to the other. This most likely occurs because the aligner itself is much stiffer towards the occlusal end compared to the gingival (free) end and it probably "grips" the tooth better. Ultimately, this could mean that attachments placed in the occlusal third of the crown could be more efficient in providing much needed aligner retention. Nonetheless, this hypothesis has been questioned (Jones et al., 2009).

Side Effects in the Three Planes

A common side effect we encountered in all the attachment setups was the vertical forces created along the long axis of the tooth (*x*-axis), which in almost all occasions were intrusive (**Figure 6**). When the tooth was rotated mesially, all setups showed an intrusive force in a quite substantial amount which in most surpassed 100cN, with the highest in the 3Shape® attachment. This far exceeds the recommended level of force needed for intrusion of 10–20 cN (Proffit et al., 2013), which of course raises questions of higher risk of root resorption. To explain this, one has to look into the biomechanics related to the premolar crown form. Due to the convexity of the crown, the force delivered to the tooth by the aligner when analyzed into the three-axial coordinate system almost always comes with an intrusive component which seems to be independent of any attachment used. This phenomenon has been well-demonstrated by Hahn et al. (Hahn et al., 2010) and is also known as the "watermelon seed" effect (Brezniak, 2008).

Interestingly, when the tooth was rotated distally, a few attachments demonstrated an extrusive force as side effect. This probably has to do with the shape of the tooth we used, and with the *in vitro* nature of our setup: in the absence of an occlusal forces aligner, re-engagement does not occur. Therefore, opposite forces can appear if the attachment is disengaged.

The vertical rectangular attachments also showed the highest moments in the *Y*-axis (mesio-distal). During the distal derotation, this was expressed as buccal root torque and during mesial derotation as lingual root torque, for all attachment types. Firstly, the non-symmetric crown form is to blame for this which does not allow for perfect rotation around the long axis. Secondly, it seems like due to the aforementioned crown anatomy, the aligner can "slide" more easily in the lingual surface, whereas the buccal surface is gripped better through the attachment. This could mean that the presence of a lingual attachment could minimize this type of side effect. Whether this side effect could be seen clinically, however, is a different matter; we know that one of the most challenging movements to achieve with aligners is root movement (Baldwin et al., 2008; Brezniak, 2008; Gomez et al., 2015). Therefore, torque overcorrections are often advised (Simon et al., 2014). It is probably due to this aligners' inaccuracy that we do not see much lingual or buccal root torque when derotating a tooth. Finally, in the *y*-axis, just like in the *x*-axis, the NoAtt setup demonstrated moments in the lowest end of the range showing that a tooth with no attachment has the least severe side effects, but this has to be seen in the light of the reduced desired effect.

Moreover, all attachment types received a distal force during disto-rotation and a mesial force during mesio-rotation. Tipping is considered an "easy" and fairly predictable movement for aligners (Brezniak, 2008; Lombardo et al., 2017), and in contrast to what is valid for the root movement, this side effect could more easily become a clinical reality. This is important in extraction cases where both bodily movement and derotation are needed as it could increase the tipping of the tooth in the extraction space. This is crucial especially for the lower teeth as tipping seems to be more frequently seen in the mandible (Baldwin et al., 2008), due to the presence of a thicker cortical bone which makes bone resorption and thus translation more challenging.

Finally, when it comes to the *z*-axis (bucco-lingual), again, Group 1 VRecUP and VRecDOWN attachments exhibited the highest forces of more than 250cN (lingual during disto-rotation and buccal during mesio-rotation). This is probably related to the aforementioned premolar crown anatomy, which is not a perfect cylinder, but also to the attachment itself; it seems like the vertical rectangular attachments offer a much better "grip".

The study comes with some limitations. The first one is of course the *in vitro* nature of the study itself. Despite the fact that we tried to replicate the oral wet conditions by lubricating the inside of the aligners with artificial saliva, there is an absence of occlusal forces, which might have an impact. Nevertheless, there are clinical implications in this investigation that a clinician orthodontist may find useful as clear aligners, whether produced in-house or not, have become a very popular treatment modality. In addition, it might be difficult to generalize the results of this study to other teeth than premolars, purely due to the difference in the dental anatomy. Nonetheless, the main principles probably apply to other teeth as well. Moreover, the material we have used is not the actual proprietary type of material used by Invisalign® (SmartTrack): the first reason was it was not feasible to use it, then that we wanted to have the same setting for testing all the different setups. Last, at the time the experimental part was carried on, we did not have access to the new SmartForce optimized attachments currently used from Invisalign®.

CONCLUSION

- Attachments should be considered necessary, at least for derotations of more rounded teeth like premolars.
- It seems that rotations above 1° generate moments, which are too high from a clinical point of view. Therefore, aligner steps of no more than 1–1.5° should be recommended for effective derotation of a premolar.
- The vertical rectangular attachments, due to their large flat active surface, perform best when derotating a premolar, but receive the most side effects in terms of tipping, torque, and intrusive force.
- Derotation of a premolar without any attachment was less efficient, despite showing the least side effects,

DATA AVAILABILITY STATEMENT

The raw data supporting the conclusion of this article will be made available by the authors, without undue reservation.

AUTHOR CONTRIBUTIONS

NF contributed to the conceptualization and study design, data extraction and software handling, data analysis, writing of the original draft and subsequent revisions, and editing. MD contributed to the study design, data analysis, supervision, and revisions. MC contributed to supervision, revisions, and editing. PC contributed to the conceptualization and study design, data curation, data analysis, research protocol, supervision, revisions, and editing. All authors approved the submitted version.

ACKNOWLEDGMENTS

We thank Dirk Leonhardt, Department of Dentistry and Oral Health, Aarhus University, Aarhus, Denmark, for laboratory work and for constructive discussions about the set-up.

REFERENCES

Align Technology (2015). *SmartForce Features and Attachments. Designed to HelpYou Treat with Confidence*. Amsterdam: Publ.: Align Technology. Available at: : https://s3.amazonaws.com/learn-invisalign/docs/SmartForce FeaturesandAttachments_en-gb-en.pdf.

Baldwin, D. K., King, G., Ramsay, D. S., Huang, G., and Bollen, A.-M. (2008). Activation Time and Material Stiffness of Sequential Removable Orthodontic Appliances. Part 3: Premolar Extraction Patients. *Am. J. Orthod. Dentofacial Orthopedics* 133 (6), 837–845. doi:10.1016/j.ajodo.2006.06.025

Bowman, S. J. (2017). Improving the Predictability of clear Aligners. *Semin. Orthod.* 23, 65–75. doi:10.1053/j.sodo.2016.10.005

Brezniak, N. (2008). The Clear Plastic Appliance. *The Angle Orthodontist* 78 (2), 381–382. Available at: http://www.ncbi.nlm.nih.gov/pubmed/18251593. doi:10.2319/0003-3219(2008)078[0381:tcpa]2.0.co;2

Cortona, A., Rossini, G., Parrini, S., Deregibus, A., and Castroflorio, T. (2020). Clear Aligner Orthodontic Therapy of Rotated Mandibular Round-Shaped Teeth: A Finite Element Study. *Angle Orthod.* 90 (2), 247–254. doi:10.2319/020719-86.1

Dasy, H., Dasy, A., Asatrian, G., Rózsa, N., Lee, H.-F., and Kwak, J. H. (2015). Effects of Variable Attachment Shapes and Aligner Material on Aligner Retention. *Angle Orthod.* 85 (6), 934–940. doi:10.2319/091014-637.1

Elkholy, F., Mikhaiel, B., Repky, S., Schmidt, F., and Lapatki, B. G. (2019). Effect of Different Attachment Geometries on the Mechanical Load Exerted by PET-G A-ligners during D-erotation of M-andibular C-anines. *J. Orofac Orthop.* 80 (6), 315–326. doi:10.1007/s00056-019-00193-7

Gomez, J. P., Peña, F. M., Martínez, V., Giraldo, D. C., and Cardona, C. I. (2015). Initial Force Systems during Bodily Tooth Movement with Plastic Aligners and Composite Attachments: A Three-Dimensional Finite Element Analysis. *Angle Orthod.* 85 (3), 454–460. doi:10.2319/050714-330.1

Hahn, W., Engelke, B., Jung, K., Dathe, H., Fialka-Fricke, J., Kubein-Meesenburg, D., et al. (2010). Initial Forces and Moments Delivered by Removable Thermoplastic Appliances during Rotation of an Upper central Incisor. *The Angle Orthodontist* 80 (2), 239–246. doi:10.2319/033009-181.1

Haouili, N., Kravitz, N. D., Vaid, N. R., Ferguson, D. J., and Makki, L. (2020). Has Invisalign Improved? A Prospective Follow-Up Study on the Efficacy of Tooth Movement with Invisalign. *Am. J. Orthod. Dentofacial Orthopedics* 158 (3), 420–425. doi:10.1016/j.ajodo.2019.12.015

Jones, M. L., Mah, J., and O'Toole, B. J. (2009). Retention of Thermoformed Aligners with Attachments of Various Shapes and Positions. *J. Clin. Orthod.* 43 (2), 113–117. Available at: www.jco-online.com.

Karras, T., Singh, M., Karkazis, E., Liu, D., Nimeri, G., and Ahuja, B. (2021). Efficacy of Invisalign Attachments: A Retrospective Study. *Am. J. Orthod. Dentofacial Orthopedics* 160 (2), 250–258. doi:10.1016/j.ajodo.2020.04.028

Kesling, H. D. (1945). The Philosophy of the Tooth Positioning Appliance. *Am. J. Orthod. Oral Surg.* 31 (6), 297–304. doi:10.1016/0096-6347(45)90101-3

Kravitz, N. D., Kusnoto, B., BeGole, E., Obrez, A., and Agran, B. (2009). How Well Does Invisalign Work? A Prospective Clinical Study Evaluating the Efficacy of Tooth Movement with Invisalign. *Am. J. Orthod. Dentofacial Orthopedics* 135 (1), 27–35. doi:10.1016/j.ajodo.2007.05.018

Lombardo, L., Arreghini, A., Ramina, F., Huanca Ghislanzoni, L. T., and Siciliani, G. (2017). Predictability of Orthodontic Movement with Orthodontic Aligners: a Retrospective Study. *Prog. Orthod.* 18 (1), 35. Available at: http://progressinorthodontics.springeropen.com/articles/10.1186/s40510-017-0190-0. doi:10.1186/s40510-017-0190-0

Papadimitriou, A., Mousoulea, S., Gkantidis, N., and Kloukos, D. (2018). Clinical Effectiveness of Invisalign® Orthodontic Treatment: a Systematic Review. *Prog. Orthod.* 19, 37. Available at: https://progressinorthodontics.springeropen.com/articles/10.1186/s40510-018-0235-z.

Proffit, W., Fields, H., Jr, and Sarver, D. (2013). *Contemporary Orthodontics*. sixth edition. Maryland Heights, Missouri: Mosby, Elsevier Inc.

Raveli, T. B., Raveli, D. B., Mathias Almeida, K. C., and Pinto, A. D. S. (2017). Molar Uprighting: A Considerable and Safe Decision to Avoid Prosthetic Treatment. *Open Dent J.* 11 (1), 466–475. Available at: /pmc/articles/PMC5646130/.

Roscoe, M. G., Meira, J. B. C., and Cattaneo, P. M. (2015). Association of Orthodontic Force System and Root Resorption: A Systematic Review. *Am. J. Orthod. Dentofacial Orthopedics* 147 (5), 610–626. doi:10.1016/j.ajodo.2014.12.026

Rossini, G., Parrini, S., Castroflorio, T., Deregibus, A., and Debernardi, C. L. (2015). Efficacy of clear Aligners in Controlling Orthodontic Tooth Movement: A Systematic Review. *Angle Orthodontist. Allen Press. Inc.* 85, 881–889. doi:10.2319/061614-436.1

Rosvall, M. D., Fields, H. W., Ziuchkovski, J., Rosenstiel, S. F., and Johnston, W. M. (2009). Attractiveness, Acceptability, and Value of Orthodontic Appliances. *Am. J. Orthod. Dentofacial Orthopedics* 135 (3), e1–276. doi:10.1016/j.ajodo.2008.07.011

Savignano, R., Valentino, R., Razionale, A. V., Michelotti, A., Barone, S., and D'Antò, V. (2019). Biomechanical Effects of Different Auxiliary-Aligner Designs for the Extrusion of an Upper Central Incisor: A Finite Element Analysis. *J. Healthc. Eng.* 2019, 1–9. doi:10.1155/2019/9687127

Sheridan, J. J. (2004). THE READERS ' CORNER. *J. Clin Orthod.* 38 (10), 543–544.

Simon, M., Keilig, L., Schwarze, J., Jung, B. A., and Bourauel, C. (2014). Treatment Outcome and Efficacy of an Aligner Technique-Rregarding Incisor Torque, Premolar Derotation and Molar Distalization. *BMC Oral Health* 14 (68), 68. doi:10.1186/1472-6831-14-68

Theodorou, C. I., Kuijpers-Jagtman, A. M., Bronkhorst, E. M., and Wagener, F. A. D. T. G. (2019). Optimal Force Magnitude for Bodily Orthodontic Tooth Movement with Fixed Appliances: A Systematic Review. *Am. J. Orthod. Dentofacial Orthopedics* 156 (5), 582–592. doi:10.1016/j.ajodo.2019.05.011

Viecilli, R. F., Chen, J., Katona, T. R., and Roberts, W. E. (2009). Force System Generated by an Adjustable Molar Root Movement Mechanism. *Am. J. Orthod. Dentofacial Orthopedics* 135 (2), 165–173. doi:10.1016/j.ajodo.2007.02.058

Conflict of Interest: The authors declare that the research was conducted in the absence of any commercial or financial relationships that could be construed as a potential conflict of interest.

frontiers | Frontiers in Materials

ORIGINAL RESEARCH
published: 14 April 2022
doi: 10.3389/fmats.2022.811251

Control of Orthodontic Tooth Movement by Nitric Oxide Releasing Nanoparticles in Sprague-Dawley Rats

*Derrick Crawford[1], Tommy C. Lau[1], Megan C. Frost[2] and Nan E. Hatch[1]**

[1]Department of Orthodontics and Pediatric Dentistry, School of Dentistry, University of Michigan, Ann Arbor, MI, United States, [2]Department of Kinesiology and Integrative Physiology, Michigan Technological University, Houghton, MI, United States

Orthodontic treatment commonly requires the need to prevent movement of some teeth while maximizing movement of other teeth. This study aimed to investigate the influence of locally injected nitric oxide (NO) releasing nanoparticles on orthodontic tooth movement in rats. Materials and Methods: Experimental tooth movement was achieved with nickel-titanium alloy springs ligated between the maxillary first molar and ipsilateral incisor. 2.2 mg/kg of silica nanoparticles containing S-nitrosothiol groups were injected into the mucosa just mesial to 1st molar teeth immediately prior to orthodontic appliance activation. NO release from nanoparticles was measured *in vitro* by chemiluminescence. Tooth movement was measured using polyvinyl siloxane impressions. Bones were analyzed by microcomputed tomography. Local tissue was assessed by histomorphometry. Results: Nanoparticles released a burst of NO within the first hours at approximately 10 ppb/mg particles that diminished by 10 × to approximately 1 ppb/mg particles over the next 1–4 days, and then diminished again by tenfold from day 4 to day 7, at which point it was no longer measurable. Molar but not incisor tooth movement was inhibited over 50% by injection of the NO releasing nanoparticles. Inhibition of molar tooth movement occurred only during active NO release from nanoparticles, which lasted for approximately 1 week. Molar tooth movement returned to control levels of tooth movement after end of NO release. Alveolar and long bones were not impacted by injection of the NO releasing nanoparticles, and serum cyclic guanosine monophosphate (cGMP) levels were not increased in animals that received the NO releasing nanoparticles. Root resorption was decreased and periodontal blood vessel numbers were increased in animals with appliances that were injected with the NO releasing nanoparticles as compared to animals with appliances that did not receive injections with the nanoparticles. Conclusion: Nitric oxide (NO) release from S-nitrosothiol containing nanoparticles inhibits movement of teeth adjacent to the site of nanoparticle injection for 1 week. Additional studies are needed to establish biologic mechanisms, optimize efficacy and increase longevity of this orthodontic anchorage effect.

Keywords: orthodontic, nitric oxide, biomaterial, nanoparticle, tooth movement, controlled release, rodent model

Edited by:
Paolo M. Cattaneo,
University of Melbourne, Australia

Reviewed by:
Jose Mauro Granjeiro,
National Institute of Metrology, Quality and Technology, Brazil
Miguel Ángel Garcés-Villalá,
Catholic University San Antonio of Murcia, Spain

***Correspondence:**
Nan E. Hatch
nhatch@umich.edu

Specialty section:
This article was submitted to Biomaterials,
a section of the journal Frontiers in Materials

Received: 08 November 2021
Accepted: 21 March 2022
Published: 14 April 2022

Citation:
Crawford D, Lau TC, Frost MC and Hatch NE (2022) Control of Orthodontic Tooth Movement by Nitric Oxide Releasing Nanoparticles in Sprague-Dawley Rats.
Front. Mater. 9:811251.
doi: 10.3389/fmats.2022.811251

INTRODUCTION

Orthodontic treatment is common because untreated malocclusion negatively impacts oral function (eating, speech) and causes physical, psychological and social disability (Sun et al., 2017). Approximately 15% of the U.S. population has a severe dental malocclusion that negatively impacts function and social acceptability (Proffit et al., 1998). This translates to a prevalence of over 48 million people in the U.S. with significant orthodontic treatment need. Treatment of such severe cases requires precise control of individual teeth, including the ability to prevent movement of some teeth while maximizing movement of other teeth (**Figure 1**). In orthodontics, the term anchorage refers to methods for preventing undesirable tooth movement. Currently, orthodontic anchorage relies on auxiliary mechanical devices. In some cases, more control is desired than is clinically achieved (Clemmer and Hayes, 1979; Chen et al., 2007; Al-Awadhi et al., 2015; Kim et al., 2016a). As a result, treatment times can be extended and/or an ideal occlusion may not be achieved. Longer treatment times increase the risk for negative sequelae such as decalcification/demineralization, caries and tooth root resorption (Sameshima and Sinclair, 2001; Gonzales et al., 2008; Feldens et al., 2015; Kim et al., 2016b; Pastro et al., 2018).

Orthodontic tooth movement is a bone modeling process in which orthodontic forces shift teeth within sockets causing hypoxia, fluid flow and tissue stretch/compression. These mechanical changes stimulate sterile inflammatory signaling, recruitment and activity of osteoclasts and osteoblasts, and tooth movement beyond the constraints of the original tooth socket (Masella and Meister, 2006; Jiang et al., 2016). Nitric oxide (NO) is a signaling molecule that was previously hypothesized to mediate orthodontic tooth movement (Yoo et al., 2004). NO was originally identified as "endothelial-derived relaxing factor". NO release from endothelial cells leads to the production of cGMP which has paracrine effects on nearby smooth muscle cells leading to a vasodilation response (Griffith et al., 1984; Ignarro, 1990; Lowenstein and Snyder, 1992). In addition to its vascularization effect (Griffith et al., 1984; Shih and Claffey, 1998), NO has inflammatory and immunomodulatory (Marcinkiewicz and Chain, 1993; Eun et al., 2000) functions. NO is known to alter inflammatory cytokine and chemokine production, alter osteoblast and osteoclast bone anabolism/ catabolism, and enhance vascularization and blood flow (Kalyanaraman et al., 2017; Vanhoutte et al., 2017; Gozdzik et al., 2018; Gantner et al., 2020). Physiologic effects of NO are limited by the location and timing of NO production, because NO has a short half-life and small diffusional distance (Lancaster, 1997; Vaughn et al., 1998). Therefore, an NO producing biomaterial is essential for therapeutic application of NO. NO producing biomaterials are currently under investigation for viral infection (Garren et al., 2021), cancer (Khan et al., 2020), inflammation, obesity, cardiovascular disease (Bladowski et al., 2020; Król and Kepinska, 2020), and cervical ripening for birth (Ghosh et al., 2016). Based upon these prior findings, in this study we investigate the efficacy of NO released from S-nitrosothiol containing silica nanoparticles for control of orthodontic tooth movement.

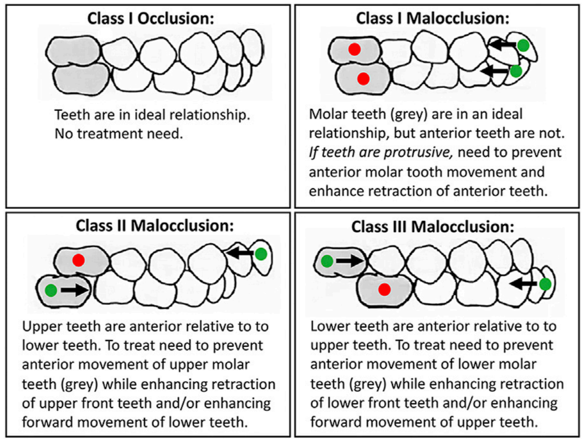

FIGURE 1 | Many malocclusions require differential orthodontic tooth movement to achieve ideal functional and esthetic outcomes. Teeth that need inhibition of movement for successful treatment are marked with a red dot. Teeth that need enhancement of movement for successful treatment are marked with a green dot. Arrows mark direction of desired tooth movement.

MATERIALS AND METHODS

Formulation of Nitric Oxide Releasing Nanoparticles

NO releasing, silica nanoparticles were fabricated at room temperature according to the method previously developed by Frost and Meyerhoff (Frost and Meyerhoff, 2005). Briefly, 7–10 nm fumed silica particles were derivatized with 3-aminopropyltrimethoxsilane to cover the particle surface. The primary amine was reacted with a self-protected thioacetone to form an amide bond and exposes a free thiol. The free thiol was then nitrosated to produce the NO donor, S-Nitroso-N-acetyl-D-penicillamine (SNAP). Residual solvent was removed by air drying of particles under vacuum overnight. Approximately 60 mg of particles were suspended in 1 ml of toluene in a 5 ml glass vial. 300 ml of t-butylnitrite was added. The reaction mixture was agitated, covered in foil and allowed to react for 2 h. The solvent was then removed and particles were vacuum dried. S-nitrosothiol containing silica nanoparticles are highly stable and were stored at room temperature in the dark before use.

In Vitro Release Kinetic Studies

Release of NO from fabricated nanoparticles was performed on nanoparticles that were saturated with deionized water and held at 37°C in a humidified chamber for the duration of the experiment (**Figure 2**). NO was quantified by ozone based chemiluminescent detection with Sievers 280i Nitric Oxide Analyzer (NOA) using 200 ml/min flow rate. 45 ppm medical grade calibration NO gas (Air Liquid Healthcare America Corp.) was used to complete the 2-point calibration of the chemiluminescent detector prior to analyses. Ambient air was used to calibrate for zero NO gas and as the sweep gas. NO was swept from the headspace of 60 mm disposable petri dish sample holders. NO measurements were taken every day for 10 min until

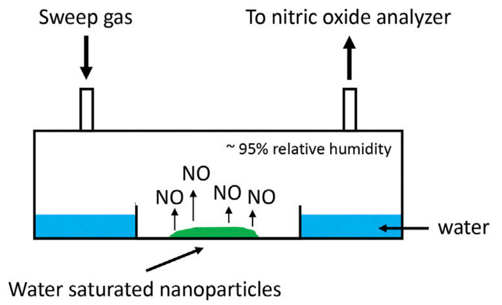

FIGURE 2 | Schematic of *in vitro* NO release kinetic analysis of nanoparticles. Nanoparticles saturated with deionized water released NO into a humidified chamber. NO was measured by chemiluminescence. Sweep gas containing no NO was ambient air.

NO was no longer detected. Data was recorded at an interval of 1/sec.

Animals and Orthodontic Appliance

In this study, we compared two experimental groups (animals that received an injection with NO releasing nanoparticle but no orthodontic appliances and animals that received an injection with NO releasing nanoparticle plus orthodontic appliances) with two control groups (animals that received an injection with saline but no orthodontic appliances and animals that received an injection with saline plus orthodontic appliances). Rats were purchased from a commercial supplier and acclimatized for 1 week prior to experimentation. Each group was comprised of eight male Sprague-Dawley rats of approximately 350 g who were randomly distributed to each group. This sample size was based upon the variability found in our prior studies in which $n = 6–8$ per group was adequate to establish significant differences in tooth movement between groups (Hudson et al., 2012; Schneider et al., 2015; Sydorak et al., 2019). Rats were housed in a controlled atmosphere of 25°C with a 12-hour light and dark cycle. They were fed a diet consisting of standard rat chow (Harlan Laboratories, Indianapolis, IN) and distilled water *ad libitum*. Based upon past studies, an a priori exclusion criteria was excessive vertical movement of the first molar. No animals had molars with significant extrusion during or after the tooth movement period, likely due to the diligence and regular attention given to the rats and their orthodontic appliances. Animals were anesthetized with isoflurane for the injection and orthodontic appliance placement (and appliance adjustment as needed). Animals were euthanized by CO_2 overdose.

Just prior to orthodontic appliance placement, each rat was injected with 30 μL of saline (control animals) or saline containing 2.2 mg/kg of nanoparticles containing S-nitrosothiol groups (experimental animals) into the gingival mucosa just mesial to the maxillary first molar teeth immediately prior to orthodontic appliance activation using a 50 ul microliter syringe and 33 gauge needles (Hamilton Company, Reno NV). As previously described (King et al., 1991; Dunn et al., 2007; Sydorak et al., 2019) for the orthodontic appliance, closed coil nickel-titanium springs to provide 50 g mesial molar force were delivered to the maxillary first molars by ligation of between the maxillary first molar and ipsilateral maxillary central incisor with stainless ligatures that were then adhered with composite. Mandibular incisors were filed down on a weekly basis to reduce appliance breakage. Orthodontic appliances were repaired and/or adjusted as needed to accommodate for continuously erupting maxillary incisors so as to maintain a horizontal force vector. All animal procedures followed federal guidelines and were approved of by the University of Michigan Institutional Animal Use and Care Committee prior to the study.

Measurements of Tooth Movement

Tooth movement was measured every 6 days by stone models made from polyvinylsiloxane impressions, as previously described (Hudson et al., 2012). The occlusal surfaces of each model were scanned (Epson Expression 10,000 XL) at 1200 dpi adjacent to a 10 mm ruler and then magnified at 20 × using imaging software (Adobe Photoshop CS5, Adobe Systems, Inc., San Jose, CA). Measurements were calibrated to the imaged ruler. Tooth movement was measured to the nearest 0.01 mm. Molar mesial movement was measured from the distal groove of the maxillary first molar to the distal surface of the maxillary third molar. Incisor distal movement was measured from the distal surface of the maxillary third molars to the mid-facial gingival margin of the ipsilateral incisor. To account for growth of the maxilla during the 18 days of orthodontic treatment, incisor distal movements were normalized using the incisor position compared to third molar position in animals without orthodontic appliances (average of 1.2 mm). Molar tooth movement did not need normalization as there was no growth displacement of the first relative to the third molar in the animals without orthodontic appliances.

Micro Computed Tomographic Bone Analyses

After 18 days of tooth movement, animals were euthanized by CO_2 overdose. Micro-CT analyses were performed to quantify alveolar and long bone volume and density between groups. Alveolar bone analysis provides information on potential effects of tooth movement and/or nanoparticles on local bone. Long bone analysis provides information on potential effects of tooth movement and/or nanoparticles on distant bone (systemic effect). Hemi-maxillae and femurs were dissected, fixed in 10% formalin for 48 h followed by transition to 70% ethanol for storage at 4C prior to analyses. Both hemi-maxillae and femur specimens were scanned using a micro-CT system (μCT100 Scanco Medical, Bassersdorf, Switzerland). Scan settings were 18 μm voxel, 70 kVp, 114 μA, 0.5 mm AL filter, and integration time of 500 ms. For femur scans, specimens were scanned over the entire length of the femur. A 0.9 mm section of trabecular bone was analyzed at the proximal metaphysis of the femur, starting 0.9 mm from the growth plate. A 0.9 mm section of cortical bone was analyzed at the mid-diaphyseal shaft. For alveolar bone, an ROI was designated as within the confines of the maxillary first molar roots, from the molar root furcation to the apex of the buccal root (**Figure 3**). This allowed measurement of bone changes within the local area of the first molar tooth ± injected particles.

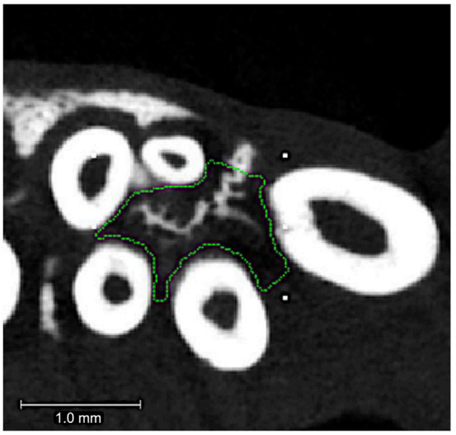

FIGURE 3 | Alveolar bone region of interest. Micro-CT axial slice image showing region of interest for the maxillary first molar intra-radicular alveolar bone. The region of interest (ROI) is outlined in green. This ROI extended from the molar root furcation to the apex of the root and did not include the tooth roots themselves. Tiny white rectangles are orientation marks placed by the operator prior to custom outlining the 3D intra-radicular ROI for analysis.

Statistical Analyses

Primary outcomes were quantitative measurements of tooth movements. Secondary outcomes were *in vitro* NO release from fabricated nanoparticles, quantitative measurements of alveolar and femur bone and histomorphometric measurements of root resorption and blood vessels. The sample size was based upon data variability found in our prior studies using this same rodent model of tooth movement (Hudson et al., 2012; Sydorak et al., 2019). Descriptive statistics (mean, standard deviation, 95% confidence intervals) were calculated. Data were checked for normality using the D'Agostino & Pearson test. Normal data were compared using an unpaired t test. Nonnormal data were compared using a Mann-Whitney test. Statistical significance was established as $p < 0.05$.

Serum Cyclic Guanosine Monophosphate Measurements

Because NO stimulates production of the secondary messenger cyclic guanosine monophosphate (cGMP) (Francis et al., 2010), cGMP can be used as a marker of NO activity (Kalyanaraman et al., 2017). Blood was obtained from animals on day 0 (before orthodontic appliance placement), and days 1, 6 and 12 after orthodontic appliance placement using a 27 gauge needle through the lateral tail vein. Serum was isolated by incubation of blood at room temperature for 40 min followed by centrifugation at 5000 rpm at 4°C. Supernatant (serum) was stored at −80°C until assay. Serum levels of cGMP were measured using a commercially available colorimetric ELISA kit (Abcam, ab133052). This ELISA is composed of a goat anti-rabbit IgG antibody precoated wells, an alkaline phosphatase conjugated-cGMP antigen, and a polyclonal rabbit antibody specific to cGMP. Colorimetric detection of cGMP was measured at 405 nm with a 570 nm correction using a SpectraMax i3 × (Molecular Devices). A standard curve was established using the commercially provided 5,000 pmol/ml stock, which was serially diluted in the commercially provided assay buffer. Final concentrations of 500, 100, 20, 4, 0.8 and 0 pmol/ml were used for standard curve preparation. cGMP levels are reported as pmol/ml by comparison to the standard curve. Due to well number limitations, serum isolated on days 0 and 1 were analyzed separately from serum isolated on days 6 and 12,, resulting in slightly different background levels for the negative control and the experimental samples for days 0 and 1 vs. days 6 and 12. Serum from each animal (n = 8 per group) was individually analyzed.

Quantitative Histomorphometry

Hemi-maxillae were dissected, fixed in 10% neutral buffered formalin and decalcified in 10% EDTA for 6 weeks. 6 mm sections axial sections were taken from the coronal third of the root (**Figure 4**). We quantified the coronal third of the root to ensure that sections were of similar apical depths by using the molar root furcation as a reference and to view all five roots of the tooth. Sections were stained with hematoxylin and eosin (H&E) for visualization of all roots plus periodontal ligament and surrounding alveolar bone of the first molar tooth. Histomorphometry was performed on the smaller distobuccal and buccal (intermediate) tooth roots, as smaller roots are more prone to resorption due to orthodontic tooth movement (Gonzales et al., 2008; Cuoghi et al., 2014). *ImageJ* software (National Institutes of Health) was utilized to quantify percent resorption per tooth root and number blood vessels within the periodontal ligament (PDL). Roots that were conjoined or otherwise undefined were excluded. This resulted in final buccal root samples sizes of $n = 8$ for control animals with no appliance and saline injections, $n = 5$ for control animals with the orthodontic appliance and saline injections, $n = 8$ for experimental animals with no appliance and nanoparticles injection, and $n = 6$ for experimental animals with the orthodontic appliance and nanoparticles injection. This resulted in final distobuccal root samples sizes of $n = 8$ for control animals with no appliance and saline injections, $n = 7$ for control animals with the orthodontic appliance and saline injections, $n = 8$ for experimental animals with no appliance and nanoparticles injection, and $n = 7$ for experimental animals with the orthodontic appliance and nanoparticles injection. Percent root resorption was calculated using the difference between the estimated original elliptical root area and the actual root area. Blood vessels located within the PDL space were counted and qualified as compressed or not compressed. Three separate axial sections from each hemi-maxilla were analyzed then averaged per animal for comparison across groups.

RESULTS

Animal Status

One animal died during the initial appliance placement procedure due to an adverse reaction to the anesthesia and was excluded from

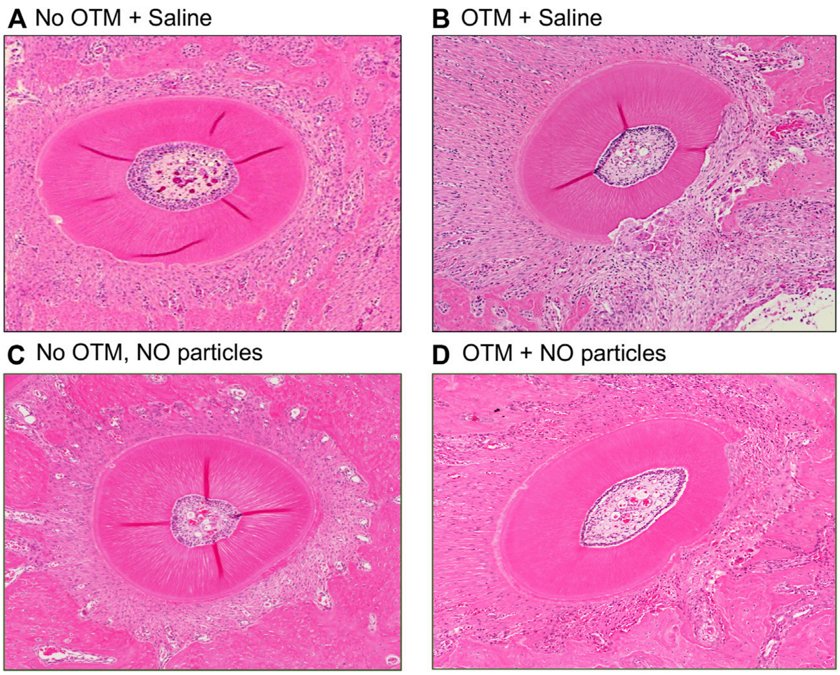

FIGURE 4 | NO releasing biomaterial inhibits molar but not incisor tooth movement. **(A)** Mesial molar tooth movement over the 18-day experimental period. Means ± standard deviations are shown. Animals that had orthodontic appliances plus NO releasing nanoparticles showed significantly diminished mesial molar tooth movement at all time points as compared to animals that had orthodontic appliances but not NO releasing nanoparticles. $^{*}p < 0.05$, $^{**}p < 0.005$ between groups. Note diminished slope of tooth movement for animals with NO releasing nanoparticles compared to that for animals without NO releasing nanoparticles from days 1–6 that increases to match that of animals without NO releasing nanoparticles by days 12–18. **(B)** Distal incisor tooth movement at the end of the 18-day experimental period. No significant differences were found for incisor movement between groups (PBS mean = 1.92, NO mean = 1.90, 95% confidence interval of difference between the means = −0.26 to +0.22). Whisker plots showing medians, interquartile range, minimum and maximum values are shown.

the study. This animal was replaced with another rat. All other animals were included with no adverse reactions to anesthesia, appliance placement or tooth movement, and followed until day 18 when they were euthanized, such that final animal numbers for tooth movement and micro-CT measurements were $n = 8$ per group. No significant differences in initial animal weights were seen between any of the groups. Prior to injections and orthodontic appliance placement, animals with orthodontic appliances weighed 359 ± 20 g (mean ± standard deviation), and 379 ± 13 g in the PBS and nanoparticle groups, respectively. Prior to injections, animals without orthodontic appliances weighed 364 ± 15 g (mean ± standard deviation), and 383 ± 27 g in the PBS and nanoparticle groups, respectively. At day 18, animals with orthodontic appliances weighed 427 ± 18 g, and 427 ± 29 g in the PBS and nanoparticle groups, respectively. At day 18, the animals without orthodontic appliances weighed 441 ± 31 g and 467.6 ± 30 g in the PBS and NO nanoparticle groups, respectively. No significant differences in final animal weights were seen between any of the groups.

Tooth Movement

As stated above, experimental animals that received an injection of the NO releasing nanoparticles included a group that had orthodontic appliances and a group that did not have orthodontic appliances. Control animals that received a single injection of saline also included a group that had orthodontic appliances and a group that did not have orthodontic appliances. All injections were performed into the gingival mucosa just mesial to the maxillary first molar tooth just prior to orthodontic appliance placement. The single injection of 2.2 mg/kg nanoparticles significantly reduced the amount of mesial molar tooth movement as compared to the amount of cumulative mesial molar tooth movement seen in animals that received saline injections at day 6 (0.12 ± 0.01 vs. 0.27 ± 0.02 mm, $p <$ 0.001), day 12 (0.27 ± 0.04 vs. 0.47 ± 0.05 mm, $p < 0.01$) and day 18 (0.53 ± 0.07 vs. 0.75 ± 0.06 mm, $p < 0.05$) (**Figure 5A**). The single injection of NO releasing silica nanoparticles did not significantly influence the amount of distal incisor tooth movement as compared to that seen in animals that received saline injections (day 18, 1.90 ± 0.08 vs. 1.92 ± 0.08, not significant) (**Figure 5B**).

Silica Nanoparticle Nitric Oxide Release Kinetics and Relationship to Tooth Movement

In vitro release kinetic studies using the same batch of formulated nanoparticles that was used *in vivo* revealed that the nanoparticles released a burst of NO within the first hours at 10.0 ± 0.32 ppb/mg particles (1.8^{-12} ± 5.8^{-14} nmol/mg particles that diminished by 10x to 1.0 ± 0.05 ppb/mg particles (1.8^{-13} ± 8.6^{-15} nmol/mg

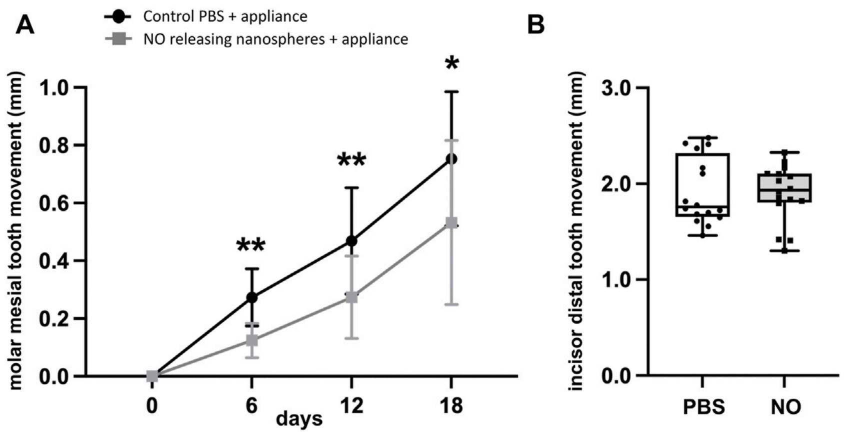

FIGURE 5 | Histology of the distobuccal root after 18 days ± orthodontic tooth movement. Hematoxylin and eosin (H&E) stained representative images of the distobuccal root of the first molar of **(A)** animals that received control saline injections and no orthodontic appliances, **(B)** animals that received control saline injections and had orthodontic appliances, **(C)** animals that received experimental nanoparticles injections and no orthodontic appliances, and **(D)** animals that received experimental nanoparticles injections and had orthodontic appliances. OTM = orthodontic tooth movement, saline = PBS = phosphate buffered saline.

particles over the next 1–4 days, and then diminished again by tenfold from day 4 to day 7, at which point it was no longer measurable (**Figure 6A**).

Based upon the *in vitro* release data showing loss of NO release by approximately day 7 *in vitro*, it seemed likely that the effect of the NO releasing nanoparticles was likely lost by the final time point of 18 days *in vivo*. Therefore, to gain a better appreciation for orthodontic anchorage (inhibition of mesial molar movement without any effect on distal incisor movement) at earlier time points, we calculated the amount of molar movement separately, between days 0–6, 6–12 and 12–18. While cumulative tooth movement was significant at all time points, comparisons of intermediate time periods (0–6, 6–12, and 12–18) show that tooth inhibition in the NO releasing group occurred only during days 0–6, with no significant inhibition noted between days 6–12 or 12–18 (**Figures 6B–D**). This is also evident when viewing the cumulative molar tooth movement data in that the difference between slopes of the experimental (received NO nanoparticles) and control (received saline) groups diminished over time (**Figure 5A**). That tooth movement returned to control rates after release of NO is worth noting because this indicates that no rebound effect occurred after cessation of exposure to NO. From this data, we also calculated the average percent inhibition of mesial molar tooth movement in the NO releasing nanoparticle group compared with the control group. Animals injected with the nanoparticles had 54% less molar movement at day 6, 42% less cumulative molar movement at day 12 and 29% less cumulative molar movement at day 18.

Local Alveolar Bone Parameters

To evaluate local effects of the delivered NO releasing biomaterial on alveolar bone investing the tooth adjacent to the site of injection and under orthodontic forces, first molar intra-radicular bone quality parameters were measured via micro CT. Sample size was $n = 8$ specimen per group. No differences in bone volume fraction, bone mineral density or tissue mineral density were seen between animals that received saline vs. animals that received that NO releasing nanoparticles, regardless of orthodontic appliance placement, at day 18 of the tooth movement experiments (**Table 1**). As expected, bone volume fraction, bone mineral density and tissue mineral density were significantly reduced in animals with orthodontic appliances compared to those without orthodontic appliances, regardless of NO delivery.

Long Bone Parameters

To evaluate potential systemic effects that local injections of the experimental NO releasing biomaterial might have on bones distant from the site of injection, femur cortical and trabecular bone were analyzed by micro CT. Sample size was $n = 8$ specimen per group. No differences in trabecular bone volume fraction, trabecular number, trabecular thickness or trabecular spacing were seen between animals that received saline vs. animals that received that NO releasing nanoparticles, regardless of orthodontic appliance placement, at day 18 of the tooth movement experiments (**Table 2**). One parameter (trabecular bone volume fraction) was significantly diminished in animals with appliances compared to animals without appliances in the NO releasing nanoparticle groups. No differences in cortical bone volume fraction, bone mineral density and tissue mineral density were seen between animals that received saline vs. animals that received that NO releasing nanoparticles. In addition, no differences in cortical bone parameters were seen between animals with orthodontics appliances and animals without orthodontic appliances (**Table 3**).

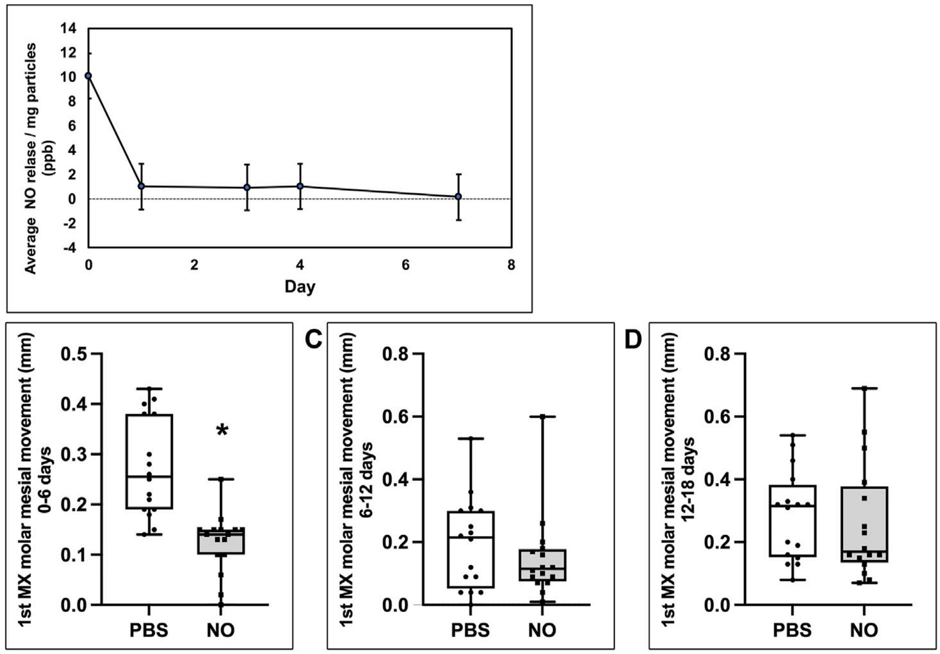

FIGURE 6 | Inhibition of molar tooth movement coincides with NO release from N-nitrosothiol nanoparticles. **(A)** NO *in vitro* release profile from nanoparticles. Results show an initial burst release followed by stable NO release until day 4 upon which NO release decreases to non-measurable levels by day 7. **(B,C,D)** Mesial molar tooth movements on days 1–6 **(B)**, 6–12 **(C)** and 12–18 **(D)**. Whisker plots showing medians, interquartile range, minimum and maximum values are shown. Mesial molar tooth movement is significantly inhibited by over 50% during days 1–6 of the experimental period. *$p < 0.001$. No significant inhibition of mesial molar tooth movement is seen during days 6–12 or days 12–18 of the experimental period.

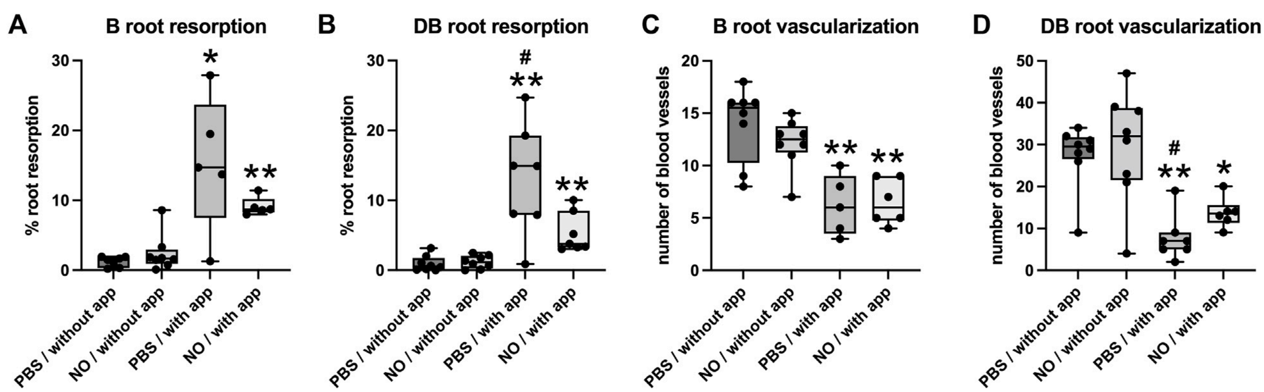

FIGURE 7 | Histomorphometry of root resorption and PDL vascularization of the buccal and distobuccal roots of the maxillary first molar after 18 days ± orthodontic tooth movement. Whisker plots showing medians, interquartile range, minimum and maximum values are shown. **(A,B)** Root resorption is significantly increased in animals that underwent tooth movement compared to those that did not have orthodontic appliances on both buccal and distobuccal roots. **(C,D)** Blood vessel numbers in the PDL were significantly decreased in animals that underwent tooth movement compared to those that did not have orthodontic appliances on both buccal and distobuccal roots. Significantly less root resorption was seen in animals that underwent tooth movement and received injections of NO releasing nanoparticles compared to animals that underwent tooth movement and received injections of saline for the distobuccal root **(B)**. Significantly more blood vessels were seen in animals that underwent tooth movement and received injections of NO releasing nanoparticles compared to animals that underwent tooth movement and received injections of saline for the distobuccal root **(D)**. *$p < 0.05$ compared to group without tooth movement, **$p < 0.005$ compared to group without tooth movement, $^{\#}p < 0.05$ compared to group that received nanoparticle injections. Without app = no orthodontic appliances/no orthodontic tooth movement, with app = with orthodontic appliances/with orthodontic tooth movement, PBS = phosphate buffered saline.

TABLE 1 | Intra-radicular alveolar bone quality measures.

	Bone volume fraction (%)	Bone mineral density (mg/cc)	Tissue mineral density (mg/cc)
No appliances	Mean ± SD: 0.70 ± 0.03 95% CI: 0.68 0.72	Mean ± SD: 714 ± 31 95% CI: 686–743	Mean ± SD: 999 ± 15 95% CI: 985–1021
No Appliances + NO releasing nanoparticles	Mean ± SD: 0.72 ± 0.04 95% CI: 0.67–0.76	Mean ± SD: 736 ± 41 95% CI: 685–787	Mean ± SD: 1004 ± 19 95% CI: 981–1027
Appliances	Mean ± SD: 0.34 ± 0.19** 95% CI: 0.11–0.57	Mean ± SD: 372 ± 170** 95% CI: 162–583	Mean ± SD: 950 ± 29** 95% CI: 913–986
Appliances + NO releasing nanoparticles	Mean ± SD: 0.45 ± 0.08** 95% CI: 0.38–0.52	Mean ± SD: 475 ± 77** 95% CI: 411–539	Mean ± SD: 979 ± 13* 95% CI: 968–990

*$p < .005$, **$p < .001$ vs. no appliances.*

TABLE 2 | Trabecular bone quality measures.

	Bone volume fraction (%)	Trabecular number (1/mm)	Trabecular thickness (mm)	Trabecular separation (mm)
No appliances	Mean ± SD: 0.31 ± 0.07 95% CI: 0.25–0.37	Mean ± SD: 4.7 ± 0.6 95% CI: 4.3–5.2	Mean ± SD: 0.088 ± 0.006 95% CI: 0.83–0.93	Mean ± SD: 0.20 ± 0.03 95% CI: 0.17–0.22
No Appliances + NO releasing nanoparticles	Mean ± SD: 0.34 ± 0.06 95% CI: 0.30–0.39	Mean ± SD: 4.8 ± 0.6 95% CI: 4.3–5.3	Mean ± SD: 0.093 ± 0.004 95% CI: 0.90–0.95	Mean ± SD: 0.19 ±0.04 95% CI: 0.16–0.22
Appliances	Mean ± SD: 0.35 ± 0.06 95% CI: 0.30–0.40	Mean ± SD: 4.8 ± 0.5 95% CI: 4.4–5.2	Mean ± SD: 0.094 ± 0.007 95% CI: 0.89–0.100	Mean ± SD: 0.19 ± 0.04 95% CI: 0.17–0.21
Appliances + NO releasing nanoparticles	Mean ± SD: 0.30 ± 0.03 95% CI: 0.27–0.32	Mean ± SD: 4.4 ± 0.4 95% CI: 4.1–4.8	Mean ± SD: 0.089± 0.003 95% CI: 0.96–0.91	Mean ± SD: 0.21 ± 0.03 95% CI: 0.19–0.24

No significant differences.

TABLE 3 | Cortical bone quality measures.

	Bone volume fraction (%)	Bone mineral density (mg/cc)	Tissue mineral density (mg/cc)
No appliances	Mean ± SD: 0.62 ± 0.03 95% CI: 0.59–0.64	Mean ± SD: 731 ± 26 95% CI: 709–753	Mean ± SD: 1141 ± 17 95% CI: 1126–1155
No Appliances + NO releasing nanoparticles	Mean ± SD: 0.63 ± 0.03 95% CI: 0.60–0.65	Mean ± SD: 746 ± 38 95% CI: 714–778	Mean ± SD: 1146 ± 23 95% CI: 1127–1165
Appliances	Mean ± SD: 0.60 ± 0.03 95% CI: 0.58–0.63	Mean ± SD: 718 ± 33 95% CI: 690–746	Mean ± SD: 1145 ± 20 95% CI: 1129–1161
Appliances + NO releasing nanoparticles	Mean ± SD: 0.60 ± 0.02 95% CI: 0.59–0.62	Mean ± SD: 716 ± 18 95% CI: 701–731	Mean ± SD: 1139 ± 13 95% CI: 1127–1150

No significant differences.

Serum Cyclic Guanosine Monophosphate Measurements

Because NO cannot be directly measured *in vivo*, to determine if the injected NO releasing nanoparticles altered NO signaling systemically, we measured serum levels of cGMP, the primary direct downstream target of NO (Friebe and Koesling, 2009). Results show that no change in circulating cGMP levels occurred in any of the control or experimental groups, before or after injection of the NO releasing nanoparticles (**Supplementary Figure S1**).

Root Resorption and Vascularization

Histomorphometric measurements of root resorption revealed significantly greater resorption of distobuccal and buccal (intermediate) tooth roots in animals with orthodontic appliances as compared to animals without orthodontic appliance (**Figure 7**). In addition, resorption of the distobuccal root was significantly lower in animals with appliances that were injected with the NO releasing nanoparticles as compared to animals with appliances that did not receive injections with the nanoparticles.

Blood vessel quantification revealed that the number of blood vessels located within the PDL of distobuccal and buccal (intermediate) tooth roots was significantly lower in animals with orthodontic appliances as compared to animals without orthodontic appliance. In addition, the number of PDL blood vessels within the distobuccal root was significantly higher in animals with appliances that were injected with the NO releasing nanoparticles as compared to animals with appliances that did not receive injections with the nanoparticles (**Figure 7**). Blood vessels were compressed in all animals with orthodontic appliances and were not compressed in animals with no appliances.

DISCUSSION

Because no fixed intraoral anatomical anchor exists, orthodontic forces can create both desirable and undesirable tooth movements. During orthodontic treatment, precisely controlled anchorage (inhibition of undesired tooth movement to enhance favorable tooth movement) is often critical to effectively establish a stable, highly functional occlusion. Contemporary orthodontists utilize various mechanical techniques to enhance orthodontic anchorage, but such techniques can lead to negative side effects, and are dependent upon patient compliance and/or an appropriate anatomic location for placement (Cole, 2002; Jambi et al., 2013; Janson et al., 2013; Jambi et al., 2014; Kuroda and Tanaka, 2014; Al-Awadhi et al., 2015; Arponen et al., 2020). In addition, even appliances that utilize skeletal anchorage, such as temporary anchorage devices (TADs), while effective, do not provide 100% anchorage (Jambi et al., 2014; Kaipatur et al., 2014; Becker et al., 2018). Biological methods which influence orthodontic tooth movement at a cell and molecular level could provide alternative adjunctive methods for inhibition of undesired tooth movement.

Nitric Oxide (NO) plays a critical role in orthodontic tooth movement. Expression of nitric oxide synthase (NOS) isoforms iNOS and eNOS increase in PDL cells and local osteocytes upon application of orthodontic force (Nilforoushan and Manolson, 2009; Tan et al., 2009). This is not surprising given that tooth movement leads to fluid shear stress on local PDL cells and osteocytes, and shear stress stimulates expression of eNOS and NO production (Fox et al., 1996; Zaman et al., 1999; Davis et al., 2001; Kalyanaraman et al., 2018). Orthodontic tooth movement also stimulates the expression of inflammatory cytokines (Lowney et al., 1995; Uematsu et al., 1996; Alhashimi et al., 2001; Kaku et al., 2008), and cytokines stimulate expression of iNOS and NO production (Ralston et al., 1995; Huang, 2000). Previous studies showed that local injection of L-arginine (NO precursor) increased tooth movement in rats (Shirazi et al., 2002; Akin et al., 2004), while local injection of L-NAME (NOS inhibitor) inhibited tooth movement in rats (Hayashi et al., 2002; Shirazi et al., 2002). These NO manipulation during tooth movement studies appear to indicate that stimulation of NO production is bone catabolic, enhancing osteoclast activity and orthodontic tooth movement. Yet, it is well known that the efficacy of manipulating NO through these methods (delivery of L-arginine and/or L-NAME) is likely inadequate for optimal changes in NO efficacy (Anastasio et al., 2020). For this reason, here we utilized an NO producing biomaterial to establish NO effects on tooth movement.

In this study we show for the first time that nitric oxide (NO) delivery via injected NO releasing nanoparticles inhibits orthodontic movement of teeth adjacent to the site of injection. This tooth movement effect is likely due to the bone anabolic effects of NO. Our results are consistent with other reports showing that endogenous and exogenous NO has bone anabolic effects. Genetic ablation of eNOS in mice leads to decreased bone mineral density and cortical thinning with reduced osteoblast numbers and mineral apposition rate (Armour et al., 2001). Genetic ablation of iNOS in mice with hind limb suspension (mechanical unloading) do not increase bone formation after reloading (Watanuki et al., 2002). Genetic ablation of nNOS leads to diminished trabecular bone mineral density with reduced bone remodeling by 10 weeks in mice (van't Hof et al., 2004). Together, these studies indicate that loss of any of the three NOS isoforms and therefore NO production, diminishes bone anabolism. Other studies also showed that NO is an essential mediator of the bone anabolic effects of both estrogen and mechanical loading in mice (Armour et al., 2001; Rangaswami et al., 2009; Rangaswami et al., 2010; Marathe et al., 2012). NO releasing biomaterials were more recently proposed for better treatment of bone fractures and osteoporosis (Anastasio et al., 2020). In addition, of particular relevance to the current study, intraperitoneal injections of an NO producing biomaterial into female ovariectomized mice was shown to increase cGMP levels and downstream signaling, increase osteoprogenitor proliferation, increase osteoblast gene expression, reduce osteocyte apoptosis, reduce osteoclast numbers and reduce bone resorption. Overall, the NO biomaterial treated mice had significantly increased trabecular bone mass when compared to non-treated mice (Kalyanaraman et al., 2017), demonstrating that NO delivered via NO releasing biomaterials are bone anabolic, not catabolic, and would therefore be inhibitory to tooth movement.

Orthodontists and patients want efficient and consistently successful treatment outcomes. The results shown here provide a novel approach for control of tooth movement based upon emerging technologies for drug delivery and advances in our knowledge of biologic processes that control orthodontic tooth movement. Results of this study show that injection of the NO releasing nanoparticles inhibited tooth movement by over 50% for approximately 1 week after injection. While these results are striking, this study does have limitations, including the need for earlier time points for bone and tissue analyses. *In vitro* release data of NO indicated loss of NO release from nanoparticles after approximately 1 week, but this data was calculated later, leading the *in vivo* study to last for 18 days of orthodontic tooth movement. This resulted in assay of isolated tissues that had not been exposed to NO for approximately 2 weeks. In addition to the need for assay of tissues during NO release, future studies should also investigate utilization of lower force levels in the rodent model (Ren et al., 2004), utilize nanoparticles that do not release NO as a better control, and include a deeper characterization including electron microscopy of the nanoparticles and the nanoparticles-tissue interaction. It is also important to recognize that the NO *in vitro* release studies performed here were performed in deionized water. NO release from biomaterials is influenced by environmental conditions (He and Frost, 2016) such that NO release levels *in vivo* are likely different from that seen *in vitro*. In future studies it will also be important to perform cytotoxicity studies, as nano size silica nanoparticles may exhibit toxicity (Murugadoss et al., 2017). In future studies we plan to utilize biocompatible and biodegradable polymer nanoparticles for delivery of NO producing S-nitrosothiol groups (Kapoor et al., 2015; Elmowafy et al., 2019) to avoid silica based toxicity. Regardless, toxicology studies should be performed regardless of the nanoparticle material used.

The nanoparticles used in this study were configured to incorporate the NO generating S-nitrosothiol molecules but not configured for control of burst release, amount of NO release or duration of release. Results shown here demonstrate that NO was released from the nanoparticles at an initial burst level of 10 ppb/mg particles that decreased by 10x to steady state levels of 1 ppb/mg particles over the next 1–4 days, and then diminished again by tenfold from day 4 to day 7, at which point it was no longer measurable. The burst release was likely generated by trace transition metals that are ubiquitous in physiological environments. In future studies we aim to eliminate the initial burst release by formulating the nanoparticles with aqueous solution containing the chelating agent EDTA (ethylenediaminetetraacetic acid) and/or by coating with a thin film of PLGA (polylactic-co-glycolic acid). We also aim to increase nanoparticle loading of S-nitrosothiol particles to increase NO release levels and to incorporate controlled triggers for NO release, to increase efficacy and control longevity of effect. Of great importance to potential clinical translation, results also showed that inhibition of molar tooth movement only occurred during the period of NO release. After NO release, tooth movement returned to rates seen in control animals. No rebound effect (Teixeira, 2013; Anastasilakis et al., 2021) (increased rate of tooth movement) after end of NO release was seen.

As stated previously, NO influences the production of inflammatory signaling mediators, alters bone cell function, and enhances vascularization. All of these processes are potentially relevant to orthodontic tooth movement. The histomorphometry results shown here indicate that NO release from the nanoparticles significantly increased the number of blood vessels in the PDL of the distobuccal root of the maxillary first molar during tooth movement. While such results were not found for the buccal root, this was likely due to the fact that a smaller sample size was available for buccal root blood vessel quantification due to challenges in definition of the PDL space around this tooth root in animals that had orthodontic appliances. The increased blood vessel count around the distobuccal root in animals with the NO releasing nanoparticles indicates that the NO releasing nanoparticles had vascular effects. NO induces vasodilation, vasopermeability and angiogenesis (Rajendran et al., 2019). The results shown here indicate that the inhibitory tooth movement effects of the NO releasing nanoparticles are likely due to increased blood flow leading to increased oxygen tension in local tissues. Such an effect would decrease the local hypoxia that is induced upon orthodontic tooth movement, leading to diminished induction of downstream signaling and diminished orthodontic tooth movement. Future more comprehensive studies are required to definitively establish that changes in hypoxic signaling mediate the tooth movement properties of the NO releasing nanoparticles.

DATA AVAILABILITY STATEMENT

The raw data supporting the conclusion of this article will be made available by the authors, without undue reservation.

ETHICS STATEMENT

The animal study was reviewed and approved by the University of Michigan Institutional Animal Use and Care Committee.

AUTHOR CONTRIBUTIONS

DC, MCF and NEH contributed to conception and design of the study. DC, MCF and TL generated data. DC, MCF, TL and NEH analyzed data and performed the statistical analysis. DC wrote the first draft of the manuscript. TL, MCF and NEH wrote sections of the manuscript. All authors contributed to manuscript revision, read, and approved the submitted version.

FUNDING

This study was supported by a University of Michigan Rackham Student Research Award (to DC), a University of Michigan School of Dentistry Le Gro Graduate Student Research Award (to DC) and the University of Michigan School of Dentistry Wolverine Fund for Orthodontic Excellence.

ACKNOWLEDGMENTS

The authors would like to thank Michelle Lynch at the University of Michigan School of Dentistry for her assistance with micro computed tomography.

SUPPLEMENTARY MATERIAL

The Supplementary Material for this article can be found online at: https://www.frontiersin.org/articles/10.3389/fmats.2022.811251/full#supplementary-material

Supplementary Figure S1 | Serum cGMP Levels. cGMP levels in serum at indicated time points were measured by ELISA as measure of NO signaling. Day 0 is prior to ± orthodontic appliance placement. Days 1, 6, and 12 are after ± orthodontic appliance placement. Results show that cGMP levels were not evident in any group at any time point, are always below the negative control data point. Negative and positive control data points differ between days 0, 1 and days 6, 12 because the ELISA had to be performed on two different plates due to well number limitations.

REFERENCES

Akin, E., Gurton, A. U., and Olmez, H. (2004). Effects of Nitric Oxide in Orthodontic Tooth Movement in Rats. *Am. J. Orthod. Dentofacial Orthop.* 126 (5), 608–614. doi:10.1016/S0889540604004494

Al-Awadhi, E. A., Garvey, T. M., Alhag, M., Claffey, N. M., and O'Connell, B. (2015). Efficacy of the Nance Appliance as an anchorage-reinforcement Method. *Am. J. Orthod. Dentofacial Orthopedics* 147 (3), 330–338. doi:10.1016/j.ajodo.2014.11.014

Alhashimi, N., Frithiof, L., Brudvik, P., and Bakhiet, M. (2001). Orthodontic Tooth Movement and De Novo Synthesis of Proinflammatory Cytokines. *Am. J. Orthod. Dentofacial Orthopedics* 119 (3), 307–312. doi:10.1067/mod.2001.110809

Anastasilakis, A. D., Makras, P., Yavropoulou, M. P., Tabacco, G., Naciu, A. M., and Palermo, A. (2021). Denosumab Discontinuation and the Rebound Phenomenon: A Narrative Review. *J. Clin. Med.* 10 (1). doi:10.3390/jcm10010152

Anastasio, A. T., Paniagua, A., Diamond, C., Ferlauto, H. R., and Fernandez-Moure, J. S. (2020). Nanomaterial Nitric Oxide Delivery in Traumatic Orthopedic Regenerative Medicine. *Front. Bioeng. Biotechnol.* 8, 592008. doi:10.3389/fbioe.2020.592008

Armour, K. E., Armour, K. J., Gallagher, M. E., Gödecke, A., Helfrich, M. H., Reid, D. M., et al. (2001). Defective Bone Formation and Anabolic Response to Exogenous Estrogen in Mice with Targeted Disruption of Endothelial Nitric Oxide Synthase**This Study Was Supported by grants from the Arthritis Research Campaign (UK) and the Medical Research Council (UK). *Endocrinology* 142 (2), 760–766. doi:10.1210/endo.142.2.7977

Arponen, H., Hirvensalo, R., Lindgren, V., and Kiukkonen, A. (2020). Treatment Compliance of Adolescent Orthodontic Patients with Headgear Activator and Twin-Block Appliance Assessed Prospectively Using Microelectronic Wear-Time Documentation. *Eur. J. Orthod.* 42 (2), 180–186. doi:10.1093/ejo/cjaa001

Becker, K., Pliska, A., Busch, C., Wilmes, B., Wolf, M., and Drescher, D. (2018). Efficacy of orthodontic mini implants for en masse retraction in the maxilla: a systematic review and meta-analysis. *Int. J. Implant Dent* 4 (1), 35. doi:10.1186/s40729-018-0144-4

Bladowski, M., Gawrys, J., Gajecki, D., Szahidewicz-Krupska, E., Sawicz-Bladowska, A., and Doroszko, A. (2020). Role of the Platelets and Nitric Oxide Biotransformation in Ischemic Stroke: A Translative Review from Bench to Bedside. *Oxid Med. Cel Longev* 2020, 2979260. doi:10.1155/2020/2979260

Chen, Y.-J., Chang, H.-H., Huang, C.-Y., Hung, H.-C., Lai, E. H.-H., and Yao, C.-C. J. (2007). A Retrospective Analysis of the Failure Rate of Three Different Orthodontic Skeletal anchorage Systems. *Clin. Oral Implants Res.* 18 (6), 768–775. doi:10.1111/j.1600-0501.2007.01405.x

Clemmer, E. J., and Hayes, E. W. (1979). Patient Cooperation in Wearing Orthodontic Headgear. *Am. J. Orthod.* 75 (5), 517–524. doi:10.1016/0002-9416(79)90070-8

Cole, W. A. (2002). Accuracy of Patient Reporting as an Indication of Headgear Compliance. *Am. J. Orthod. Dentofacial Orthopedics* 121 (4), 419–423. doi:10.1067/mod.2002.122369

Cuoghi, O. A., Aiello, C. A., Consolaro, A., Tondelli, P. M., and Mendonça, M. R. (2014). Resorption of Roots of Different Dimension Induced by Different Types of Forces. *Braz. Oral Res.* 28. doi:10.1590/1807-3107bor-2014.vol28.0013

Davis, M. E., Cai, H., Drummond, G. R., and Harrison, D. G. (2001). Shear Stress Regulates Endothelial Nitric Oxide Synthase Expression through C-Src by Divergent Signaling Pathways. *Circ. Res.* 89 (11), 1073–1080. doi:10.1161/hh2301.100806

Dunn, M. D., Park, C. H., Kostenuik, P. J., Kapila, S., and Giannobile, W. V. (2007). Local Delivery of Osteoprotegerin Inhibits Mechanically Mediated Bone Modeling in Orthodontic Tooth Movement. *Bone* 41 (3), 446–455. doi:10.1016/j.bone.2007.04.194

Elmowafy, E. M., Tiboni, M., and Soliman, M. E. (2019). Biocompatibility, Biodegradation and Biomedical Applications of Poly(lactic Acid)/poly(lactic-Co-Glycolic Acid) Micro and Nanoparticles. *J. Pharm. Investig.* 49, 347–380. doi:10.1007/s40005-019-00439-x

Eun, J.-S., Suh, Y.-H., Kim, D.-K., and Jeon, H. (2000). Regulation of Cytokine Production by Exogenous Nitric Oxide in Murine Splenocyte and Peritoneal Macrophage. *Arch. Pharm. Res.* 23 (5), 531–534. doi:10.1007/bf02976585

Feldens, C. A., Dos Santos Dullius, A. I., Kramer, P. F., Scapini, A., Busato, A. L. S., and Vargas-Ferreira, F. (2015). Impact of Malocclusion and Dentofacial Anomalies on the Prevalence and Severity of Dental Caries Among Adolescents. *Angle Orthod.* 85 (6), 1027–1034. doi:10.2319/100914-722.1

Fox, S. W., Chambers, T. J., and Chow, J. W. (1996). Nitric Oxide Is an Early Mediator of the Increase in Bone Formation by Mechanical Stimulation. *Am. J. Physiol.* 270 (6 Pt 1), E955–E960. doi:10.1152/ajpendo.1996.270.6.E955

Francis, S. H., Busch, J. L., Corbin, J. D., and Sibley, D. (2010). cGMP-Dependent Protein Kinases and cGMP Phosphodiesterases in Nitric Oxide and cGMP Action. *Pharmacol. Rev.* 62 (3), 525–563. doi:10.1124/pr.110.002907

Friebe, A., and Koesling, D. (2009). The Function of NO-Sensitive Guanylyl Cyclase: what We Can Learn from Genetic Mouse Models. *Nitric Oxide* 21 (3-4), 149–156. doi:10.1016/j.niox.2009.07.004

Frost, M. C., and Meyerhoff, M. E. (2005). Synthesis, Characterization, and Controlled Nitric Oxide Release fromS-Nitrosothiol-Derivatized Fumed Silica Polymer Filler Particles. *J. Biomed. Mater. Res.* 72A (4), 409–419. doi:10.1002/jbm.a.30275

Gantner, B. N., LaFond, K. M., and Bonini, M. G. (2020). Nitric Oxide in Cellular Adaptation and Disease. *Redox Biol.* 34, 101550. doi:10.1016/j.redox.2020.101550

Garren, M. R., Ashcraft, M., Qian, Y., Douglass, M., Brisbois, E. J., and Handa, H. (2021). Nitric Oxide and Viral Infection: Recent Developments in Antiviral Therapies and Platforms. *Appl. Mater. Today* 22, 100887. doi:10.1016/j.apmt.2020.100887

Ghosh, A., Lattey, K. R., and Kelly, A. J. (2016). Nitric Oxide Donors for Cervical Ripening and Induction of Labour. *Cochrane Database Syst. Rev.* 12, CD006901. doi:10.1002/14651858.CD006901.pub3

Gonzales, C., Hotokezaka, H., Yoshimatsu, M., Yozgatian, J. H., Darendeliler, M. A., and Yoshida, N. (2008). Force Magnitude and Duration Effects on Amount of Tooth Movement and Root Resorption in the Rat Molar. *Angle Orthod.* 78 (3), 502–509. doi:10.2319/052007-240.1

Gozdzik, W., Zielinski, S., Zielinska, M., Ratajczak, K., Skrzypczak, P., Rodziewicz, S., et al. (2018). Beneficial Effects of Inhaled Nitric Oxide with Intravenous Steroid in an Ischemia-Reperfusion Model Involving Aortic Clamping. *Int. J. Immunopathol Pharmacol.* 32, 394632017751486. doi:10.1177/0394632017751486

Griffith, T. M., Edwards, D. H., Lewis, M. J., Newby, A. C., and Henderson, A. H. (1984). The Nature of Endothelium-Derived Vascular Relaxant Factor. *Nature* 308 (5960), 645–647. doi:10.1038/308645a0

Hayashi, K., Igarashi, K., Miyoshi, K., Shinoda, H., and Mitani, H. (2002). Involvement of Nitric Oxide in Orthodontic Tooth Movement in Rats. *Am. J. Orthod. Dentofacial Orthopedics* 122 (3), 306–309. doi:10.1067/mod.2002.126151

He, W., and Frost, M. C. (2016). Direct Measurement of Actual Levels of Nitric Oxide (NO) in Cell Culture Conditions Using Soluble NO Donors. *Redox Biol.* 9, 1–14. doi:10.1016/j.redox.2016.05.002

Huang, P. L. (2000). Mouse Models of Nitric Oxide Synthase Deficiency. *J. Am. Soc. Nephrol.* 11 Suppl 16 (Suppl. 16), S120–S123. doi:10.1681/asn.v11suppl_2s120

Hudson, J. B., Hatch, N., Hayami, T., Shin, J. M., Stolina, M., Kostenuik, P. J., et al. (2012). Local Delivery of Recombinant Osteoprotegerin Enhances Postorthodontic Tooth Stability. *Calcif Tissue Int.* 90 (4), 330–342. doi:10.1007/s00223-012-9579-4

Ignarro, L. J. (1990). Nitric Oxide. A Novel Signal Transduction Mechanism for Transcellular Communication. *Hypertension* 16 (5), 477–483. doi:10.1161/01.hyp.16.5.477

Jambi, S., Thiruvenkatachari, B., O'Brien, K. D., and Walsh, T. (2013). Orthodontic Treatment for Distalising Upper First Molars in Children and Adolescents. *Cochrane Database Syst. Rev.* 10, CD008375. doi:10.1002/14651858.CD008375.pub2

Jambi, S., Walsh, T., Sandler, J., Benson, P. E., Skeggs, R. M., and O'Brien, K. D. (2014). Reinforcement of anchorage during Orthodontic Brace Treatment with Implants or Other Surgical Methods. *Cochrane Database Syst. Rev.* (8), CD005098. doi:10.1002/14651858.CD005098.pub3

Janson, G., Sathler, R., Fernandes, T. M. F., Branco, N. C. C., and de Freitas, M. R. (2013). Correction of Class II Malocclusion with Class II Elastics: a Systematic

Review. *Am. J. Orthod. Dentofacial Orthopedics* 143 (3), 383–392. doi:10.1016/j.ajodo.2012.10.015

Jiang, N., Guo, W., Chen, M., Zheng, Y., Zhou, J., Kim, S. G., et al. (2016). Periodontal Ligament and Alveolar Bone in Health and Adaptation: Tooth Movement. *Front. Oral Biol.* 18, 1–8. doi:10.1159/000351894

Kaipatur, N., Wu, Y., Adeeb, S., Stevenson, T., Major, P., and Doschak, M. (2014). A Novel Rat Model of Orthodontic Tooth Movement Using Temporary Skeletal Anchorage Devices: 3D Finite Element Analysis and *In Vivo* Validation. *Int. J. Dent* 2014, 917535. doi:10.1155/2014/917535

Kaku, M., Motokawa, M., Tohma, Y., Tsuka, N., Koseki, H., Sunagawa, H., et al. (2008). VEGF and M-CSF Levels in Periodontal Tissue during Tooth Movement. *Biomed. Res.* 29 (4), 181–187. doi:10.2220/biomedres.29.181

Kalyanaraman, H., Ramdani, G., Joshua, J., Schall, N., Boss, G. R., Cory, E., et al. (2017). A Novel, Direct NO Donor Regulates Osteoblast and Osteoclast Functions and Increases Bone Mass in Ovariectomized Mice. *J. Bone Miner Res.* 32 (1), 46–59. doi:10.1002/jbmr.2909

Kalyanaraman, H., Schall, N., and Pilz, R. B. (2018). Nitric Oxide and Cyclic GMP Functions in Bone. *Nitric Oxide* 76, 62–70. doi:10.1016/j.niox.2018.03.007

Kapoor, D. N., Bhatia, A., Kaur, R., Sharma, R., Kaur, G., and Dhawan, S. (2015). PLGA: a Unique Polymer for Drug Delivery. *Ther. Deliv.* 6 (1), 41–58. doi:10.4155/tde.14.91

Khan, F. H., Dervan, E., Bhattacharyya, D. D., McAuliffe, J. D., Miranda, K. M., and Glynn, S. A. (2020). The Role of Nitric Oxide in Cancer: Master Regulator or Not? *Int. J. Mol. Sci.* 21 (24). doi:10.3390/ijms21249393

Kim, J.-W., Lee, N.-K., Sim, H.-Y., Yun, P.-Y., and Lee, J.-H. (2016). Failure of Orthodontic Mini-Implants by Patient Age, Sex, and Arch; Number of Primary Insertions; and Frequency of Reinsertions after Failure: An Analysis of the Implant Failure Rate and Patient Failure Rate. *Int. J. Periodontics Restorative Dent* 36 (4), 559–565. doi:10.11607/prd.2675

Kim, S., Katchooi, M., Bayiri, B., Sarikaya, M., Korpak, A. M., and Huang, G. J. (2016). Predicting Improvement of Postorthodontic white Spot Lesions. *Am. J. Orthod. Dentofacial Orthopedics* 149 (5), 625–633. doi:10.1016/j.ajodo.2015.10.025

King, G. J., Keeling, S. D., and Wronski, T. J. (1991). Histomorphometric Study of Alveolar Bone Turnover in Orthodontic Tooth Movement. *Bone* 12 (6), 401–409. doi:10.1016/8756-3282(91)90029-i

Król, M., and Kepinska, M. (2020). Human Nitric Oxide Synthase-Its Functions, Polymorphisms, and Inhibitors in the Context of Inflammation, Diabetes and Cardiovascular Diseases. *Int. J. Mol. Sci.* 22 (1). doi:10.3390/ijms22010056

Kuroda, S., and Tanaka, E. (2014). Risks and Complications of Miniscrew anchorage in Clinical Orthodontics. *Jpn. Dental Sci. Rev.* 50 (4), 79–85. doi:10.1016/j.jdsr.2014.05.001

Lancaster, J. R., Jr. (1997). A Tutorial on the Diffusibility and Reactivity of Free Nitric Oxide. *Nitric Oxide* 1 (1), 18–30. doi:10.1006/niox.1996.0112

Lowenstein, C. J., and Snyder, S. H. (1992). Nitric Oxide, a Novel Biologic Messenger. *Cell* 70 (5), 705–707. doi:10.1016/0092-8674(92)90301-r

Lowney, J. J., Norton, L. A., Shafer, D. M., and Rossomando, E. F. (1995). Orthodontic Forces Increase Tumor Necrosis Factor α in the Human Gingival Sulcus. *Am. J. Orthod. Dentofacial Orthopedics* 108 (5), 519–524. doi:10.1016/s0889-5406(95)70052-8

Marathe, N., Rangaswami, H., Zhuang, S., Boss, G. R., and Pilz, R. B. (2012). Pro-survival Effects of 17β-Estradiol on Osteocytes Are Mediated by Nitric Oxide/cGMP via Differential Actions of cGMP-dependent Protein Kinases I and II. *J. Biol. Chem.* 287 (2), 978–988. doi:10.1074/jbc.m111.294959

Marcinkiewicz, J., and Chain, B. M. (1993). Differential Regulation of Cytokine Production by Nitric Oxide. *Immunology* 80 (1), 146–150.

Masella, R. S., and Meister, M. (2006). Current Concepts in the Biology of Orthodontic Tooth Movement. *Am. J. Orthod. Dentofacial Orthopedics* 129 (4), 458–468. doi:10.1016/j.ajodo.2005.12.013

Murugadoss, S., Lison, D., Godderis, L., Van Den Brule, S., Mast, J., Brassinne, F., et al. (2017). Toxicology of Silica Nanoparticles: an Update. *Arch. Toxicol.* 91 (9), 2967–3010. doi:10.1007/s00204-017-1993-y

Nilforoushan, D., and Manolson, M. F. (2009). Expression of Nitric Oxide Synthases in Orthodontic Tooth Movement. *Angle Orthod.* 79 (3), 502–508. doi:10.2319/0003-3219(2009)079[0502:eonosi]2.0.co;2

Pastro, J. D. V., Nogueira, A. C. A., Salvatore de Freitas, K. M., Valarelli, F. P., Cançado, R. H., de Oliveira, R. C. G., et al. (2018). Factors Associated to Apical Root Resorption after Orthodontic Treatment. *Todentj* 12, 331–339. doi:10.2174/1874210601812010331

Proffit, W. R., Fields, H. W., Jr., and Moray, L. J. (1998). Prevalence of Malocclusion and Orthodontic Treatment Need in the United States: Estimates from the NHANES III Survey. *Int. J. Adult Orthodon Orthognath Surg.* 13 (2), 97–106.

Rajendran, S., Shen, X., Glawe, J., Kolluru, G. K., and G. Kevil, C. (2019). Nitric Oxide and Hydrogen Sulfide Regulation of Ischemic Vascular Growth and Remodeling. *Compr. Physiol.* 9 (3), 1213–1247. doi:10.1002/cphy.c180026

Ralston, S. H., Ho, L. P., Helfrich, M. H., Grabowski, P. S., Johnston, P. W., and Benjamin, N. (1995). Nitric Oxide: a Cytokine-Induced Regulator of Bone Resorption. *J. Bone Miner Res.* 10 (7), 1040–1049. doi:10.1002/jbmr.5650100708

Rangaswami, H., Schwappacher, R., Marathe, N., Zhuang, S., Casteel, D. E., Haas, B., et al. (2010). Cyclic GMP and Protein Kinase G Control a Src-Containing Mechanosome in Osteoblasts. *Sci. Signal.* 3 (153), ra91. doi:10.1126/scisignal.2001423

Rangaswami, H., Marathe, N., Zhuang, S., Chen, Y., Yeh, J.-C., Frangos, J. A., et al. (2009). Type II cGMP-dependent Protein Kinase Mediates Osteoblast Mechanotransduction. *J. Biol. Chem.* 284 (22), 14796–14808. doi:10.1074/jbc.m806486200

Ren, Y., Maltha, J. C., and Kuijpers-Jagtman, A. M. (2004). The Rat as a Model for Orthodontic Tooth Movement-Aa Critical Review and a Proposed Solution. *Eur. J. Orthod.* 26 (5), 483–490. doi:10.1093/ejo/26.5.483

Sameshima, G. T., and Sinclair, P. M. (2001). Predicting and Preventing Root Resorption: Part II. Treatment Factors. *Am. J. Orthod. Dentofacial Orthopedics* 119 (5), 511–515. doi:10.1067/mod.2001.113410

Schneider, D. A., Smith, S. M., Campbell, C., Hayami, T., Kapila, S., and Hatch, N. E. (2015). Locally Limited Inhibition of Bone Resorption and Orthodontic Relapse by Recombinant Osteoprotegerin Protein. *Orthod. Craniofac. Res.* 18 (Suppl. 1), 187–195. doi:10.1111/ocr.12086

Shih, S. C., and Claffey, K. P. (1998). Hypoxia-mediated Regulation of Gene Expression in Mammalian Cells. *Int. J. Exp. Pathol.* 79 (6), 347–357. doi:10.1046/j.1365-2613.1998.00088.x

Shirazi, M., Nilforoushan, D., Alghasi, H., and Dehpour, A. R. (2002). The Role of Nitric Oxide in Orthodontic Tooth Movement in Rats. *Angle Orthod.* 72 (3), 211–215. doi:10.1043/0003-3219(2002)072<0211:TRONOI>2.0.CO;2

Sun, L., Wong, H. M., and McGrath, C. P. (2017). Relationship between the Severity of Malocclusion and Oral Health Related Quality of Life: A Systematic Review and Meta-Analysis. *Oral Health Prev. Dent* 15 (6), 503–517. doi:10.3290/j.ohpd.a38994

Sydorak, I., Dang, M., Baxter, S. J., Halcomb, M., Ma, P., Kapila, S., et al. (2019). Microsphere Controlled Drug Delivery for Local Control of Tooth Movement. *Eur. J. Orthod.* 41 (1), 1–8. doi:10.1093/ejo/cjy017

Tan, S. D., Xie, R., Klein-Nulend, J., van Rheden, R. E., Bronckers, A. L. J. J., Kuijpers-Jagtman, A. M., et al. (2009). Orthodontic Force Stimulates eNOS and iNOS in Rat Osteocytes. *J. Dent Res.* 88 (3), 255–260. doi:10.1177/0022034508330861

Teixeira, M. Z. (2013). Rebound Effect of Modern Drugs: Serious Adverse Event Unknown by Health Professionals. *Rev. Assoc. Med. Bras (1992)* 59 (6), 629–638. doi:10.1016/j.ramb.2013.05.003

Uematsu, S., Mogi, M., and Deguchi, T. (1996). Interleukin (IL)-1β, IL-6, Tumor Necrosis Factor-α, Epidermal Growth Factor, and β2-Microglobulin Levels Are Elevated in Gingival Crevicular Fluid during Human Orthodontic Tooth Movement. *J. Dent Res.* 75 (1), 562–567. doi:10.1177/00220345960750010801

van't Hof, R. J., Macphee, J., Libouban, H., Helfrich, M. H., and Ralston, S. H. (2004). Regulation of Bone Mass and Bone Turnover by Neuronal Nitric Oxide Synthase. *Endocrinology* 145 (11), 5068–5074. doi:10.1210/en.2004-0205

Vanhoutte, P. M., Shimokawa, H., Feletou, M., and Tang, E. H. C. (2017). Endothelial Dysfunction and Vascular Disease - a 30th Anniversary Update. *Acta Physiol.* 219 (1), 22–96. doi:10.1111/apha.12646

Vaughn, M. W., Kuo, L., and Liao, J. C. (1998). Effective Diffusion Distance of Nitric Oxide in the Microcirculation. *Am. J. Physiology-Heart Circulatory Physiol.* 274 (5), H1705–H1714. doi:10.1152/ajpheart.1998.274.5.h1705

Watanuki, M., Sakai, A., Sakata, T., Tsurukami, H., Miwa, M., Uchida, Y., et al. (2002). Role of Inducible Nitric Oxide Synthase in Skeletal Adaptation to Acute Increases in Mechanical Loading. *J. Bone Miner Res.* 17 (6), 1015–1025. doi:10.1359/jbmr.2002.17.6.1015

Yoo, S. K., Warita, H., and Soma, K. (2004). Duration of Orthodontic Force Affecting Initial Response of Nitric Oxide Synthase in Rat Periodontal Ligaments. *J. Med. Dent Sci.* 51 (1), 83–88.

Zaman, G., Pitsillides, A. A., Rawlinson, S. C. F., Suswillo, R. F. L., Mosley, J. R., Cheng, M. Z., et al. (1999). Mechanical Strain Stimulates Nitric Oxide Production by Rapid Activation of Endothelial Nitric Oxide Synthase in Osteocytes. *J. Bone Miner Res.* 14 (7), 1123–1131. doi:10.1359/jbmr.1999.14.7.1123

Conflict of Interest: The authors declare that the research was conducted in the absence of any commercial or financial relationships that could be construed as a potential conflict of interest.

Publisher's Note: All claims expressed in this article are solely those of the authors and do not necessarily represent those of their affiliated organizations, or those of the publisher, the editors and the reviewers. Any product that may be evaluated in this article, or claim that may be made by its manufacturer, is not guaranteed or endorsed by the publisher.